Norwegian University of Life Sciences
Faculty of chemistry, biotechnology and food science

Philosophiae Doctor (PhD)
Thesis 2020:36

Cell-shape regulation in *Streptococcus pneumoniae*: EloR/KhpA, a new regulatory pathway administering cellelongation

Regulering av celleform hos *Streptococcus pneumoniae*: EloR/KhpA, en ny reguleringsvei for celle-elongering

Anja Ruud Winther

Cell-shape regulation in *Streptococcus pneumoniae*: EloR/KhpA, a new regulatory pathway administering cell elongation

Regulering av celleform hos *Streptococcus pneumoniae*: EloR/KhpA, en ny reguleringsvei for celle-elongering

Philosophiae Doctor (PhD) Thesis

Anja Ruud Winther

Norwegian University of Life Sciences

Faculty of chemistry, biotechnology and food science

Ås (2020)

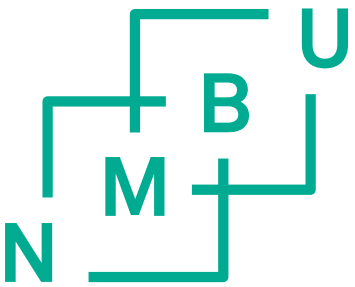

Thesis number 2020:36

ISSN 1894-6402

ISBN 978-82-575-1700-7

Table of contents

Acknowledgements

First of all, I want to thank my amazing supervisors, Dr. Daniel Straume and Prof. Sigve Håvarstein. Together, they have an extensive knowledge of cell division in *Streptococcus pneumoniae* and every possible laboratory technique you'll ever need. I've learned so much over the course of this project, and because of them it's been fun (most of the time) and educational.

The whole MolMik group also deserves a huge THANK YOU for the great time I've had over the last 4 years. We've had parties, snuggle hooks, bubble breakfasts, julekalender and ice cream breaks in the sun. We have also attended some great conferences over the years. My top memories include Daniel and myself in a bar alone, because Gro had to go to bed at 9 pm, the PizzaHut incident in Paris with Gro, and seeing all the amazing sites in Jerusalem with Morten, particularly the wailing wall, despite the lack of results after all my wailing.

I want to thank Zhian for our early morning gossiping and coffee drinking. You are the only one that gets to work before me, and you make every morning better. Vi er den harde kjernen. You also have crazy PCR skills, and I am grateful for being able to utilize those to the fullest. Gro, you are always in a good mood and you make everyone smile. I can ask you about anything – academic or not – and you always make time for me. We will always be bound together by our hate of liver-lollipops.

It's been nice to have a fellow "noisy music" lover in the group, Daniel. Together, we can withstand Celine Dion and Karpe Diem. And Morten, when you least expect it, I will come by and decorate your office for Christmas, Halloween or a Game of Thrones marathon.

Having people around you in a similar situation is always helpful, and I've been lucky enough to have Ine, Kasia and Maria. With fellow PhD-students one can complain about the harsh PhD-life, ask stupid questions that are embarrassing to take to your supervisor, and support each other after having made the same mistake for the third time. Thank you for the complaining sessions (Kasia), baby-talk (Ine), and arranging Hangouts coffee-breaks during corona-quarantine (Maria).

Danae, Marita, Anette, Janette and Ingvild: I haven't known you for long, but you are all part of making MolMik a great place to be. And Marita, starting a 40-days challenge 3 weeks before quarantine hits is a BAD idea. I'm holding you responsible!

Acknowledgements

My family also deserves a big thank you. My parents and sister are nothing but supportive and inspiring. I would never be here without you! And my dear husband who survives my rants when lab work isn't going my way, shares my joy when it does, and takes all my worries away. You and Jenny keep me grounded, motivated and happy.

Anja Ruud Winther

Oppegård 2020

Summary

The oval shaped *Streptococcus pneumoniae* utilizes both septal and peripheral peptidoglycan (PG) synthesis in order to maintain its shape. The protein complexes responsible for synthesizing PG are called the elongasome and the divisome, and as the names imply the elongasome synthesizes peripheral PG while the divisome synthesizes the PG responsible for dividing the cell into two [1]. The core of the elongasome and the divisome is the essential class B penicillin binding proteins (PBPs) 2b and 2x, respectively. PBP2b and PBP2x are transpeptidases creating peptide cross-links in PG between glycan strands [1, 2]. They work alongside the glycosyltransferases RodA and FtsW, respectively, to incorporate new PG into the existing PG sacculus [3-5]. The elongasome and divisome activities must be precisely coordinated throughout the cell cycle, but detailed knowledge about the control systems the cells possess to manage these PG machineries are lacking. In the current work, I present a pathway for regulation of elongation that has emerged recently: the EloR/KhpA complex. EloR and KhpA both contain RNA binding domains commonly seen in proteins involved in transcriptional or post-transcriptional regulation [6-8]. We and others have found that in order to survive the loss of *pbp2b*, *S. pneumoniae* can create suppressor mutations in the genes encoding EloR, KhpA and MltG rendering the protein products inactive [9, 10]. Our results show that EloR and KhpA work as a complex controlling cell elongation, most likely in a pathway including StkP, a Ser/Thr kinase known to have a regulatory role in cell division [11-15], and the essential lytic transglycosylase MltG.

In paper I we show that the loss of EloR resulted in shorter cells in the laboratory strain R6. We confirmed that EloR is phosphorylated by StkP and conclude that it is likely that phosphorylation of EloR leads to release of bound RNA, stimulating elongation. We speculate that the reason PBP2b and RodA are essential in a wild type background is that these proteins are required in cells where the muralytic activity of MltG has a normal function. The reason *pbp2b* and *rodA* can be deleted in an Δ*eloR* mutant may be that the MltG activity is reduced without EloR present.

In paper II we show that EloR interacts directly with a small RNA binding protein called KhpA. Using 3D modelling and site directed mutagenesis we identified the interaction surface between the two proteins and two amino acid residues important for this interaction. We could use this information to investigate how cells reacted to the loss of complex formation between the two

proteins. A study by Zheng et al., 2017 showed that a *khpA* deletion mutant phenocopies an *eloR* deletion mutant [9]. We demonstrate in paper II that EloR and KhpA is one functional unit, and if the direct interaction between EloR and KhpA is broken, the cells behave like a Δ*eloR* or Δ*khpA* mutant, i.e. PBP2b/RodA become redundant. We also show that KhpA depends upon EloR interaction to reach its midcell localization.

In addition to two RNA binding domains (KH-II and R3H) at the C-terminal end, EloR has a Jag-domain with unknown function at its N-terminus. In the final manuscript, paper III, we set out to unravel the function of the Jag domain. We found that the Jag domain is critical for midcell localization of EloR. Furthermore, by screening for protein-protein interactions between EloR and other elongasome proteins, the Jag domain was found to interact with the cytoplasmic domain of the lytic transglycosylase MltG. We hypothesize that the EloR/KhpA complex is recruited to midcell through the Jag-MltG interaction where it somehow controls the muralytic activity of MltG, either through protein – protein interaction or by RNA binding.

Sammendrag

Den ovale bakterien *Streptococcus pneumoniae* benytter både septal og perifer peptidoglykansyntese for å opprettholde celleformen. Proteinkompleksene som er ansvarlige for å syntetisere peptidoglykan (PG) kalles elongasomet og divisomet, og som navnene tilsier syntetiserer elongasomet perifert PG mens divisomet syntetiserer PG som er ansvarlig for å dele cellen i to [1]. Kjernevirksomheten i elongasomet og divisomet utføres av de essensielle klasse B penicillinbindende proteinene (PBP) 2b og 2x. PBP2b og PBP2x er transpeptidaser som danner peptid-kryssbindinger mellom glykantrådene i PG [1, 2]. De jobber sammen med glykosyltransferasene RodA og FtsW for å inkorporere ny PG i det eksisterende PG nettverket [3-5]. Elongasom- og divisom-aktivitetene må være nøyaktig koordinerte gjennom hele cellesyklusen, men detaljert kunnskap om hvordan cellene kontrollerer disse PG-maskineriene mangler. I dette prosjektet presenterer jeg en vei for regulering av elongering som nylig har blitt oppdaget: EloR/KhpA-komplekset. EloR og KhpA inneholder begge RNA-bindende domener som ofte finnes hos proteiner involvert i transkripsjonell eller post-transkripsjonell regulering [6-8]. Vi og andre har oppdaget at for å overleve tapet av *pbp2b* kan *S. pneumoniae* skape suppressormutasjoner i genene som koder for EloR, KhpA og MltG, slik at proteinproduktene blir inaktive [9, 10]. Resultatene våre viser at EloR og KhpA fungerer som et kompleks som kontrollerer celle-elongering sammen med StkP, en Ser/Thr-kinase kjent for å ha en regulerende rolle i celledeling [11-15], og den essensielle lytiske transglykosylasen MltG.

I artikkel I viste vi at tapet av EloR resulterte i kortere celler i laboratoriestammen R6. Vi bekreftet at EloR fosforyleres av StkP og konkluderer med at det er sannsynlig at fosforylering av EloR fører til at RNA frigis og dermed stimulerer elongering. Vi spekulerer at PBP2b og RodA er essensielle i en villtype bakgrunn fordi disse proteinene er nødvendige i celler der den muralytiske aktiviteten til MltG har normal funksjon. Årsaken til at *pbp2b* og *rodA* kan fjernes i en Δ*eloR* stamme kan være at MltG-aktiviteten er redusert i fravær av EloR.

I artikkel II viser vi at EloR interagerer direkte med et lite RNA-bindende protein kalt KhpA. Ved hjelp av 3D-modellering og innføring av punktmutasjoner identifiserte vi interaksjonsflaten mellom de to proteinene, samt to aminosyrer som er viktige for denne interaksjonen. Vi brukte denne informasjonen til å undersøke hvordan celler reagerte på tap av EloR/KhpA interaksjonen.

En studie av Zheng et al., 2017 viste at en *khpA* delesjonsmutant fenokopierer en *eloR* delesjonsmutant [9]. Vi viser i artikkel II at EloR og KhpA er en funksjonell enhet, og hvis den direkte interaksjonen mellom EloR og KhpA brytes, oppfører cellene seg som en Δ*eloR* eller Δ*khpA* mutant, dvs. cellene kan leve fint uten PBP2b/RodA. Vi viser også at KhpA er avhengig av å binde EloR for å plasseres i delingssonen i cellen.

I tillegg til to RNA bindende domener (KH-II og R3H) ved C-terminal ende, har EloR et Jag-domene med ukjent funksjon ved sin N-terminale ende. I manuskriptet, artikkel III, tok vi sikte på å avdekke funksjonen til Jag-domenet. Vi fant ut at Jag-domenet er essensielt for EloRs lokalisering til septum. Videre, ved å screene for protein-protein-interaksjoner mellom EloR og andre elongasom proteiner, ble det oppdaget at Jag-domenet interagerer med det cytoplasmatiske domenet til den lytiske transglykosylasen MltG. Vi antar at EloR/KhpA-komplekset rekrutteres til cellens delingssone ved at Jag-domenet interagerer med MltG hvor det på en eller annen måte styrer den muralytiske aktiviteten til MltG, enten gjennom protein-protein-interaksjon eller ved RNA-binding.

List of papers

Paper I Stamsås, G. A., D. Straume, **A. Ruud Winther**, M. Kjos, C. A. Frantzen and L. S. Håvarstein (2017). "Identification of EloR (Spr1851) as a regulator of cell elongation in *Streptococcus pneumoniae*." Molecular microbiology **105**(6): 954-967.

Paper II **Winther, A. R.**, M. Kjos, G. A. Stamsås, L. S. Håvarstein and D. Straume (2019). "Prevention of EloR/KhpA heterodimerization by introduction of site-specific amino acid substitutions renders the essential elongasome protein PBP2b redundant in *Streptococcus pneumoniae*." Scientific Reports **9**(1): 3681.

Paper III **Winther, A. R.**, M. Kjos, L. S. Håvarstein, D. Straume (2020). "EloR interacts with the lytic transglycosylase MltG at midcell in *Streptococcus pneumoniae* R6." unpublished.

1. Introduction

Streptococcus pneumoniae, or the pneumococcus, is a Gram-positive, ellipsoid shaped bacterium belonging to the Mitis group of streptococci (Figure 1). It is a potential pathogen that resides in the nasopharynx of approximately 10 percent of the adult human population [16]. Pneumococci can spread from the nasopharynx to the ear, the sinuses, the bronchi, and even to the blood stream, causing sepsis. Yong children and the elderly are most at risk of infection, and WHO has estimated that around one million children die of pneumococcal disease every year. After the discovery of penicillin by Alexander Fleming in 1928, several antimicrobial drugs have been introduced, making the treatment of these bacterial infections efficient. Despite their success, the inevitable rise of drug resistant pneumococci and other pathogens has become a major threat to modern medicine. This was already predicted by Fleming in his Nobel lecture in 1945.

It is estimated that 23 thousand people died as a result of infections with antibiotic resistant bacteria in the US in 2013. Seven thousand of these cases were caused by drug resistant *S. pneumoniae*, costing the US government 96 million dollars in medical expenses [17]. Because pneumococci can become natural competent for genetic transformation, they can take up DNA from their surroundings in a process known as horizontal gene transfer. Antibiotic resistance genes can thus be quickly acquired and shared with other pneumococcal strains. The accelerating magnitude of drug resistance among pathogens will soon make lifesaving procedures such as chemotherapy and surgeries high risk treatments. Proper antibiotic use within agriculture and medicine is instrumental to slow the spread and development of resistance. Regardless, we also need to develop new antimicrobials that can be used alone or in combination with existing drugs to fight present and future drug resistant bacteria. Two promising targets for such new drugs are the bacterial cell division machineries. This is because many of the processes involved are essential and conserved in bacteria, and not found in humans. Without the ability to divide and elongate, the pneumococcal cells cannot survive and multiply. Inhibition of penicillin binding proteins (PBPs), which are enzymes constructing the bacterial cell wall, with β-lactam antibiotics exemplifies the success of a cell division targeting antibiotic. Exploiting the potential of novel components of the division and elongation machineries as drug targets, however, requires extensive knowledge about which proteins are involved, their functions, interactions and their mode of action. It is also of high

academic and public interest to address how these fundamental events take place in a bacterium's life.

The work presented here describes the discovery and characterization of a novel and conserved regulatory pathway that is essential for cell elongation in *S. pneumoniae*, i.e. synthesis of lateral cell wall during cell division. Two RNA binding (possibly ssDNA) proteins named EloR and KhpA are key players in this pathway. Unraveling their functions in pneumococcal cell elongation have been the focus of the current research.

1.1 The pneumococcal cell wall

Bacteria have a colossal structure wrapping the cytoplasmic membrane called the cell wall. It functions to maintain the cell shape, serves as an anchor for other extracellular components such as proteins, and protects the cell from lysing due to the high turgor pressure. The Gram-positive cell wall of pneumococci is made up of peptidoglycan (PG), teichoic acids, and proteins (Figure 1). Most pneumococcal strains also have polysaccharides attached to the cell wall (a so-called capsule), helping the cells in evading the host immune system. Further description of capsule biosynthesis will not be given here.

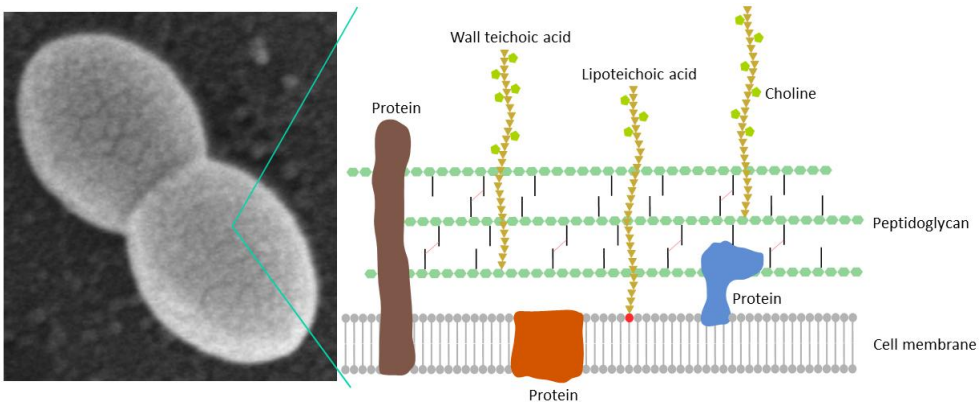

Figure 1. Micrograph of *S. pneumoniae* and a simplified overview of the pneumococcal cell wall structure which consists of protein, peptidoglycan, wall teichoic acid, lipoteichoic acid, and capsule (not depicted). Scanning electron microscopy image curtesy of Katarzyna Wiaroslawa Piechowiak.

1.1.1 Pneumococcal cell wall structure

The main component of the cell wall is PG. It is made up of glycan chains of disaccharide units consisting of N-acetylglucosamine (GlcNAc) and N-acetylmuramic acid (MurNAc). MurNAc residues have a pentapeptide attached to it (Figure 2A), which is involved in crosslinking the glycan chains. In *S. pneumoniae* the PG chains consist of at least 25 disaccharide units [18]. This length is relatively long if one compares with chain lengths of *Escherichia coli* (5-10 units) and *Staphylococcus aureus* (3-10 units) [19, 20]. The pentapeptides in pneumococcal PG have the composition L-Alanine – iso-D-Glutamine – L-Lysine – D-Alanine – D-Alanine. When incorporated into the PG layer, the pentapeptide precursor can have three different fates. It can be part of a direct cross-link, a branched cross-link, or be trimmed to tetra- or tripeptides by DD-carboxylases and LD-carboxylases (Figure 2B) [21].

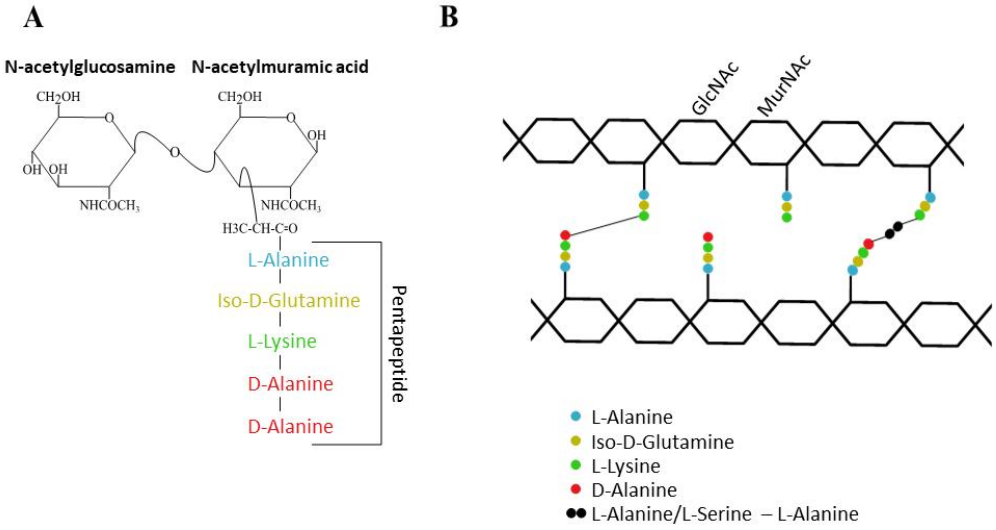

Figure 2. A) Structure of the GlcNAc-MurNAc-pentapeptide unit that makes up pneumococcal PG, and B) a simplified view of a mature PG polymer including the main three different states of the pentapeptide precursor.

Cross-links in PG are made between the pentapeptides on neighboring glycan chains. A direct cross-link is between the L-Lys at position three of one peptide and the D-Ala at position four of a neighboring peptide, expelling the D-Ala at position 5 in the second peptide. In addition, the D-

Ala in position four of the second peptide can be cross-linked with the ε amino group on L-Lys of a third peptide. In this way, dimers, trimers and tetramers are formed in the PG. In a branched cross-link a dipeptide connects L-Lys and D-Ala between two peptides. The dipeptide in a branched cross-link consists of either an L-Alanine or an L-Serine followed by an invariable L-Alanine [22]. The glycan chains in PG are further modified by various degree of N-deacetylation of GlcNAc [23], O-acetylation of MurNAc [24] and attachment of teichoic acids on MurNAc [18].

1.1.2 Pneumococcal peptidoglycan synthesis

The synthesis of peptidoglycan starts in the cytoplasm and involves a cascade of enzymatic reactions. MurABCDEF sequentially add the amino acids that make up the pentapeptide attached to MurNAc. Then, the enzyme MraY transfers this complex to a transport lipid, creating lipid I. GlcNAc is added to lipid I by MurG, producing lipid II [25]. A complex made up of MurT and GatD adds an amide group to the α-carboxyl group of γ-D-Glutamine, creating iso-D-Glutamine, a modification essential for efficient cross-linking of the PG in *S. pneumoniae* [26]. Some of the lipid II precursors are branched by adding the dipeptide (L-Ala/L-Ser – L-Ala) to the ε amino group on L-Lys in position three on the pentapeptide [27, 28]. First, MurM adds an L-Alanine or L-Serine while MurN adds an L-Alanine. Lipid II is then flipped across the membrane by MurJ [29]. Outside the membrane, lipid II is polymerized by glycosyltransferases such as RodA, FtsW and class A PBPs (see section 1.1.3 and 1.1.4) transferring the disaccharide to the growing PG chain [3-5]. Glycan chains are then incorporated into the PG sacculus by transpeptidase reactions performed by PBPs.

1.1.3 The penicillin binding proteins

PBPs have a central role in PG synthesis. Pneumococci hold six PBPs, three class A PBPs (PBP1a, PBP1b, PBP2a) that harbor both transglycosylase and transpeptidase activity, two class B PBPs (PBP2b, PBP2x) that harbor only transpeptidase activity, and one low molecular weight PBP (PBP3) with DD-carboxylase activity. The transglycosylase activity of the PBPs is utilized to polymerase PG monomers into longer glycan chains, while the transpeptidase activity is vital for creating peptide cross links between the neighboring PG chains [1, 2]. As mentioned above, non-

crosslinked pentapeptides being part of the growing PG layer can be trimmed to tripeptides by the DD-carboxypeptidase PBP3 (removes D-Ala in position 5) and the L, D-carboxypeptidase LdcB (removes D-Ala in position 4) [30, 31]. Tripeptides have limited cross-linking opportunities (only ε amino group on lysine 3) and stem peptide trimming is thus believed to be important for regulating the amount of cross links in PG or to functioning as a marker distinguishing between new and old PG [30, 32].

The PG saculus in *S. pneumoniae* is formed by a combination of lateral and septal PG synthesis. There have been disagreements on whether there are two protein complexes (the divisome and the elongasome) producing septal and peripheral PG, or whether all proteins involved in PG synthesis are part of one larger complex. Based on cell morphology in depletion experiments and protein localization studies, cell elongation or septation appear to progress even if the other is compromised. Depletion of PBP2b results in cells compressed in the longitude axis leading to the conclusion that PBP2b is a part of the peripheral machinery known as the elongasome (Figure 3A) [33]. Depletion of PBP2x, on the other hand, results in elongated lemon shaped cells, indicating that this PBP is an essential part of the divisome (Figure 3B) [33]. Super-resolution microscopy techniques showing that PBP2x and PBP2b localize slightly different during the division process, suggest that there are two separate complexes at work [34, 35]. Also supporting this notion is the fact that inactivation or depletion of other assumed members of the elongasome (RodA, MreD, CozE and DivIVA) result in spherical cells, while cells depleted of the PBP2x partner FtsW and the deletion of GpsB (considered to be part of the divisome) results in elongated cells [36-38]. Based on the results discussed here, production of new PG in *S. pneumoniae* is carried out by two protein complexes henceforth referred to as the divisome and the elongasome.

The genes encoding bifunctional class A PBPs can be knocked out individually. It is also possible to obtain Δ*pbp1b*/Δ*pbp1a* and Δ*pbp1b*/Δ*pbp2a* double mutants. The combined deletion of *pbp1a* and *pbp2a* is lethal, indicating a functional redundancy between these two PBPs [39]. Vigouroux et al., 2019 show that class A PBPs are not important for maintaining cell shape during growth of *E. coli*, but rather repair damage in PG, and are required for structural integrity of the cell wall [42]. Recent studies indicate that the same is true in pneumococci: A study by Straume et al., 2020 shows that the class A PBPs most likely work independently of the elongasome and divisome, and that they process new and imperfect PG made by the divisome into mature PG [36]. It has been

shown that CozE is important for directing the activity of PBP1a to the division zone [40], while MacP is important for PBP2a activity in *S. pneumoniae* [41]. It is hence reasonable to believe that the class A PBPs might make up functional units important for PG remodeling and damage repair with dedicated protein partners that are important for positioning, timing, and activation [36, 42].

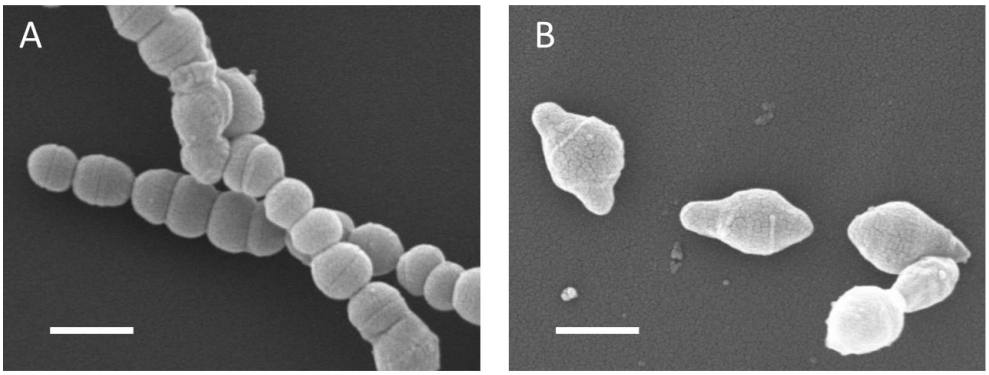

Figure 3. Pneumococcal cells depleted of A) PBP2b and B) PBP2x. When the level of PBP2b is critically low, the cells stop elongating and become compressed along the longitudinal axis. Limiting concentration of PBP2x on the other hand results in elongated cells without septum formation. Scale bars are 1 μm. Scanning electron microscopy image curtesy of Kari Helene Berg.

1.1.4 The monofunctional PBP2x and PBP2b work in concert with dedicated transglycosylases

The class A PBPs have been assumed to be the only proteins in charge of polymerizing the PG sacculus. Recent studies, on the other hand, point to the Shape Elongation Division and Sporulation (SEDS) proteins RodA and FtsW to be the main PG polymerizing enzymes working together with the monofunctional PBP2b and PBP2x. PBP2b/RodA and PBP2x/FtsW make up the core functional units of the elongasome and the divisome, respectively [3-5, 43]. Meeske et al., 2016 found that the Rod complex (the elongasome) in the rod-shaped *Bacillus subtilis* could function without the class A PBPs present, indicating that there is another enzyme with transglycosylase activity in the elongasome [4]. They reasoned that the same would be the case for the divisome. RodA and FtsW were found to be these unknown enzymes based on secondary structure homology. They also showed that RodA can promote polymerization of glycan strands *in vitro*.

The same conclusion was reached regarding RodA by Cho et al., 2016 through their studies on *E. coli* [3]. These results have been verified by findings proving that purified FtsW can function as a PG polymerase as long as it has a class B PBP interaction partner [5].

1.1.5 Teichoic acids

Pneumococci harbor two types of teichoic acids in their cell envelope. Wall teichoic acids (WTA), which make up 40 to 50% of the pneumococcal cell wall material [18], and lipoteichoic acids (LTA). The lack of WTA is severally harmful to cell growth, whereas a mutant unable to incorporate LTA is viable [44, 45]. The teichoic acids are important binding sites for a range of surface proteins and are important virulence factors helping the bacterial cells evade the host immune system [46, 47]. WTA and LTA are made up of identical structures, which are four to eight repeating units of a pseudo-pentasaccharide consisting of AATGal (2-acetamido-4-amino-2,4,6-trideoxy-D-galactose, a rare positively charged amino sugar), D-glucose, ribitol 5-phosphate, two N-acetyl-D-galactosaminyl residues, and one or two phosphocholine residues. WTA are attached to the cell wall through a phosphodiester bond to O6 of MurNAc in PG [48]. LTAs have a glycolipid anchor [47]. A rarity found tethering the pneumococcal LTA and WTA is phosphocholine residues. These are important anchors for choline binding proteins such as LytA, LytB, and CbpD. The amount of choline per pentasaccharide repeat is strain specific: R6 contains two choline residues per pentasaccharide repeat, while D39 and Rx1 usually contain one residue per repeat [47].

The genes encoding the proteins and enzymes that synthesize teichoic acids are clustered into three operons: lic1, lic2, and lic3. These operons hold genes encoding enzymes that produce the repeat units, proteins and enzymes for choline uptake and modification, phosphotransferases that couples phosphocholine to the teichoic acid repeat units, and a teichoic acid flippase [47, 49]. The flippase (TacF) is specific for teichoic acids that contain choline, making sure only correctly synthesized teichoic acids are flipped to the outside of the membrane [50].

1.2 Initiation and regulation of cell wall synthesis in *S. pneumoniae*

Dividing one bacterial cell into two daughter cells is a complicated process that requires coordination of several events, including chromosome segregation, cellular growth and cell wall synthesis. Expansion of the PG sacculus is instrumental for cell growth of dividing cells, and it is performed by the abovementioned PG synthesis machineries that insert new PG material into the existing PG layer. This involves both cleavage of bonds in the old PG and incorporation of new PG. The essentiality of the PG layer underlines the need for tight regulation of these protein complexes, for which mis-regulation often is lethal to the cells. In rod shaped bacteria, such as *B. subtilis* and *E. coli*, there are two PG synthesizing machineries. The elongasome is directed to the periphery of the cell by the actin homologue MreB, maintaining the elongated cell shape. The divisome is directed to midcell by the tubulin-like protein FtsZ that polymerizes into filaments with a directional movement called FtsZ treadmilling [35, 51]. The treadmilling was referred to as the Z-ring, but newer insights into movement dynamics show that FtsZ does not form a ring, but dynamic filaments that grow by adding FtsZ-GTP on the plus side and shedding FtsZ-GDP on the minus side [51]. This treadmilling drives PG synthesis in a constricting ring at the division zone that eventually divides one cell into two.

Pneumococci lack MreB, but regardless of this display both septal and peripheral PG synthesis. In *S. pneumoniae* FtsZ monomers assemble at the midcell defined by MapZ (also known as LocZ) in the early stages of cell division [52, 53]. The moving FtsZ filaments are anchored to the membrane through interactions with various proteins, including FtsA. The assembly of these early cell division proteins recruits the rest of the components belonging to the divisome and the elongasome. These include peptidoglycan polymerases, transpeptidases, regulatory and scaffolding proteins, and PG remodeling enzymes [54]. Rod shaped bacteria have the Min and nucleoid occlusion systems to ensure that FtsZ assembles the division machinery at midcell, and that both new daughter cells end up with one copy of the chromosome [55]. *S. pneumoniae* lacks homologues to both these systems. However, two independent studies by Fleurie et al., 2014 and Holečková et al., 2015 showed that the protein MapZ arrives at the division site before FtsZ. As the cells start to elongate, MapZ will split into two rings that move with peripheral PG synthesis towards the future division zones of the new daughter cells, while FtsZ stays behind at the current division site. At

later stages of the division process the FtsZ filaments splits into two and move towards MapZ at the future division sites [52, 53].

During the process of cell elongation and division in pneumococci, the divisome constructs the septal PG that eventually divides the cell into two new daughter cells, while the elongasome produces the peripheral PG, maintaining the slightly elongated shape of the pneumococci (Figure 4A and 4B). The activity of these two cell-wall synthesizing machineries are monitored and strictly regulated during the cell cycle. Although many proteins taking part in these PG synthesizing machineries are yet to be discovered, a selection of proteins is known to function in either the divisome or the elongasome. Proteins connected to the divisome are PBP2x, FtsZ, FtsA, FtsW, FtsE, FtsX, ZapA, ZapB, EzrA, GpsB, LytB (more details can be found in the following references [5, 35, 47, 56, 57]). Proteins considered to be part of the elongasome include MltG, RodZ, MreC, MreD, RodA, CozE, DivIVA, and PBP2b (for extensive details see references [10, 37, 40, 47, 58, 59]) (Figure 5). Additional proteins involved in PG synthesis are the class A PBPs which where until recently believed to be the main players in PG polymerization through their transglycosylation activity. Since RodA and FtsW have been assigned this function, class A PBPs probably have other supporting functions during cell division. As mentioned in section 1.1.3, the emerging view is that the class A PBPs fill in gaps left by the divisome and possibly the elongasome, maturing the PG to its final form [36, 42].

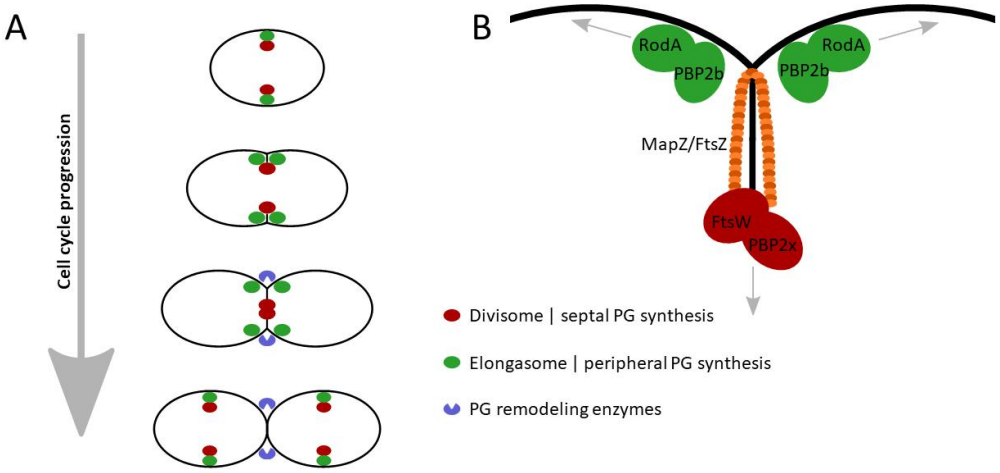

Figure 4. Simplified cartoon depicting pneumococcal cell division. A) Cell division in *S. pneumoniae* including the speculative positions of the elongasome, divisome, and PG remodeling enzymes throughout the cell cycle. B) A somewhat more detailed view of the placement of the elongasome and divisome during cell elongation and division.

1.2.1 Coordination of lateral and septal PG synthesis in *S. pneumoniae*

Key signals informing the bacterium at which stage of cell division it is in, and how these signals are relayed into activation and deactivation of the PG synthesis machineries have been sought for decades, however, proved difficult to identify. Hence, not much is known about the regulation of the PBPs and SEDS proteins regarding production of new PG. One study shows that the balance between MreC and MreD is important for complex formation between PBP2 (homolog to pneumococcal PBP2b) and RodA in *E. coli* [58]. According to this study, MreC can interact with PBP2 and have a positive effect on the complex formation between PBP2 and RodA based on conformational changes in PBP2. MreD has a negative effect on the complex formation [58]. What regulates the balance between MreC and MreD, however, is not known. Others have found that the complex formation between the homologues of PBP2b and RodA in *Thermus thermophilus* is essential for their activity. The complex between the two proteins can adopt several conformations representing the inactive form or promoting TG or TP activity. It is speculated that MreC might be involved in regulating the equilibrium between the different conformations [60]. As cell division is a conserved process, it is likely that a similar model is true for *S. pneumoniae*.

Two key proteins in control of cell division in *S. pneumoniae* are the kinase StkP and its cognate phosphatase PhpP. *stkP* and *phpP* form an operon, and StkP and PhpP are important for regulation of several cellular processes such as transformation, virulence and cell division [61]. StkP is a eukaryotic-type Ser/Thr kinase with an N-terminal intracellular kinase domain, a membrane spanning α-helix, and four extracellular penicillin-binding protein and Ser/Thr kinase-associated (PASTA) domains on the C-terminus [62]. The PASTA domains can bind peptidoglycan and are thought to sense external signals related to cell wall integrity and convey these to the inside of the cell [63]. This transfer of information happens through autophosphorylation. StkP then phosphorylates a selection of proteins of which some (MapZ, DivIVA, MacP, FtsZ, FtsA and MurC) are known to have a role in PG synthesis and cell division [41, 52, 53, 64-66]. PhpP, which is a cytoplasmic protein, modulates the activity of StkP by dephosphorylation of the StkP kinase domain and of StkP's protein targets [11, 14]. What decides the phosphorylation/ dephosphorylation balance between the two is not known. In the process of cell division, it is possible that StkP uses its extracellular PASTA domains to sense the state of the cell wall and then affect PG synthesis through phosphorylation of proteins involved in the process [11]. It has been shown that the PASTA domains of StkP respond to the thickness of the cell wall and the final separation of daughter cells via the PG hydrolase LytB [15]. Little is known about how the activities of the divisome and elongasome are coordinated, but StkP and its phosphorylation targets probably play a key role. More research is needed to unveil how these proteins regulate PG synthesis in *S. pneumoniae*.

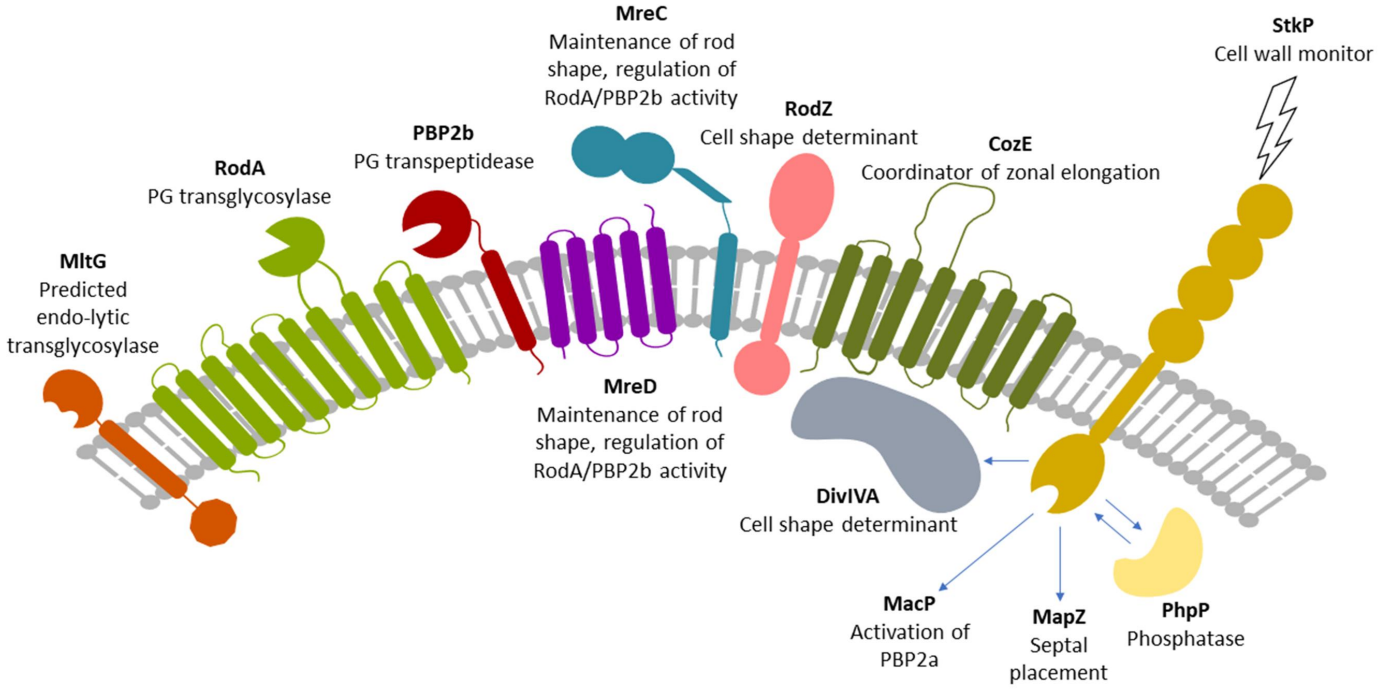

Figure 5 Overview of some of the proteins known to be part of the elongasome. Their functions/predicted functions are indicated [10, 37, 40, 47, 58]. StkP is also included as this kinase seems to be important in switching between septal and peripheral PG synthesis.

2. Aim of the study

When this work was initiated, there was little knowledge about how *S. pneumoniae* regulated its cell division, including the synthesis of new PG. The pneumococcus has two modes of PG synthesis, peripheral and septal. The peripheral synthesis is performed by the machinery known as the elongasome, while septal synthesis is carried out by the divisome. Together, the elongasome and the divisome are responsible for the ovococcal shape of the pneumococci. The regulation of division and elongation must therefore be timed perfectly in order to maintain cell shape. StkP, a Ser/Thr kinase, and its cognate phosphatase PhpP are considered to be key players in this regulation [11-15], but the how, when and where are still a mystery. This work has focused on discovering proteins that are important for the regulation of PG synthesis by exploiting pneumococci's ability to acquire mutations combined with whole genome sequencing. It was attempted to evoke suppressor mutations by deleting the genes encoding the essential PBP2b and PBP2x, core members of the elongasome and divisome, respectively. The identified suppressor mutants would be studied further to uncover the function of the proteins, resulting in new knowledge concerning the regulation of PG synthesis.

The hope is that in the future, what we know about regulation of PG synthesis can be utilized to develop new antimicrobial substances and strategies to fight the rising population of antibiotic resistant bacteria. Development of such compounds requires knowledge about essential cellular processes, such as PG synthesis.

3. Main results and discussion

3.1 Discovery of EloR as a regulator of cell elongation in *S. pneumoniae*

In paper I we performed an initial genetic screen to search for mutations that allowed survival without the essential PBP2b (elongasome) or PBP2x (divisome). Only suppressors surviving without PBP2b were obtained. Among the six suppressor mutants, three displayed mutations in the *mltG* gene, previously reported by Tsui et al., 2016. The three remaining suppressors had mutations in the *spr1851* gene resulting in truncated versions of the Spr1851 protein, rendering it nonfunctional. We discovered that in a Δ*spr1851* background, both *pbp2b* and *rodA* were no longer essential, indicating that in the absence of Spr1851, the pneumococci are no longer dependent upon cell elongation. We therefore hypothesized that this protein functions as a regulator of cell elongation. This was confirmed with morphology and cell shape distribution studies which showed that the Δ*spr1851* mutant grew in chains with cells that appeared shorter compared to the wild type cells. Based on these results, we named the protein EloR for elongasome regulating protein. A study published at the same time as our discovery confirmed the morphology in a Δ*spr1851* mutant [67]. The same study showed that over-expression of EloR resulted in elongated cells, a result that fits into our hypothesis about regulation of cell elongation.

EloR is a cytoplasmic protein made up of 328 amino acids distributed into three domains: An N-terminal Jag domain with unknown function and two RNA (possibly ssDNA) binding domains, KH-II and R3H, at the C-terminal end of the protein. The Jag domain is separated from the two RNA binding domains by a linker region (Figure 6). Proteins containing KH-II and R3H domains usually bind RNA to modulate gene expression [7, 8]. Interestingly, EloR is one of the phosphorylation targets of the key cell division regulator StkP (Ser/Thr kinase). Since EloR has been shown to be phosphorylated on threonine 89, close to its Jag domain, we wanted to investigate the effect of this phosphorylation with regards to cell elongation [64, 67].

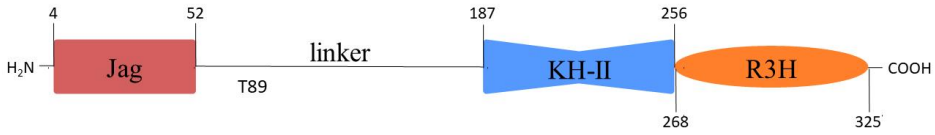

Figure 6. Schematic representation of EloR including predicted domain borders. EloR consists of a Jag domain of unknown function, a linker region with unknown structure and function containing the T89 phosphorylation target of StkP, and two ssRNA binding domains, KH-II and R3H.

3.2 Pneumococcal cell elongation requires the phosphorylated form of EloR

To test the effect of EloR phosphorylation, a phosphoablative version of EloR (EloR^{T89A}) was expressed in substitute of the wild type gene in *S. pneumoniae*. This resulted in cells with morphology and cell shape distribution similar to the Δ*eloR* knockout strain (length/width ratio of 1.65 ± 0.37 in the phosphoablative mutant and 1.56 ± 0.33 in the knockout mutant versus 1.91 ± 0.45 in the wild type strain). This experiment revealed two important features: (i) that StkP plays an important role in regulating the activity of EloR and thus cell elongation, and (ii) that the phosphorylated form of EloR is the elongasome stimulating form. Based on this, we hypothesize that EloR functions as a switch that activate cell elongation at the appropriate time during cell division in a phosphorylation dependent manner administered by StkP. It was then natural to test how the cells would respond to expressing a phosphomimetic form of EloR (EloR^{T89E}) with the assumption that this mutation would produce abnormally elongated cells. Surprisingly however, the EloR^{T89E} mutant proved to be even shorter than the phosphoablative mutant. Further investigations of several clones with the phosphomimicing mutation in EloR revealed that they had acquired truncation mutations in either the gene encoding MreC or the gene encoding RodZ. These are both considered to be part of the elongasome. It is likely that the stress of having a constitutively active elongasome, in the form of the phosphomimicing EloR, is alleviated by truncation of other elongasome genes, rendering the elongasome inactive. Similar mutations were found in strains where the nucleic acid binding properties of EloR domains KH-II and R3H were diminished. These results indicate that the non-phosphorylated form of EloR is the RNA-binding form, and that phosphorylation results in release of the bound nucleic acid.

In order to investigate the effect of the phosphomimicing form of EloR, we attempted to overexpress EloR^{T89E} ectopically from an inducible promoter (ComRS system [68]). The wild type gene was left untouched in this strain. When cells expressed EloR^{T89E} they appeared longer compared to the uninduced cells (unpublished data), a result consistent with our previous assumption that the phosphorylated form of EloR somehow stimulates cell elongation in *S. pneumoniae*. Zheng et al., 2017 showed that their phosphoablative (T89A) and phosphomimicing (T89E, T89D) forms of EloR did not affect cell morphology nor growth rate in their laboratory strain D39 [9]. The different results concerning the phosphorylation state of EloR in our R6 strain versus the D39 strain are difficult to explain but could be due to the accumulation of mutations found in the R6 strain [69]. Two such mutations are found in the gene encoding PBP1a, and may affect different aspects of PG synthesis, including the regulatory effect of EloR. Hopefully, these differences in genotype and phenotype in R6 and D39 can be exploited to elucidate the function and mode of action of EloR in the future.

We confirmed by immunoblotting that StkP phosphorylates EloR on T89 [64, 67] and that StkP requires its extracellular PASTA domains in order to do so. This was done by creating a series of strains with Flag-tagged EloR, perform immunoprecipitation with α-Flag antibodies on their cell lysates, and analyzing the precipitate using antibodies against the Flag-tag and phosphothreonine. The immunoprecipitation showed that Flag-EloR is indeed phosphorylated, on two positions in the protein. One phosphorylation site was lost in the phosphoablative strain, confirming that T89 is one of the two sites. Recently it was published that the second phosphorylation site is on threonine 126 [70]. Both phosphorylation sites are found in the linker region of EloR. By either deleting StkP, introducing a kinase dead StkP or removing the extracellular PASTA domains of StkP, phosphorylation on both phosphorylation sites in EloR was lost, proving that StkP requires its PASTA domains for EloR phosphorylation. This led us to the conclusion that StkP senses the status of the cell wall, for example the thickness [15] or other factors that indicate how far along the cell cycle the bacterium has progressed, and phosphorylates EloR at the appropriate time. StkP and its cognate phosphatase PhpP work in unison in *S. pneumoniae* to control several cellular processes, including cell division. PhpP has been shown to dephosphorylate EloR in strain Rx1 [67]. The balance between StkP and PhpP probably allows for fine tuning of the activity of EloR, ensuring that cell elongation is timed perfectly. The function of the second phosphorylation site is unknown to us. It might be related to an alternative pathway regulated by EloR, or perhaps it is

involved in fine-tuning EloR activity. We also introduced a C-terminally truncated MreC (MreC-T) version that was discovered when creating the phosphomimicing form of EloR and performed immunoprecipitation on the lysate of this strain (Flag-EloR, MreC-T). The result showed that a larger fraction of EloR is phosphorylated in this strain compared to the wild type strain. This might be a response to the inactivation of MreC where the cell tries to compensate for a compromised elongasome by activating more of the cellular EloR.

3.3 EloR and KhpA make up a complex that regulates cell elongation in pneumococci

A parallel study on EloR showed that the protein immunoprecipitated with a small (8.9 kDa) protein called KhpA [9]. KhpA is a cytosolic RNA binding protein consisting of only a KH-II domain. A Δ*khpA* mutant phenocopies a Δ*eloR* mutant in that the essential *pbp2b* and *rodA* genes can be deleted and the cells display a shortened morphology [9]. In paper II we exploited information from 3D modeling with site-specific point mutations and protein cross-linking to show that KhpA interacts with itself and with EloR, more specifically with the KH-II domain of EloR. As the target sequences of KH-II domains are typically short (4 nucleotides), it is reasonable to believe that in order to increase their specificity, EloR and KhpA form a complex allowing recognition of longer or multiple sequences. Next, we wanted to identify amino acid residues important for the EloR – KhpA interaction. The predicted 3D-structure of the KH-II domain of KhpA came out as expected for KH-II domains, typically three α-helices packed against a three-stranded β-sheet (α-β-β-α-α-β). The online tool ZDOCK [71] was used in order to predict the interaction surface in a KhpA homodimer. The model predicted that the α3-helices of two KhpA proteins interact antiparallel with each other. Based on this model we chose to change amino acid residues (R53K, R59K, T60Q and I61F) that were likely to be important for said interaction. When these mutated KhpA versions were employed in bacterial two hybrid (BACTH) assays, the I61F mutant stood out to be crucial for the KhpA self-interaction. A phenylalanine in position 61 abolished the interaction between KhpA proteins but kept the interaction in an EloR/KhpA complex. It was reasoned that a bulky but more polar amino acid than phenylalanine in position 61 in KhpA could prevent both self-interaction and EloR/KhpA complex formation. This was confirmed by substitution of I61 with a tyrosine. The amino acid residue corresponding to KhpA's

I61 in the KH-II domain of EloR is L239. Introduction of the mutation L239Y also eliminated the EloR/KhpA interaction. In order to prove that I61 (KhpA) and L239 (EloR) are directly involved in interactions between the two proteins, we made a *S. pneumoniae* strain expressing Flag-EloR^{L239C} and KhpA^{I61C}. We deduced that if the two amino acids are indeed involved in direct interaction in the EloR/KhpA complex, a cysteine-bridge would form between the two proteins. If this was the case, a size shift corresponding to the size of KhpA would be seen in an immunoblot when detecting Flag-EloR under nonreducing conditions. The size shift occurred, and we could conclude that EloR and KhpA physically interact.

It was already known that EloR and KhpA localize to the division zone of streptococci [9, 72]. Investigations in paper II showed that KhpA is dependent upon EloR in order to localize at midcell. In instances where KhpA could no longer self-interact but kept its ability to form a complex with EloR (KhpA^{I61F}), localization of KhpA was not affected. When EloR was knocked out or the complex formation between EloR and KhpA was disturbed (KhpA^{I61Y} or EloR^{L239Y}), on the other hand, KhpA-sfGFP was no longer concentrated in the division zone of the cell. In the EloR^{L239Y} background, KhpA could still self-interact and KhpA-sfGFP was observed throughout the cytosol of the cells. This indicates that this form of KhpA might have another function in the cell that is not important for the EloR-pathway. The *khpA* gene shares an operon with a gene encoding the ribosomal S16 protein RpsP, which is an essential component of the 30S ribosomal unit [73]. Curiously, this co-expression seems to be conserved in many Gram-positive bacteria (*Streptococcus*, *Lactococcus*, *Enterococcus*, *Bacillus* and *Lactobacillus*). One possible function of self-interacting KhpA could thus be that the complex is involved with ribosomal function through protein – protein interactions or perhaps through binding to rRNA or mRNA protruding from the ribosome. This may affect the translation rate of specific mRNAs. Confirmation of such a function for KhpA requires further investigations.

Homologs of EloR and KhpA are widespread among Gram-positive bacteria, and are found in genera such as Streptococcus, Bacillus, Clostridium, Listeria, Enterococcus, Lactobacillus and Lactococcus. It is interesting that we find both EloR and KhpA in several rod shaped species (Bacilli, Clostridia, Listeria and Lactobacilli) considering that elongation in these bacteria depends on the actin like protein MreB shown to direct the synthesis of new peptidoglycan along the cell length axis, while elongation in Streptococci, Enterococci or Lactococci is MreB independent [74].

During the course of this work Myrbråten and co-workers showed that depletion of EloR/KhpA in the rod-shaped *Lactobacillus plantarum* significantly reduced the cell length [75]. In sum, this shows that EloR/KhpA is a conserved pathway regulating cell elongation in many Gram-positive bacteria including MreB-dependent rods.

3.4 The essential PBP2b becomes expendable when the EloR/KhpA interaction is broken

Since there is a direct interaction between EloR and KhpA, we hypothesized that the reason a Δ*khpA* mutant phenocopies a Δ*eloR* mutant is because the EloR/KhpA complex works as one functional unit, and that the elongasome becomes redundant when the EloR-KhpA interaction is disrupted. In order to verify this, we investigated the strains expressing $KhpA^{I61F}$ and $KhpA^{I61Y}$ with respect to morphology and cell shape distribution. Our hypothesis was confirmed: in a background where KhpA can no longer self-interact but is still able to interact with EloR ($KhpA^{I61F}$), the cell morphology and cell shape distribution were similar to wild type cells. In a background where the EloR/KhpA complex can no longer form ($KhpA^{I61Y}$ or $EloR^{L239Y}$), on the other hand, morphology and cell shape distribution were similar to the Δ*khpA* and Δ*eloR* mutants. We also found that in cells where the EloR/KhpA complex cannot form, the essential elongasome proteins PBP2b and RodA are no longer essential, indicating that elongasome activity is no longer necessary. The loss of complex formation between KhpA and EloR leads to reduced elongation, most likely due to loss of RNA binding. As concluded previously, phosphorylation of EloR in a wild type background probably leads to RNA release, stimulating cell elongation. When the ability to bind RNA is abolished by site directed mutations, elongation will be continuously stimulated. This is likely not tolerated in *S. pneumoniae* and the reduced elongation that follows additional suppressor mutations (*rodZ* and *mreC*) allows for deletion of *pbp2b* and *rodA*. Why then is a Δ*khpA* mutant viable without suppressor mutations? The RNA binding is abolished (i.e. stimulation of elongation), but cells become shorter. This is a paradox that we at present do not understand.

The reason *pbp2b* and *rodA* are essential in wild type cells may be that without these, other elongasome proteins are not regulated properly and elongation becomes uncontrolled, leading to cell death. In a Δ*eloR* and Δ*khpA* mutant this effect of the elongasome is somehow alleviated. The

mechanism behind this is unknown, but we have previously speculated that the lytic transglycosylase MltG is involved and that it might be the uncontrolled actions of MltG that is lethal to the cell [72]. This is discussed in the next section.

3.5 The KhpA/EloR complex interacts with MltG at the septal region

In paper I and II we show that EloR is found at midcell were it co-localize with FtsZ during cell division. In the work presented in paper III we sought to reveal what part of EloR directs it to the division zone. The Jag domain of EloR is connected to the two RNA binding domains KH-II and R3H via a linker region with an unknown function and structure (Figure 1). In paper III, we used fluorescent imaging to look at cells expressing the Jag and linker domains of EloR fused with mKate. This revealed that the Jag domain is essential for the protein's localization to the division zone. In order to find the interaction partner facilitating this midcell localization, we screened our BACTH library, looking for positive hits. One such match was MltG, a protein shown to be part of the elongasome [10]. MltG consists of a cytosolic domain, a membrane spanning α-helix, and an extracellular lytic transglycosylase domain. The protein has homology to *E. coli* MltG and is thus predicted to be an endolytic murein transglycosylase [10]. BACTH assays and co-IP showed that EloR does indeed interact with MltG, more specifically with the cytosolic domain of MltG. The *mltG* gene is essential under wild type conditions, but suppressor mutations in *mltG* allows for the removal of *pbp2b* and *rodA*. The current hypothesis is that deletion of *pbp2b* or *rodA* results in a situation where the muralytic activity of MltG becomes lethal to the cells, but that this is alleviated in mutants with compromised EloR/KhpA function. The idea is that EloR/KhpA has a regulatory role on the MltG activity. No definitive evidence has been published about what the function of MltG is. It has been hypothesized that MltG releases glycan strands polymerized by PBP1a for crosslinking by RodA/PBP2b in order to terminate glycan chain elongation [10]. Another possibility is that MltG opens the peripheral PG meshwork to allow new material to be incorporated by RodA/PBP2b. This function must be tightly regulated – if MltG were able to open the PG layer at will, the layer would quickly be weakened, and cell lysis would occur. MltG activity seems to be lethal without RodA/PBP2b present and *vice versa*, maybe because this complex is necessary for filling in the gaps that MltG makes. Based on the results discussed above, we propose

a model where MltG opens the PG layer for insertion of new PG by RodA/PBP2b. StkP/EloR/KhpA are involved in tight regulation of this process (Figure 7).

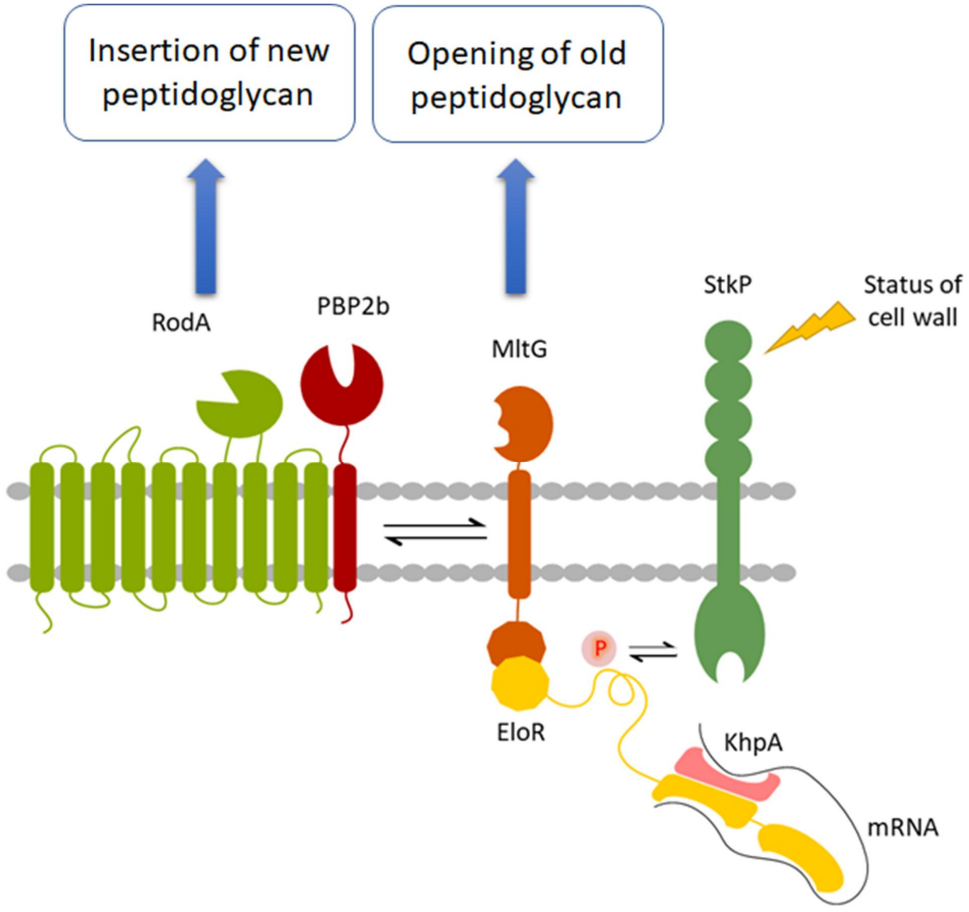

Figure 7. Simplified model for the actions of EloR, KhpA and MltG. StkP senses the status of the cell wall and stimulates EloR through phosphorylation. MltG is stimulated to open the PG layer in order for RodA/PBP2b to insert new PG material which elongates the cells.

4. Concluding remarks

A significant question during our research into EloR and KhpA has been whether or not they act in the same pathway. The fact that they co-precipitate [9] and that a Δ*khpA* mutant phenocopies a Δ*eloR* mutant strongly indicate that EloR and KhpA are part of the same functional unit. In this work we also demonstrated that they interact directly with each other via their KH-II domains and that this interaction is crucial for the pneumococcus to elongate properly. This represents conclusive evidence that EloR and KhpA work through the same pathway. Taking into account that the elongasome is dispensable (*pbp2b* and *rodA* can be deleted) under conditions where the EloR/KhpA complex cannot form, i.e. deletion of either genes or disrupting their protein interaction, it is reasonable to believe that the EloR/KhpA complex has a regulatory role in elongasome function. Since the EloR activity depends on phosphorylation by StkP, a kinase known to take part in the control of cell division and cell elongation through phosphorylation of a range of different protein targets, we believe EloR/KhpA is part of a regulatory pathway, that under the command of StkP sets the timing point when the pneumococcal cell should elongate or not during cell division. Considering that both EloR and KhpA harbor RNA binding domains typically found in proteins that have a regulatory role in transcription or post-transcription, a probable scenario is that the EloR/KhpA/MltG complex controls the expression of one or several elongasome proteins by binding/releasing RNA(s) and hence inhibiting/promoting expression of specific protein(s). When EloR is phosphorylated by StkP, the complex releases its bound target, and cell elongation can proceed. To the best of my knowledge, the EloR/KhpA-pathway represents the first line of evidence directly linking RNA-binding proteins with regulation of cell cycle progression in Gram-positive bacteria. Identification of the RNA binding targets of EloR/KhpA will be crucial to solve this puzzle.

5. References

1. Zapun, A., T. Vernet, and M.G. Pinho, *The different shapes of cocci.* FEMS microbiology reviews, 2008. **32**(2): p. 345-360.
2. Sauvage, E., et al., *The penicillin-binding proteins: structure and role in peptidoglycan biosynthesis.* FEMS microbiology reviews, 2008. **32**(2): p. 234-258.
3. Cho, H., et al., *Bacterial cell wall biogenesis is mediated by SEDS and PBP polymerase families functioning semi-autonomously.* Nature microbiology, 2016. **1**: p. 16172.
4. Meeske, A.J., et al., *SEDS proteins are a widespread family of bacterial cell wall polymerases.* Nature, 2016.
5. Taguchi, A., et al., *FtsW is a peptidoglycan polymerase that is functional only in complex with its cognate penicillin-binding protein.* Nature microbiology, 2019: p. 1.
6. Grishin, N.V., *KH domain: one motif, two folds.* Nucleic acids research, 2001. **29**(3): p. 638-643.
7. Grishin, N.V.J.T.i.b.s., *The R3H motif: a domain that binds single-stranded nucleic acids.* 1998. **23**(9): p. 329-330.
8. Valverde, R., L. Edwards, and L.J.T.F.j. Regan, *Structure and function of KH domains.* 2008. **275**(11): p. 2712-2726.
9. Zheng, J.J., et al., *Absence of the KhpA and KhpB (JAG/EloR) RNA-binding proteins suppresses the requirement for PBP2b by overproduction of FtsA in* Streptococcus pneumoniae *D39.* Molecular microbiology, 2017. **106**(5): p. 793-814.
10. Tsui, H.C.T., et al., *Suppression of a deletion mutation in the gene encoding essential PBP2b reveals a new lytic transglycosylase involved in peripheral peptidoglycan synthesis in* Streptococcus pneumoniae *D39.* 2016. **100**(6): p. 1039-1065.
11. Beilharz, K., et al., *Control of cell division in* Streptococcus pneumoniae *by the conserved Ser/Thr protein kinase StkP.* Proceedings of the National Academy of Sciences, 2012. **109**(15): p. E905-E913.
12. Fleurie, A., et al., *Mutational dissection of the S/T-kinase StkP reveals crucial roles in cell division of* Streptococcus pneumoniae*.* 2012. **83**(4): p. 746-758.
13. Fleurie, A., et al., *Interplay of the serine/threonine-kinase StkP and the paralogs DivIVA and GpsB in pneumococcal cell elongation and division.* 2014. **10**(4): p. e1004275.
14. Osaki, M., et al., *The StkP/PhpP signaling couple in* Streptococcus pneumoniae*: cellular organization and physiological characterization.* 2009. **191**(15): p. 4943-4950.
15. Zucchini, L., et al., *PASTA repeats of the protein kinase StkP interconnect cell constriction and separation of* Streptococcus pneumoniae*.* Nature microbiology, 2017.
16. Henriques-Normark, B. and E.I. Tuomanen, *The pneumococcus: epidemiology, microbiology, and pathogenesis.* Cold Spring Harbor perspectives in medicine, 2013. **3**(7): p. a010215.
17. Frieden, T., *ANTIBIOTIC RESISTANCE THREATS in the United States.* 2013.
18. Bui, N.K., et al., *Isolation and analysis of cell wall components from* Streptococcus pneumoniae*.* Analytical biochemistry, 2012. **421**(2): p. 657-666.
19. Harz, H., K. Burgdorf, and J.-V. Höltje, *Isolation and separation of the glycan strands from murein of* Escherichia coli *by reversed-phase high-performance liquid chromatography.* Analytical biochemistry, 1990. **190**(1): p. 120-128.
20. Boneca, I.G., et al., *Characterization of* Staphylococcus aureus *cell wall glycan strands, evidence for a new β-N-acetylglucosaminidase activity.* Journal of Biological Chemistry, 2000. **275**(14): p. 9910-9918.

21. Hoyland, C.N., et al., *Structure of the LdcB LD-carboxypeptidase reveals the molecular basis of peptidoglycan recognition.* 2014. **22**(7): p. 949-960.
22. Vollmer, W., D. Blanot, and M.A. De Pedro, *Peptidoglycan structure and architecture.* FEMS microbiology reviews, 2008. **32**(2): p. 149-167.
23. Vollmer, W. and A.J.J.o.B.C. Tomasz, *The* pgdA *gene encodes for a peptidoglycan N-acetylglucosamine deacetylase in* Streptococcus pneumoniae. 2000. **275**(27): p. 20496-20501.
24. Crisóstomo, M.I., et al., *Attenuation of penicillin resistance in a peptidoglycan O-acetyl transferase mutant of* Streptococcus pneumoniae. 2006. **61**(6): p. 1497-1509.
25. Typas, A., et al., *From the regulation of peptidoglycan synthesis to bacterial growth and morphology.* Nature Reviews Microbiology, 2012. **10**(2): p. 123.
26. Zapun, A., et al., *In vitro reconstitution of peptidoglycan assembly from the Gram-positive pathogen* Streptococcus pneumoniae. 2013. **8**(12): p. 2688-2696.
27. Filipe, S.R., M.G. Pinho, and A. Tomasz, *Characterization of the murMN operon involved in the synthesis of branched peptidoglycan peptides* in Streptococcus pneumoniae. Journal of Biological Chemistry, 2000. **275**(36): p. 27768-27774.
28. Filipe, S.R. and A.J.P.o.t.N.A.o.S. Tomasz, *Inhibition of the expression of penicillin resistance in* Streptococcus pneumoniae *by inactivation of cell wall muropeptide branching genes.* 2000. **97**(9): p. 4891-4896.
29. Sham, L.-T., et al., *MurJ is the flippase of lipid-linked precursors for peptidoglycan biogenesis.* 2014. **345**(6193): p. 220-222.
30. Hakenbeck, R. and M. Kohiyama, *Purification of Penicillin-Binding Protein 3 from* Streptococcus pneumoniae. The FEBS Journal, 1982. **127**(2): p. 231-236.
31. Barendt, S.M., L.-T. Sham, and M.E.J.J.o.b. Winkler, *Characterization of mutants deficient in the L, D-carboxypeptidase (DacB) and WalRK (VicRK) regulon, involved in peptidoglycan maturation of* Streptococcus pneumoniae *serotype 2 strain D39.* 2011. **193**(9): p. 2290-2300.
32. Abdullah, M.R., et al., *Structure of the pneumococcal l, d-carboxypeptidase DacB and pathophysiological effects of disabled cell wall hydrolases DacA and DacB.* 2014. **93**(6): p. 1183-1206.
33. Berg, K.H., et al., *Effects of low PBP2b levels on cell morphology and peptidoglycan composition in* Streptococcus pneumoniae *R6.* Journal of bacteriology, 2013. **195**(19): p. 4342-4354.
34. Tsui, H.C.T., et al., *Pbp2x localizes separately from Pbp2b and other peptidoglycan synthesis proteins during later stages of cell division of* Streptococcus pneumoniae *D39.* Molecular microbiology, 2014. **94**(1): p. 21-40.
35. Perez, A.J., et al., *Movement dynamics of divisome proteins and PBP2x: FtsW in cells of* Streptococcus pneumoniae. Proceedings of the National Academy of Sciences, 2019. **116**(8): p. 3211-3220.
36. Straume, D., et al., *Class A PBPs have a distinct and unique role in the construction of the pneumococcal cell wall.* 2020. **117**(11): p. 6129-6138.
37. Straume, D., et al., *Identification of pneumococcal proteins that are functionally linked to penicillin-binding protein 2b (PBP2b).* Molecular microbiology, 2017. **103**(1): p. 99-116.
38. Land, A.D., et al., *Requirement of essential P bp2x and GpsB for septal ring closure in* Streptococcus pneumoniae *D 39.* 2013. **90**(5): p. 939-955.
39. Paik, J., et al., *Mutational analysis of the* Streptococcus pneumoniae *bimodular class A penicillin-binding proteins.* Journal of bacteriology, 1999. **181**(12): p. 3852-3856.
40. Fenton, A.K., et al., *Erratum: CozE is a member of the MreCD complex that directs cell elongation in* Streptococcus pneumoniae. 2017. **2**(3): p. 17011.
41. Fenton, A.K., et al., *Phosphorylation-dependent activation of the cell wall synthase PBP2a in* Streptococcus pneumoniae *by MacP.* 2018. **115**(11): p. 2812-2817.

42. Vigouroux, A., et al., *Cell-wall synthases contribute to bacterial cell-envelope integrity by actively repairing defects.* 2019: p. 763508.
43. Emami, K., et al., *RodA as the missing glycosyltransferase in* Bacillus subtilis *and antibiotic discovery for the peptidoglycan polymerase pathway.* Nature microbiology, 2017. **2**: p. 16253.
44. Heß, N., et al., *Lipoteichoic acid deficiency permits normal growth but impairs virulence of* Streptococcus pneumoniae. 2017. **8**(1): p. 1-13.
45. Morona, J.K., R. Morona, and J.C.J.P.o.t.N.A.o.S. Paton, *Attachment of capsular polysaccharide to the cell wall of* Streptococcus pneumoniae *type 2 is required for invasive disease.* 2006. **103**(22): p. 8505-8510.
46. Gehre, F., et al., *Role of teichoic acid choline moieties in the virulence of* Streptococcus pneumoniae. 2009. **77**(7): p. 2824-2831.
47. Vollmer, W., O. Massidda, and A. Tomasz, *The Cell Wall of* Streptococcus pneumoniae. Microbiology spectrum, 2019. **7**(3).
48. Liu, T.-Y. and E.C. Gotschlich, *Muramic acid phosphate as a component of the mucopeptide of Gram-positive bacteria.* Journal of Biological Chemistry, 1967. **242**(3): p. 471-476.
49. Baur, S., et al., *Synthesis of CDP-activated ribitol for teichoic acid precursors in* Streptococcus pneumoniae. 2009. **191**(4): p. 1200-1210.
50. Damjanovic, M., et al., *The essential* tacF *gene is responsible for the choline-dependent growth phenotype of* Streptococcus pneumoniae. Journal of bacteriology, 2007. **189**(19): p. 7105-7111.
51. Bisson-Filho, A.W., et al., *Treadmilling by FtsZ filaments drives peptidoglycan synthesis and bacterial cell division.* 2017. **355**(6326): p. 739-743.
52. Fleurie, A., et al., *MapZ marks the division sites and positions FtsZ rings in* Streptococcus pneumoniae. Nature, 2014. **516**(7530): p. 259-262.
53. Holečková, N., et al., *LocZ is a new cell division protein involved in proper septum placement in* Streptococcus pneumoniae. 2015. **6**(1): p. e01700-14.
54. Massidda, O., L. Nováková, and W. Vollmer, *From models to pathogens: how much have we learned about* Streptococcus pneumoniae *cell division?* Environmental microbiology, 2013. **15**(12): p. 3133-3157.
55. Pinho, M.G., M. Kjos, and J.-W.J.N.r.m. Veening, *How to get (a) round: mechanisms controlling growth and division of coccoid bacteria.* 2013. **11**(9): p. 601.
56. Sham, L.-T., et al., *Recent advances in pneumococcal peptidoglycan biosynthesis suggest new vaccine and antimicrobial targets.* Current opinion in microbiology, 2012. **15**(2): p. 194-203.
57. Reichmann, N.T., et al., *SEDS–bPBP pairs direct lateral and septal peptidoglycan synthesis in* Staphylococcus aureus. 2019: p. 1.
58. Liu, X., et al., *MreC and MreD balance the interaction between the elongasome proteins PBP2 and RodA.* 2019: p. 769984.
59. Alyahya, S.A., et al., *RodZ, a component of the bacterial core morphogenic apparatus.* 2009. **106**(4): p. 1239-1244.
60. Sjodt, M., et al., *Structural coordination of polymerization and crosslinking by a SEDS–bPBP peptidoglycan synthase complex.* 2020: p. 1-8.
61. Pallová, P., et al., *A eukaryotic-type serine/threonine protein kinase StkP of* Streptococcus pneumoniae *acts as a dimer in vivo.* 2007. **355**(2): p. 526-530.
62. Novakova, L., et al., *Characterization of a eukaryotic type serine/threonine protein kinase and protein phosphatase of* Streptococcus pneumoniae *and identification of kinase substrates.* 2005. **272**(5): p. 1243-1254.
63. Jones, G. and P. Dyson, *Evolution of Transmembrane Protein Kinases Implicated in Coordinating Remodeling of Gram-Positive Peptidoglycan: Inside versus Outside.* 2006. **188**(21): p. 7470-7476.

64. Sun, X., et al., *Phosphoproteomic analysis reveals the multiple roles of phosphorylation in pathogenic bacterium* Streptococcus pneumoniae. 2009. **9**(1): p. 275-282.
65. Nováková, L., et al., *Identification of multiple substrates of the StkP Ser/Thr protein kinase in* Streptococcus pneumoniae. 2010. **192**(14): p. 3629-3638.
66. Falk, S.P. and B.J.F.m.l. Weisblum, *Phosphorylation of the* Streptococcus pneumoniae *cell wall biosynthesis enzyme MurC by a eukaryotic-like Ser/Thr kinase.* 2013. **340**(1): p. 19-23.
67. Ulrych, A., et al., *Characterization of pneumococcal Ser/Thr protein phosphatase* phpP *mutant and identification of a novel PhpP substrate, putative RNA binding protein Jag.* 2016. **16**(1): p. 247.
68. Berg, K.H., et al., *Peptide-regulated gene depletion system developed for use* in Streptococcus pneumoniae. Journal of bacteriology, 2011. **193**(19): p. 5207-5215.
69. Lanie, J.A., et al., *Genome sequence of Avery's virulent serotype 2 strain D39 of* Streptococcus pneumoniae *and comparison with that of unencapsulated laboratory strain R6.* 2007. **189**(1): p. 38-51.
70. Hirschfeld, C., et al., *Proteomic Investigation Uncovers Potential Targets and Target Sites of Pneumococcal Serine-Threonine Kinase StkP and Phosphatase PhpP.* 2019. **10**.
71. Pierce, B.G., et al., *ZDOCK server: interactive docking prediction of protein–protein complexes and symmetric multimers.* Bioinformatics, 2014. **30**(12): p. 1771-1773.
72. Stamsås, G.A., et al., *Identification of EloR (Spr1851) as a regulator of cell elongation in* Streptococcus pneumoniae. Molecular microbiology, 2017. **105**(6): p. 954-967.
73. Oberto, J., et al., *The* Escherichia coli *ribosomal protein S16 is an endonuclease.* 1996. **19**(6): p. 1319-1330.
74. Busiek, K.K. and W.J.C.B. Margolin, *Bacterial actin and tubulin homologs in cell growth and division.* 2015. **25**(6): p. R243-R254.
75. Myrbråten, I.S., et al., *CRISPR Interference for Rapid Knockdown of Essential Cell Cycle Genes in* Lactobacillus plantarum. 2019. **4**(2): p. e00007-19.

PAPER I

Identification of EloR (Spr1851) as a regulator of cell elongation in *Streptococcus pneumoniae*

Gro Anita Stamsås, Daniel Straume,
Anja Ruud Winther, Morten Kjos,
Cyril Alexander Frantzen and
Leiv Sigve Håvarstein
Faculty of Chemistry, Biotechnology and Food Science,
Norwegian University of Life Sciences, NO-1432, Ås,
Norway.

DOI: https://doi.org/10.1111/mmi.13748

Summary

In a screen for mutations suppressing the lethal loss of PBP2b in *Streptococcus pneumoniae* we identified Spr1851 (named EloR), a cytoplasmic protein of unknown function whose inactivation removed the requirement for PBP2b as well as RodA. It follows from this that EloR and the two elongasome proteins must be part of the same functional network. This network also includes StkP, as this serine/threonine kinase phosphorylates EloR on threonine 89 (T89). We found that Δ*eloR* cells, and cells expressing the phosphoablative form of EloR ($EloR^{T89A}$), are significantly shorter than wild-type cells. Furthermore, the phosphomimetic form of EloR ($EloR^{T89E}$) is not tolerated unless the cell in addition acquires a truncated MreC or non-functional RodZ protein. By itself, truncation of MreC as well as inactivation of RodZ gives rise to less elongated cells, demonstrating that the stress exerted by the phosphomimetic form of EloR is relieved by suppressor mutations that reduce or abolish the activity of the elongasome. Of note, it was also found that loss of elongasome activity caused by truncation of MreC elicits increased StkP mediated phosphorylation of EloR. Together, the results support a model in which phosphorylation of EloR stimulates cell elongation, while dephosphorylation has an inhibitory effect.

Introduction

The shape of bacteria depends on the shape of their peptidoglycan sacculus. Pneumococci, which are not true cocci, have an ellipsoidal shape that results from a combination of septal and lateral peptidoglycan synthesis. The septal cross-wall is synthesized by the divisome, while peripheral cell wall elongation is carried out by the elongasome. It is not known whether pneumococcal cells alternate between septal and lateral peptidoglycan synthesis, or if these processes take place simultaneously. Whatever the case, both activities must be strictly regulated and coordinated (Zapun *et al*., 2008; Philippe *et al.*, 2014).

The peptidoglycan sacculus consists of glycan chains of alternating β-1–4-linked N-acetylmuramic acid and N-acetylglucosamine cross-linked by short peptides (Vollmer *et al.*, 2008). The synthesis of this gigantic macromolecule involves the penicillin-binding proteins (PBPs). Pneumococci produce six different PBPs: three class A PBPs (PBP1a, PBP1b and PBP2a), two class B PBPs (PBP2x and PBP2b), and the D,D-carboxypeptidase PBP3. Class A PBPs are bifunctional, that is, they catalyze both polymerization of glycan chains (transglycosylation) and cross-linking of stem peptides (transpeptidation) during peptidoglycan synthesis. Class B PBPs, on the other hand, are monofunctional transpeptidases that catalyze the formation of peptide cross-links between adjacent glycan strands (Sauvage *et al.*, 2008; Zapun *et al.*, 2008). PBP3 removes the terminal D-alanine from the pentapeptide side chain, presumably to control the extent of peptidoglycan cross-linking (Hakenbeck and Kohiyama, 1982). The class A enzymes are individually dispensible, but a PBP1a/PBP2a double deletion is lethal. In contrast, PBP2x and PBP2b, which are key component of the divisome and elongasome, respectively, are both essential (Kell *et al*., 1993; Berg *et al.*, 2013). Another essential key member of the

elongasome, RodA, was recently identified as a peptidoglycan polymerase (Meeske *et al*., 2016). Thus, RodA and PBP2b work together to synthesize the new wall material that is inserted into the lateral cell-wall during cell elongation. In addition to PBP2b and RodA, MreC, MreD, DivIVA, RodZ and CozE have been identified as important for the normal function of the pneumococcal elongasome (Alyahya *et al*., 2009; Land and Winkler, 2011; Massidda *et al*., 2013; Philippe *et al*., 2014; Fenton *et al*., 2016; Straume *et al*., 2017).

Several studies have reported that the eukaryotic-type Ser/Thr protein kinase, StkP, is a key regulator of pneumococcal cell-wall synthesis and cell division (Beilharz *et al*., 2012; Fleurie *et al*., 2012; Morlot *et al*., 2013; Fleurie *et al*., 2014b; Manuse *et al*., 2016). Deletion of StkP results in morphological alterations, increased susceptibility to environmental stresses and reduced virulence and transformability (Echenique *et al*., 2004; Beilharz *et al*., 2012; Fleurie *et al*., 2012). StkP is a bitopic membrane protein. The extracellular part consists of four PASTA domains, while the intracellular part is composed of a flexible approximately 65 amino acid juxtamembrane domain of unknown function and a kinase domain (Morlot *et al*., 2013; Manuse *et al*., 2016). Presumably, the PASTA domains detect specific external signals, which are relayed to intracellular effector proteins through activation of the kinase domain. PASTA domains have been shown to bind peptidoglycan fragments and β-lactams (Shah *et al*., 2008; Maestro *et al*., 2011; Mir *et al*., 2011). It is, therefore, possible that the PASTA domains of StkP modulate its kinase activity by recognizing specific substructures in the peptidoglycan layer. Moreover, very recently, compelling evidence that the cell wall precursor lipid II acts as signal for StkP have been reported (Hardt *et al*., 2017). The PASTA domains are also responsible for targeting StkP to the septal region, perhaps by recognizing unlinked peptidoglycan (Beilharz *et al*., 2012; Manuse *et al*., 2016; Grangeasse, 2016). *stkP* is co-transcribed with the phosphatase *phpP*, which specifically dephosphorylates StkP and StkP target proteins. Hence, the two enzymes operate as a functional couple (Novakova *et al*., 2005; Ulrych *et al*., 2016).

To fully understand the biological role of StkP, the phosphorylation targets of StkP must be identified and their functions characterized. StkP-targets reported to be involved in peptidoglycan synthesis or cell division/ elongation include MurC, GlmM, MapZ (LocZ), DivIVA, FtsZ and FtsA (Novakova *et al*., 2005; Sun *et al*., 2010; Falk and Weisblum, 2012; Fleurie *et al*., 2014a; Holeckova *et al*., 2015). Phosphoproteomic analysis has identified more than 80 phosphoproteins in *S. pneumoniae* (Sun *et al*., 2010). It is therefore likely that a number of StkP phosphorylation targets remain to be identified and characterized. One poorly characterized protein targeted by StkP is Spr1851. It belongs to a family of proteins termed Jag (*jag* = *spoIIIJ associated* gene) (Errington *et al*., 1992; Sun *et al*., 2010; Ulrych *et al*., 2016). Jag homologs are widespread among Gram-positive bacteria, but their function remains unknown. In the present study we show that Spr1851 plays an important role in the regulation of cell elongation in *S. pneumoniae*.

Results

Deletion of *spr1851* enables pneumococci to survive without a functional elongasome

PBP2b and RodA are both essential and constitute the core components of the elongasome. Previously, we have observed that PBP2b-depleted pneumococci display distinct phenotypic traits. They form long chains of oblate cells, get an altered stem peptide composition, lose immunity to the peptidoglycan hydrolase CbpD during competence and become hypersensitive to the autolysin LytA during exponential growth phase (Berg *et al*., 2013; Straume *et al*., 2017). Based on these findings, we speculated that the lethality of a *pbp2b* null mutation might be due to LytA-mediated autolysis, and that Δ*pbp2b* mutants would be viable in a Δ*lytA* background. Attempts to replace the *pbp2b* gene with the kanamycin selectable Janus cassette in *lytA*$^+$ and *lytA*$^-$ backgrounds gave no colonies on the selection plates after overnight incubation at 37°C, but a few lytA$^+$ as well as lytA$^-$ colonies appeared after 24–144 hours. This shows that PBP2b is essential also in cells lacking LytA. We picked six colonies, designated GS1–6, which were subjected to whole genome sequencing in order to locate possible suppressor mutations. Three of the isolates harboured mutations in the gene encoding the lytic transglycosylase MltG (Spr1370) (Yunck *et al*., 2016). The GS5 strain expressed a truncated form of MltG (Δaa 169–551), while the GS1 and GS2 strains produced MltG proteins with amino acid substitutions at their C-terminal ends. GS1-MltG contained only an A505V substitution, while GS2-MltG contained 16 amino acid substitutions between I477 and A505. Shortly after we had made this discovery, Tsui *et al*. (2016) published the same finding, that is, that deletion of *mltG* removes the requirement for PBP2b.

We, therefore, chose to focus on another possible Δ*pbp2b* suppressor mutation identified in the whole genome sequence analysis. The remaining isolates, GS3, GS4 and GS6, contained mutations in a gene (*spr1851*) encoding a protein of unknown function which is conserved among Gram-positive bacteria. The mutations resulted in truncations of the predicted protein products (Fig. 1A, see Supporting Information Fig. S1 for details). To verify that a non-functional *spr1851* gene is able to suppress the loss of *pbp2b*, we first replaced the complete *spr1851* gene with the Janus cassette in our wild-type strain RH425. The resulting Δspr1851 mutant showed marked growth defect compared with

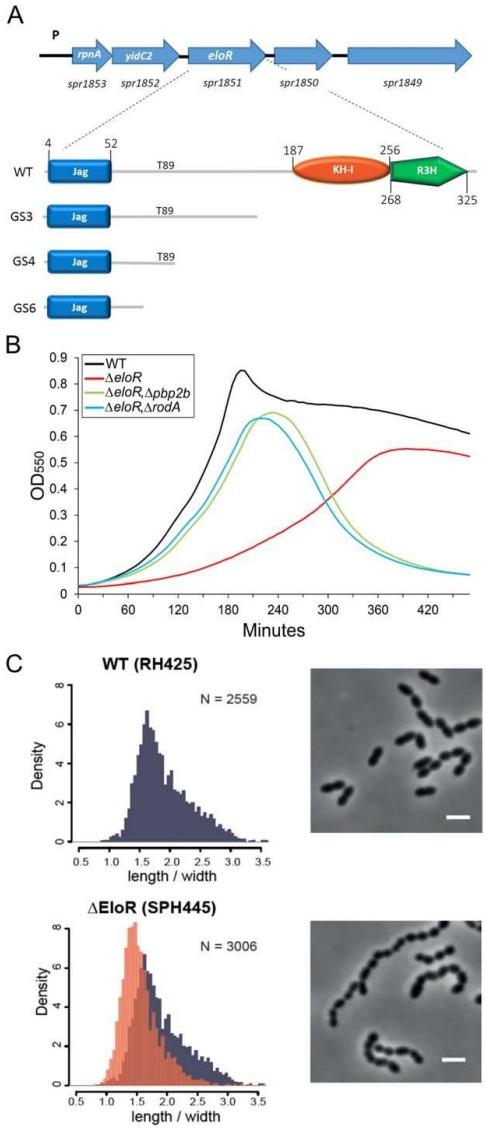

Fig. 1. Properties of a Δ*eloR* strain with respect to growth rate, cell shape distribution and morphology. Panel A. Genetic map of the *S. pneumoniae* genome region where *eloR* is located. The EloR protein consists of 328 amino acids, and is composed of an N-terminal Jag domain and two single-strand nucleic acid binding domains, KH-I and R3H, at the C-terminal end. The position of threonine 89, which is phosphorylated by StkP, and the positions of the domain boundaries are indicated. The truncated forms of EloR expressed by the suppressor mutants GS3, GS4 and GS6 are shown as schematic drawings. Panel B. Comparison of the growth rates of the SPH445 (Δ*eloR*) and RH425 (WT) strains. The reduction in growth rate caused by deletion of *eloR* is nearly abolished in strains where *pbp2b* or *rodA* (strains SPH446 and SPH447 respectively) are deleted in addition to *eloR*. Panel C. Comparison of cell shape distribution (length/width ratios) and morphology of the SPH445 (Δ*eloR*) and RH425 (WT) strains. The histogram representing the shape distribution of wild-type cells (RH425) is shown in grey, while the histogram representing the Δ*eloR* mutant strain (SPH445) is shown in orange. The number of cells counted are indicated for each plot. The lenght/width ratio of Δ*eloR* cells (1.56 ± 0.33) was significantly different from WT (1.91 ± 0.45) ($P < 0.01$, Kolmogorov–Smirnov test). Scale bars in the phase-contrast images represent 2 μm.

wild-type (Fig. 1B). Next, the Janus cassette was removed by negative selection (Sung *et al*., 2001), giving rise to the SPH445 mutant strain (see Supporting Information Table S1 for list of strains). SPH445 and the wild-type RH425 strain were transformed with the Δ*pbp2b*-amplicon described above. As expected, no transformants were obtained with the wild-type strain. The mutant strain lacking *spr1851*, however, was transformed at a normal frequency. A few colonies were picked and cultivated in liquid media for further analysis. The absence of the genes encoding Spr1851 and PBP2b in these transformants was confirmed by PCR as well as Sanger sequencing. In addition, the absence of PBP2b in one of them (SPH446) was verified by staining with Bocillin FL, a fluorescent penicillin that specifically labels PBPs (see Materials and Methods and Supporting Information Fig. S2).

Similar to PBP2b, RodA is essential in *S. pneumoniae* (Meeske *et al*., 2016; Straume *et al*., 2017). Due to the close functional relationship of these proteins, we speculated that both might be dispensable in a Δ*spr1851* background. We therefore attempted to delete the *rodA* gene in a strain lacking the *spr1851* gene. Interestingly, we succeeded in obtaining transformants that upon further characterization proved to be bona fide *rodA* deletion mutants (e.g., SPH447). Notably, the growth defect observed for the Δ*spr1851* strain is partially alleviated in the Δ*spr1851*/Δ*pbp2b* and Δ*spr1851*/Δ*rodA* double mutants (Fig. 1B). Together, these results show that pneumococci are not only able to survive without PBP2b or RodA in a Δ*spr1851* background, but the presence of these proteins are detrimental when Spr1851 is absent.

Spr1851 is involved in the regulation of cell elongation in *S. pneumoniae*

Spr1851 contains three regions with strong homology to previously described domains, namely Jag (50 aa), KH-I (76 aa) and R3H (61 aa) (Fig. 1A). The C-terminal KH-I and R3H domains are both known to bind ssRNA or ssDNA, and are typically found in proteins regulating gene expression (Grishin, 1998; Valverde *et al*., 2008; Jaudzems *et al*., 2012). The function of the N-terminal JAG domain, on the other hand, remains unknown. Considering that Spr1851 contains KH-I and R3H

domains, resides in the cytoplasm, and when absent suppresses the requirement for PBP2b and RodA, it is highly likely that Spr1851 functions to regulate the activity of the elongasome. To further corroborate this theory we used the image analysis tool MicrobeJ (Ducret *et al*., 2016) to compare the cell shape distribution (length/width ratio) of the SPH445 (Δ*spr1851*) and RH425 (WT) strains. The results showed that Δ*spr1851* mutant cells on average are significantly less elongated than wild-type cells (Fig. 1C), demonstrating that the elongasome is less active in the absence of Spr1851. Hence, we concluded that Spr1851 is involved in regulating the activity of the elongasome and named the protein EloR (elongasome regulating protein). Furthermore, to gain insight into the subcellular localization of EloR we made a C-terminal fusion to monomeric superfolder GFP, and expressed the EloR-m(sf)gfp fusion from an ectopic locus in strain RH425 as well as in the encapsulated *S. pneumoniae* D39 strain. This showed that EloR, similar to other proteins involved in cell elongation in *S. pneumoniae*, localizes to the septal area (Supporting Information Fig. S3).

StkP-mediated phosphorylation of EloR requires functional PASTA domains

EloR has been shown to be phosphorylated on threonine 89 (Sun *et al*., 2010; Ulrych *et al*., 2016). We confirmed this finding by constructing a strain, SPH449, which expresses a phosphoablative (T89A) form of EloR. To be able to immunoprecipitate and detect this mutant protein by Western blotting, a 3xFlag tag was added to its N-terminal end. Similarly, as a positive control, we constructed a strain (SPH448) in which a 3xFlag tag was added to the N-terminal end of wild-type EloR. Furthermore, to determine whether EloR is phosphorylated by StkP, we added a 3xFlag tag to wild-type EloR in a *stkP*$^{-}$ strain (SPH450) and a strain (SPH451) expressing the StkP^{K42M} mutant protein. In the latter strain, the catalytic lysine residue of StkP (K42) was changed to a methionine, generating a kinase dead protein (Fleurie *et al*., 2012). The strain (SPH448) expressing the wild-type 3xFlag-EloR protein displayed normal growth, indicating that the Flag tag does not significantly affect the functionality of the EloR protein. To detect phosphorylation of EloR *in vivo*, the Flag tagged proteins were immunoprecipitated with an anti-Flag antibody, followed by Western blotting with an anti-phosphothreonine antibody. Our results verified that EloR is phosphorylated by StkP on T89 (Sun *et al*., 2010; Ulrych *et al*. 2016). The anti-phosphothreonine antibody detected two bands of approximately equal intensity in the lane representing wild-type EloR (Fig. 2). As the upper band is missing in the strain expressing the phosphoablative (T89A) form of EloR, the upper band must represent the T89-phosphorylated form (Fig. 2). The lower band and the band detected in strain expressing EloR^{T89A} are both absent in the Δ*stkP* strain. Hence, StkP must be able to phosphorylate EloR at two different sites.

The four PASTA domains of StkP are believed to detect extracellular signals that regulate its kinase activity. To determine if the PASTA domains are required for StkP-mediated phosphorylation of EloR, we constructed a strain, SPH452 (StkP$^{\Delta PASTA}$), in which the PASTA domains (amino acids 372–659) were deleted. As demonstrated in Supporting Information Fig. S4, deletion of the PASTA domains does not affect anchoring of the StkP$^{\Delta PASTA}$ protein to the cytoplasmic membrane. Our results clearly show that EloR is not phosphorylated in the strain expressing StkP$^{\Delta PASTA}$ (Fig. 2), strongly indicating that the phosphorylation state of EloR is regulated by an extracellular signal sensed by the PASTA domains.

Further evidence that EloR is a substrate of StkP was obtained by bacterial two-hybrid analysis. We used the bacterial adenylate cyclase two-hybrid system (BACTH) to test for interactions between EloR and StkP in vivo. The system is based on the functional complementation of T18 and T25, two fragments of the catalytic domain of adenylate cyclase from Bordetella pertussis (see Materials and Methods for details). Positive interactions

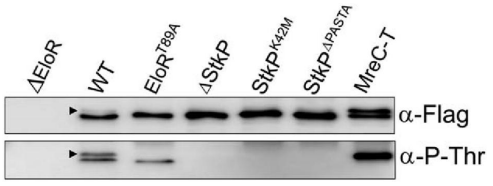

Fig. 2. Immunoblot detecting FLAG-tagged EloR with an anti-Flag antibody (α-Flag) and its phosphorylated form with an anti-phosphothreonine antibody (α-P-Thr). Lanes were loaded with immunoprecipitates (anti-FLAG antibody conjugated to agarose beads) derived from pneumococcal cell lysates as follows: ΔEloR, cells in which the *eloR* gene was deleted; WT, wild-type cells expressing FLAG-tagged EloR; EloR^{T89A}, cells expressing the FLAG-tagged phosphoablative form of EloR; ΔStkP, Δ*stkP* cells expressing FLAG-tagged EloR; StkP^{K42M}, cells expressing both FLAG-tagged EloR and a kinase dead mutant of StkP; StkP$^{\Delta PASTA}$, cells expressing both FLAG-tagged EloR and a version of StkP where the external PASTA domains were deleted; MreC-T, cells expressing both FLAG-tagged EloR and MreC$^{\Delta aa183-272}$. Arrowheads indicate the position of EloR with a phosphorylated Thr89 residue.

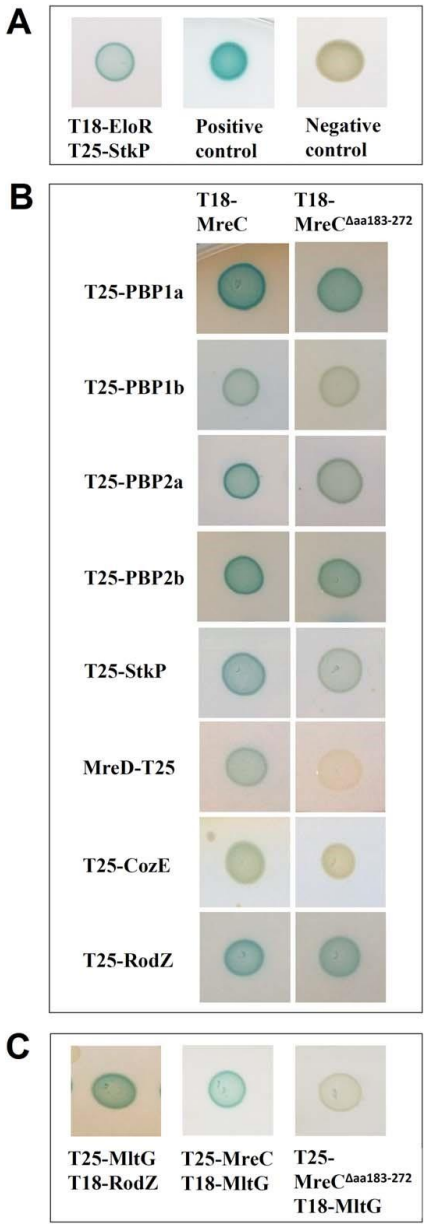

Fig. 3. Bacterial two-hybrid data on the interactions between proteins involved in cell elongation. Interactions between pairs of proteins were detected by fusing proteins of interest to adenylate cyclase fragments T18 and T25, respectively, and co-expressing the resulting fusion proteins in an E. coli cya⁻ strain as specified by the manufacturer (Euromedex). Functional complementation of T18 and T25 fragments restores adenylate cyclase activity resulting in synthesis of cAMP followed by CAP activated expression of β-galactosidase. Samples were spotted on agar plates containing X-gal and incubated for 24 h at 30°C. A colourless spot indicates a negative result, while a blue colour indicates a positive interaction between the pair of fusion proteins tested. Panel A. Interaction between EloR and the Ser/Thr protein kinase StkP. Positive and negative controls were supplied by Euromedex. Panel B. Interactions between full-length and truncated MreC and various elongasome proteins. Panel C. Interactions between the lytic transglycosylase MltG and RodZ, full-length MreC and truncated MreC respectively.

elicit cAMP synthesis followed by cAMP/CAP activated expression of β-galactosidase which converts X-gal to a blue dye. Hence, blue colonies indicate a positive reaction, while white colonies indicate non-interacting proteins. When co-expressed, the T18-EloR and T25-StkP fusion proteins gave rise to blue colonies, demonstrating that EloR and StkP interact *in vivo* (Fig. 3A).

The phosphomimetic T89E mutation (EloR^{T89E}) is not tolerated

To gain information about the biological effects of StkP mediated phosphorylation of EloR, a strain, SPH456, expressing a phosphoablative (T89A) form of EloR was constructed and compared with wild-type (RH425) and the ΔEloR mutant (SPH445). In this case, no Flag tag was added to the EloR^{T89A} protein. Analysis of their shape distribution showed that the ΔEloR and EloR^{T89A} strains have highly similar profiles, and that both on average form less elongated cells than the wild-type strain (Fig. 4; Supporting Information Fig. S5). Since deletion of EloR and removal of its phosphorylation site lead to approximately the same reduction in average cell length, it appears that the phosphoablative form of EloR represents a less active or inactive form of the protein. It follows from this that a phosphomimetic (T89E) mutant of EloR might represent the active form that stimulates the activity of the elongasome and increases cell length. To test this hypothesis we constructed an EloR^{T89E} mutant strain (SPH457) and analysed it as described above. Unexpectedly, the SPH457 pneumococci were even less elongated than SPH456 cells expressing the EloR^{T89A} mutant protein (Fig. 4; Supporting Information Fig. S5). This led us to suspect that the phosphomimetic (T89E) mutation is not tolerated and selects for suppressors. To check for possible suppressor mutations we sequenced the genomes of the SPH445 (ΔEloR), SPH456 (EloR^{T89A}) and SPH457 (EloR^{T89E}) mutant strains, and compared them to the parental strain (RH425). The genomes of the SPH445 and SPH456 strains did not contain suppressors, but a potential suppressor mutation was detected in the

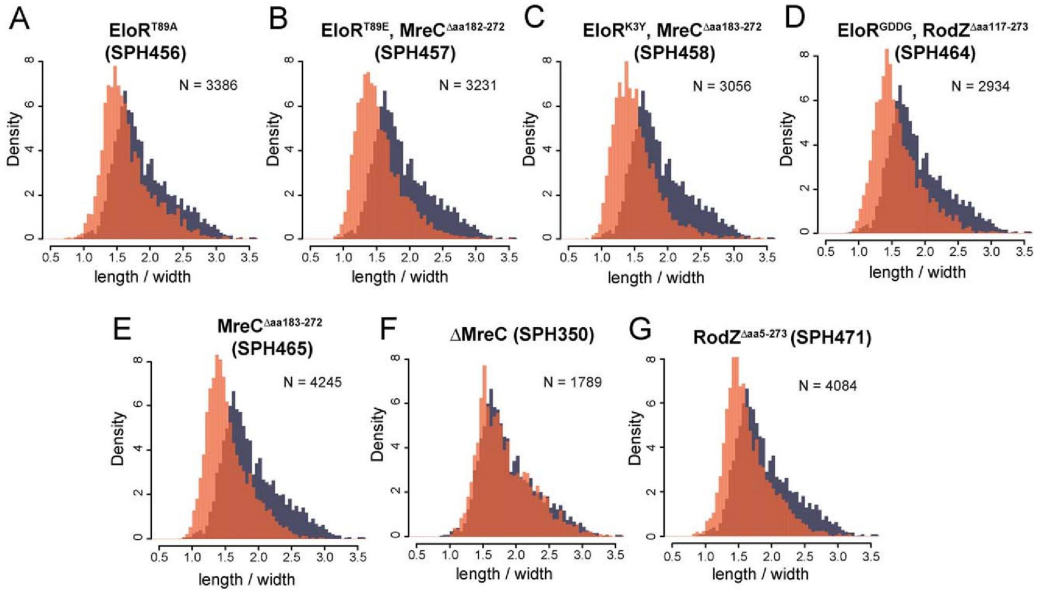

Fig. 4. Cell shape distributions. As a measurement for cell elongation, length/width ratio was computed for all counted cells and plotted as histograms (in orange color) for EloR^{T89A} (panel A, length/width ratio 1.65 ± 0.37), EloR^{T89E} with suppressor mutation MreC$^{\Delta aa182-272}$ (panel B, ratio 1.53 ± 0.35), ElorR^{K3Y} with suppressor mutation MreC$^{\Delta aa183-272}$ (panel C, ratio 1.52 ± 0.36), EloR^{GDDG} with suppressor mutation RodZ$^{\Delta aa117-273}$ (panel D, ratio 1.59 ± 0.36), MreC$^{\Delta aa183-272}$ (panel E, ratio 1.54 ± 0.34), ΔMreC (panel F, ratio 1.84 ± 0.42), RodZ$^{\Delta aa5-273}$ (panel G, ratio 1.64 ± 0.36). Wild-type RH425 (see Fig. 1C) is shown in grey for all plots for comparison. The length/width ratios of the mutant strains are significantly different from the wild-type ($P < 0.01$, Kolmogorov–Smirnov test). Phase contrast microscope images of all strains are shown in Supporting Information Fig. S5A–G. Overlaid density plots length/width ratio distributions for some of the mutants are shown in Supporting Information Fig. S5H. The number of cells counted are indicated for each plot.

genome of the strain expressing EloR^{T89E}. This mutation introduces a frameshift that causes a premature termination of *mreC* mRNA translation, resulting in the synthesis of a truncated protein (MreC$^{\Delta aa182–272}$). Pneumococcal MreC is a bitopic transmembrane protein consisting of 272 amino acids. The N-terminal approximately 8 amino acids are located in the cytoplasm, while the approximately 244 C-terminal amino acids are periplasmic (Lovering and Strynadka, 2007). The amino acid sequence of MreC$^{\Delta aa182–272}$ is identical to MreC up to amino acid K181, after which they diverge. Deletion of a single adenosine creates a frameshift that introduces a stop codon 26 amino acids downstream of K181 (see Supporting Information Fig. S6 for details).

Intriguingly, a mutation creating an almost identical truncation of the MreC protein was detected in the genome of a strain (SPH458) expressing an EloR protein in which the R3H domain was inactivated (EloR^{K3Y}). The R3H domain is characterized by the conserved Arg-X-X-X-His (R3H) sequence motif, where the arginine and histidine residues are required for nucleic acid binding (Grishin, 1998; Jaudzems *et al*., 2012). In the EloR^{K3Y} mutant strain, the Arg-X-X-X-His sequence was changed to Lys-X-X-X-Tyr (K3Y). By comparing the genome sequence of the strain expressing EloR^{K3Y} with the parental strain we detected a C to T transition in the *mreC* gene that introduced a premature stop codon after amino acid I182. The resulting truncated MreC protein was termed MreC$^{\Delta aa183–272}$.

The presence of the MreC$^{\Delta aa182–272}$ mutation in the strain (SPH457) expressing EloR^{T89E} suggested that the phosphomimetic T89E mutation exerts severe stress that is alleviated by truncation of MreC. To obtain additional evidence in support of this idea, we constructed five new EloR^{T89E} mutants and sequenced their *mreC* genes. In three of the mutants (SPH459–461) we identified the same MreC$^{\Delta aa183–272}$ mutation as described above for the SPH458 strain, while two of the mutants (SPH462 and SPH463) had a wild-type *mreC* gene. To determine whether the latter mutant strains had acquired other suppressors, their genomes were sequenced. In both of them a single adenosine was deleted in a run of eight adenosines located 3–10 bases downstream of the translational start codon of the gene encoding RodZ. RodZ is a widely conserved bitopic membrane protein known to play a role in bacterial cell elongation (Massidda *et al*., 2013; Philippe *et al*., 2014). The mutation creates a frameshift that introduces

a stop codon eleven codons downstream of the RodZ start site. Hence, it inactivates the protein.

A frameshift mutation in RodZ was also found in a strain in which the KH-I domain of EloR had been mutated (EloR^{GDDG}). KH domains contain an invariant GXXG loop in which at least one of the variable amino acids has a positively charged side chain. The loop forms contact with the sugar–phosphate backbone and is crucial for nucleotide binding. It has been reported that mutation of the two variable amino acids to aspartate (GDDG) impairs nucleic acid binding without compromising the stability of the KH domain (Hollingworth *et al*., 2012). We, therefore, constructed a mutant strain (SPH464) where the native EloR protein was exchanged with a version in which the GYHG loop were mutated to GDDG. Genome sequencing of SPH464 revealed that the five nucleotides TTTAT (nt 330–334) had been deleted in the *rodZ* gene, giving rise to a frameshift after amino acid Y116 (see Supporting Information Fig. S7 for details). The frameshift occurs in the transmembrane segment of the resulting RodZ$^{\Delta aa117–273}$ mutant protein. Thus, while the N-terminal cytoplasmic domain is still expressed, the complete extracellular part is missing. Together, the results described in this section strongly indicate that the phosphomimetic T89E mutation, and mutations that disrupt EloR's ability to bind single stranded nucleic acid, are not tolerated in *S. pneumoniae*.

MreC deletion and truncation mutants have strikingly different phenotypes

To investigate whether the truncated MreC proteins expressed by the SPH457 (EloR^{T89E}/MreC$^{\Delta aa182–272}$) and SPH458 (EloR^{K3Y}/MreC$^{\Delta aa183–272}$) strains are suppressors that alleviate the stress induced by the EloR^{T89E} and EloR^{K3Y} mutations, a strain (SPH465) was constructed in which the *mreC* gene of RH425 was replaced by the gene encoding the truncated form of MreC (MreC$^{\Delta aa183–272}$). As outlined above, the SPH457 and SPH458 strains form on average much less elongated cells than the wildtype strain (Fig. 4; Supporting Information Fig. S5). Comparison of the SHP457, SPH458 and SPH465 strains show that their cell shape distribution is virtually identical, strongly indicating that the MreC$^{\Delta aa183–272}$ mutation rather than the EloR^{T89E} or EloR^{K3Y} mutations is responsible for the cell rounding observed in the SPH457 and SPH458 strains (Fig. 4; Supporting Information Fig. S5). Comparison of the RH425 (WT) and SPH350 (Δ*mreC*) strains, on the other hand showed that the shape distribution of their cells is highly similar. Further characterization of SPH465 (MreC$^{\Delta aa183–272}$), revealed that the genes encoding PBP2b and RodA can be individually deleted in this strain. Moreover, the growth rates of the SPH465 (MreC$^{\Delta aa183–272}$) strain, and Δ*pbp2b* or Δ*rodA* mutants of this strain, are similar to wild-type (Supporting Information Fig. S8). These interesting results show that essential components of the elongasome are dispensible in strains expressing the truncated form of the MreC protein (MreC$^{\Delta aa183–272}$). In contrast, neither *pbp2b* nor *rodA* can be deleted in a wild-type or Δ*mreC* background.

Truncation of MreC alters its interactions with other components of the elongasome and stimulates StkP-mediated phosphorylation of EloR

MreC has been reported to interact with a number of proteins involved in cell division and elongation (van den Ent *et al*., 2006). As pneumococci expressing the MreC$^{\Delta aa183–272}$ protein are phenotypically different from wild-type and ΔmreC strains, we speculated that truncation of the MreC protein might disrupt its interaction with some partners in the elongasome without disturbing the interaction with others. To test this hypothesis, we used the BACTH system to study interactions between the truncated MreC protein and proteins that we in a previous screening (unpublished results) found to interact with full-length MreC. Strikingly, the results presented in Fig. 3B show that the interaction between MreC and MreD is completely lost when the 90 C-terminal amino acids of MreC are deleted. We also detected a strong reduction in the interaction between MltG and MreC$^{\Delta aa183–272}$ compared with the interaction between MltG and MreC (Fig. 3C). This result was obtained with T18-MltG and T25-MreC. When the adenylate cyclase fragments were swapped (T25-MltG and T18-MreC/T18-MreC$^{Daa183–272}$), a similar tendency was found although the difference was less evident. In addition, our results suggest that MreC$^{\Delta aa183–272}$ interacts less efficiently with the PBP1b, StkP and CozE proteins than full-length MreC (Fig. 3B). Finally, we made the interesting observation that MltG interacts very strongly with RodZ (Fig. 3C).

As the interaction between MreC$^{\Delta aa183–272}$ and StkP appears to be somewhat reduced compared with the interaction between full-length MreC and StkP, we wondered whether the truncation of MreC might affect StkP-mediated phosphorylation of EloR. To test this possibility, we constructed a strain (SPH475) expressing a 3xFlag-tagged EloR protein and a truncated MreC protein (MreC$^{Daa183–272}$). To establish the level of EloR phosphorylation in the SPH475 strain, 3xFlag-EloR was immunoprecipitated and subjected to Western blot analysis as described above. Intriguingly, we found that the level of phosphorylated EloR in this strain was much higher than in a strain expressing full-length MreC (Fig. 2).

Discussion

We identified EloR by screening for mutations that suppress the lethality caused by deletion of the gene encoding the transpeptidase PBP2b. Subsequent experiments showed that the essential peptidoglycan polymerase RodA is also

dispensable in a ΔEloR background. These findings demonstrate that pneumococci can survive without a functional elongasome in the absence of EloR. This implies that EloR and the elongasome are part of the same functional network. Although the specific function of EloR remains to be determined, several lines of evidence indicate that it has a regulatory role. Firstly, it contains two regions with strong homology to KH-I and R3H domains. Both domains have been reported to bind single stranded nucleic acid (ssNA) in a sequence-specific manner (Valverde *et al.*, 2008; Hollingworth *et al.*, 2012; Jaudzems *et al*., 2012). KH domains, which have been more extensively studied than R3H domains, are present in a variety of proteins from all domains of life. They are typically found in proteins that regulate gene expression at the transcriptional or post-transcriptional level (Valverde *et al.*, 2008). Secondly, we found that deletion of EloR significantly reduces the average cell length of the mutant strain compared with wild-type. This demonstrates that EloR is needed to stimulate elongasome-mediated lateral cell wall synthesis. Thirdly, EloR is a substrate of StkP, a transmembrane serine/threonine kinase that is involved in orchestrating the switching between septal and peripheral peptidoglycan synthesis in *S. pneumoniae* through phosphorylation of several proteins involved in cell division and elongation (Novakova *et al.*, 2005; Beilharz *et al.*, 2012; Manuse *et al.*, 2016).

To study the effect of StkP-mediated phosphorylation on T89 we constructed strains expressing the phosphoablative ($EloR^{T89A}$) and phosphomimetic ($EloR^{T89E}$) forms of EloR. The strain SPH456 expressing the phosphoablative form displayed a cell shape profile that was highly similar to that of the SPH445 strain (ΔEloR). However, in contrast to the SPH445 strain, the *pbp2b* gene could not be deleted in the SPH456 strain. This shows that the $EloR^{T89A}$ protein is not biologically inactive, but its ability to stimulate lateral cell wall synthesis is diminished. Unexpectedly, we observed that $EloR^{T89A}$ is still being phosphorylated by StkP (Fig. 2), presumably at a threonine residue located close to T89 at the surface of the protein. Since the ΔEloR and $EloR^{T89A}$ strains have somewhat different phenotypes, it is likely that phosphorylation of the alternative site affects the activity of EloR.

The strain expressing the $EloR^{T89E}$ phosphomimetic form acquired additional mutations in the *mreC* or *rodZ* gene in all cases examined. Clearly, expression of the $EloR^{T89E}$ mutant protein generates stress that is alleviated by truncation of MreC or loss of RodZ function. Truncation of MreC alone resulted in a strong reduction in average cell length, showing that this mutation reduced or inactivated lateral cell wall synthesis (Fig. 4). Similarly, the *rodZ* null mutation present in the SPH462 and SPH463 strains gives rise to less elongated cells (Fig. 4). It follows from this that alleviation of the stress imposed by the phosphomimetic T89E mutation requires suppressor mutations that downregulate or inhibit the activity of the elongasome. In pneumococci expressing truncated MreC ($MreC^{\Delta aa183–272}$), loss of elongasome activity is sensed by the cells, which attempt to compensate by strongly increasing StkP-mediated phosphorylation of EloR (Fig. 2). Together these results support a model in which $EloR^{T89E}$ and the phosphorylated form of EloR stimulate the activity of the elongasome. Since $EloR^{T89E}$ cannot be dephosphorylated by PhpP, but is permanently active throughout the cell cycle, the T89E mutation is probably lethal to the cell. Presumably, the only way to escape the lethality of an overactive elongasome is to acquire suppressors that reduce or abolish the activity of this peptidoglycan synthesizing machine.

Suppressor mutations in the *mreC* or *rodZ* genes were also found in strains expressing EloR proteins containing amino acid substitutions that reduce or abolish their ability to bind ssNA. The SPH458 ($EloR^{K3Y}$) strain acquired the $MreC^{\Delta aa183–272}$ suppressor mutation, while the $RodZ^{\Delta aa117–276}$ suppressor was acquired by the strain (SPH464) expressing the $EloR^{GDDG}$ mutant protein. Using the same reasoning as above this implies that loss of ssNA-binding activity stimulates the elongasome, while binding of target ssNA probably has an inhibitory effect. As proteins containing ssNA-binding domains are often involved in controlling protein expression by controlling transcription or translation of specific target mRNAs, it is plausible that EloR controls the expression of one or several proteins that are critical for elongasome function. Our data suggest that non-phosphorylated EloR represses target protein expression at the transcriptional or translational level by binding to specific ssDNA or ssRNA sequences. Following phosphorylation of EloR by StkP, the nucleic acid(s) in question is released and target proteins can be synthesized. Further studies are needed to verify or reject this model.

The $MreC^{\Delta aa183–272}$ mutation gives rise to a distinct and highly interesting phenotype that includes a strong reduction in cell elongation and the ability to grow and proliferate well without PBP2b or RodA. These traits distinguish the $MreC^{\Delta aa183–272}$ mutant from a ΔMreC strain. Hence, the truncated MreC protein cannot be completely inactive, but must have retained some functions. MreC is an abundant protein present at about 8500 dimers per cell (Land and Winkler, 2011). As mentioned above, the N-terminal approximately 8 amino acids of the bitopic MreC protein is cytoplasmic, while approximately 244 amino acids are located in the periplasm. The periplasmic part of MreC consists of a helix (aa 73–102) and two six-stranded β-barrels (aa 110– 272), where the second barrel is folded between strands five and six of the first barrel (van den Ent *et al*., 2006; Lovering and Strynadka, 2007). The crystal structure shows that MreC dimerizes through close contact between the N-terminal helices. There is also contact between one globular β-barrel from each monomer, while the other β-barrel is solvent exposed and in principle free to interact with another

MreC dimer. Hence, it is possible the MreC-dimers are able to form filaments *in vivo* (van den Ent *et al*., 2006). The truncated MreC$^{\Delta aa183–272}$ protein ends at position 182, which is in the middle of the first β-strand (β6) in the second C-terminal β-barrel. Thus the MreC$^{\Delta aa183–272}$ protein obviously lacks this domain. Since the nine C-terminal amino acids (aa 264–272) form a β-strand (β12) that is part of the first β-barrel, the loss of this strand probably destabilizes the domain and alters its structure. It follows from this that if MreC dimers form filaments, this will not be possible for the MreC$^{\Delta aa183–272}$ protein. It is, therefore, conceivable that loss of filament formation causes or contributes to the phenotype the SPH465 strain.

Since MreC has been reported to bind to a number of different proteins (van den Ent *et al*., 2006), we investigated whether we could detect any differences between MreC and MreC$^{\Delta aa183–272}$ with respect to protein interaction partners. The most striking result of this study was that the interaction between MreD and MreC was completely lost when the 90 C-terminal amino acids of MreC were deleted (Fig. 3B). The interaction between MreC$^{\Delta aa183–272}$ and PBP1a, PBP2a and PBP2b, on the other hand, was not affected, while the interaction between MreC$^{\Delta aa183–272}$ and PBP1b, StkP and CozE appeared to be somewhat reduced. Based on these results, it is reasonable to assume that the complete loss of interaction between MreC$^{\Delta aa183–272}$ and MreD causes, or significantly contributes to, the distinct phenotype displayed by the SPH465 (MreC$^{\Delta aa183–272}$) strain. If so, it follows that MreC/MreD interaction is required for activation of elongasome-mediated lateral cell wall synthesis. Curiously, although deletion of MreD causes pneumococci to form long chains of round or oblate cells, *pbp2b* cannot be deleted in these cells (Straume *et al*., 2017). This shows that loss of the MreC$^{\Delta aa183–272}$/MreD interaction alone cannot explain all phenotypic differences between the SPH465 strain and the strains lacking MreC or MreD. It is, therefore, likely that the unique properties of the MreC$^{\Delta aa183–272}$ mutant protein result from the fact that it is no longer able to interact with some MreC partners, while retaining the ability to interact with others (e.g., the PBPs) (Fig. 3B).

In the present study we show that the genes encoding the essential proteins PBP2b and RodA can be readily deleted in a ΔEloR background. Hence, lateral peptidoglycan synthesis per se is not essential for viability in *S. pneumoniae*. So why is deletion of PBP2b and RodA lethal in a wild-type background? The finding that deletion of *mltG* also supresses the requirement for PBP2b and RodA (Tsui *et al*., 2016; current study) points toward MltG as the lethal factor. As MltG is an essential muralytic enzyme, misregulation of this enzyme might have fatal consequences. It is conceivable that deletion of PBP2b, RodA and other essential components of the elongasome results in uncontrolled MltG activity that kills the bacterial cells. To gain support for this hypothesis, we tested whether EloR regulates the expression of the MltG protein. Comparison of MltG levels in wild-type (SPH473) and Δ*eloR* (SPH474) cells expressing Flag tagged MltG proteins revealed no significant differences (Supporting Information Fig. S9). Neither is EloR required for septal localization of MltG, as MltG localizes to the septum in wild-type as well as Δ*eloR* cells (Supporting Information Fig. S9). Instead, our results indicate that EloR regulates the muralytic activity of MltG. Presumably, *pbp2b* and *rodA* can be deleted in a Δ*eloR* mutant because the activity of the elongasome, including MltG, is strongly reduced in this genetic background. This supposition is supported by the finding that pneumococcal transformants expressing EloR^{T89E} always contain a truncated MreC or nonfunctional RodZ protein. The MreC$^{\Delta aa183–272}$ suppressor mutation strongly reduces the interaction between MreC and MltG, while the Δ*rodZ* suppressor mutation completely abolishes the interaction between RodZ and MltG. Hence, both suppressor mutations probably reduce or modulate the muralytic activity of MltG in a way that helps the cell survive the stress imposed by the phosphomimetic EloR^{T89E} mutant protein. The finding that PBP2b and RodA can be deleted in a strain expressing the truncated MreC$^{\Delta aa183–272}$ protein, further supports this model.

In conclusion, our results demonstrate that EloR regulates cell elongation in *S. pneumoniae*. The PASTA domains of StkP sense one or more external signals which are relayed to EloR by transfer of a phosphoryl group. We obtained strong evidence that the phosphorylated form of EloR stimulates cell elongation, while the non-phosphorylated form is less active or inactive. Of note, we observed that strains expressing EloR^{T89E} always acquired suppressor mutations that gave rise to a less active or inactive elongasome, demonstrating that the constitutively activated phosphomimetic form of EloR is not tolerated (Fig. 5). Furthermore, the finding that StkP-mediated phosphorylation of EloR increases strongly in a MreC$^{\Delta aa183–272}$ mutant, suggests that StkP monitors the activity of the elongasome and responds to changes that reduce or abolish its activity (Fig. 5). Several elongasome proteins have been reported to be essential (Massidda *et al*., 2013; Tsui *et al*., 2016). Our data suggest that they are not essential by themselves. Instead, we propose that their absence leads to misregulation of the muralytic enzyme MltG, whose unrestrained activity will be lethal to the pneumococcal cell.

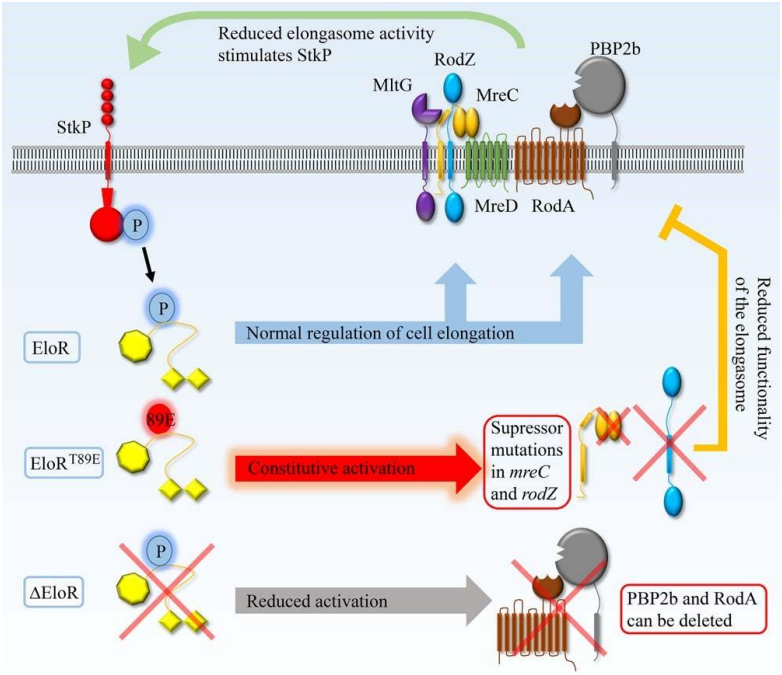

Fig. 5. Model depicting EloR mediated regulation of the pneumococcal elongasome. At the appropriate stage of the cell cycle, the extracellular PASTA domains of StkP sense an unknown signal linked to elongasome activity that is relayed to EloR through the transfer of a phosphoryl group. Our results indicate that the phosphorylated form of EloR activates the elongasome, resulting in synthesis of new peptidoglycan that is inserted into the existing peptidoglycan layer. Cells expressing the phosphomimetic form of EloR (EloR^{T89E}) always acquire suppressor mutations in *mreC* or *rodZ* that strongly reduce elongasome activity. This implies that the suppressors alleviate the stress imposed by a constantly activated elongasome. Deletion of the gene encoding EloR results in short, rounded, cells that are able to survive without the essential elongasome components PBP2b and RodA.

Experimental procedures

Bacterial strains, cultivation and transformation

Bacterial strains used in this study are listed in the Supporting Information Table S1. Strains of *Escherichia coli* were grown in Luria Bertani broth with shaking or on LB agar plates at 30°C or 37°C. When appropriate, the following antibiotic concentrations were used in the growth medium: ampicillin = 100 μg/ml and kanamycin = 50 μg/ml. Chemically competent *E. coli* was transformed by typical heatshock at 42°C for 30 seconds. *S. pneumoniae* was grown in C medium (Lacks and Hotchkiss, 1960) at 37°C without shaking. When selecting for *S. pneumoniae* transformants, the pneumococcus was grown on Todd-Hewitt agar plates in an oxygen-depleted chamber using AnaeroGen™ bags from Oxoid. Gene knockouts or introduction of point mutations in the *S. pneumoniae* genome were performed by natural transformation. Pneumococcal cultures (1 ml) growing exponentially at OD_{550}= 0.05–0.1 were mixed with 100–200 ng of the transforming DNA and CSP to a final concentration of 250 ng/ml. After 2 hours of incubation at 37°C, transformants were selected on TH-agar containing the appropriate antibiotic (kanamycin= 400 μg/ml, streptomycin= 200 μg/ml and tetracycline = 1 μg/ml).

When following the growth of *S. pneumoniae* over time, pneumococcal strains where grown in 96-well Corning NBS clear-bottom plates in a Synergy H1 Hybrid Reader (BioTek). First, cells were grown to exponential growth phase (OD_{550}= 0.2–0.3) in 5 ml volumes, collected by centrifugation at 4000*g* and resuspended in fresh C medium to OD_{550}= 0.05. Then 300 μl cell culture were transferred to each well of the microtiter plate and incubated in the Synergy H1 Hybrid Reader under normal atmosphere at 37°C. OD_{550} was measured automatically every 5 minutes.

Construction of DNA amplicons

DNA amplicons used to transform *S. pneumoniae* were constructed by overlap extension PCR based on the principle of Higuchi *et al.* (1988). Gene knockouts created in this study were made by using the Janus cassette (Sung *et al.*, 2001), or in some cases a tetracycline resistance cassette. Basically, approximately 1000 bp flanking regions upstream and downstream of a desired target gene were fused the 5′ and 3′ end of the knockout cassette as described in previous works (Johnsborg *et al.*, 2008; Eldholm *et al.*, 2010). By using a streptomycin resistant strain, the Janus cassette can be deleted by replacing it with a DNA fragment containing flanking sequences that are homologous to the corresponding regions flanking the Janus cassette in the genome. Primers used to create DNA amplicons in the present work are listed in the

Supporting Information Table S2. All constructs were verified by PCR and Sanger sequencing.

PBP2b suppressor mutants

Based on our previous work with PBP2b, which showed that cells depleted for PBP2b becomes very sensitive to LytA (Berg *et al.*, 2013), we chose to knock out *pbp2b* in both a LytA$^-$ and a LytA$^+$ background. A fragment carrying the Janus cassette fused to the flanking regions of *pbp2b* was transformed into strain RH4 (LytA$^-$) and RH6 (LytA$^+$) according to standard procedure (see above). After incubating the transformation mixture for 2 hours at 37°C, cells were pelleted, resuspended in 200 µl TH medium and plated on TH-agar. After 24 hours of incubation at 37°C, three colonies had appeared on the plate containing the LytA$^-$ strain. PCR confirmed that two of the three transformants were *bona fide* Δ*pbp2b* knockouts. Of the two correct Δ*pbp2b* mutants, one was genome sequenced and named G1 (Supporting Information Table S1). The plate with the LytA$^-$ strain also contained 3 colonies after 24 hours of incubation, 5 colonies after 48 hours and approximately 20 new colonies after 6 days of incubation. PCR screening identified five transformants to be *bona fide* Δ*pbp2b* mutants (GS2–GS6). Strain GS1–GS6 were genome sequenced to identify possible suppressor mutations.

Whole genome sequencing

The strains RH425, GS1–GS6, SPH445 and SPH456– SPH464 were grown in 10 ml C medium and collected at 4000*g* when reaching OD_{550}= 0.4. Genomic DNA was isolated by using the NucleoBondv® AXG 100 kit from Macherey–Nagel according to the manufacturer's protocol. DNA library was created by using the Nextera XT DNA Library Preparation Kit (Illumina) by following the protocol of the manufacturer, and genome sequencing was done by using an Illumina MiSeq. The RH425 raw sequences were assembled to the reference genome *S. pneumoniae* R6 (NC_003098.1) using SPAdes v3.10.0 (Bankevich *et al.*, 2012) and annotated using the Prokka pipeline (Seemann, 2014). Genomic analysis of the GS1–GS6, SPH445 and SPH456–464 sequences, including sequence mapping, coverage calculation, variant calling and visualization, was performed using Geneious v8.1.9 (Kearse *et al.*, 2012). Mean sequencing coverage was 503.

SDS-PAGE and immunoblotting

To detect Flag-EloR and its phosphorylated form, Flag-EloR was first isolated from a 50 ml cell culture by performing an immunoprecipitation assay using Anti-Flag antibodies conjugated to agarose beads (ANTI-FLAG® M2 Affinity Gel, Sigma). RH425 (WT) and pneumococci expressing Flag-EloR in different genetic backgrounds (SPH448–SPH452) were harvested at OD_{550}= 0.3, and auto-lysed in 1 ml of binding buffer (50 mM Tris-HCl [pH 5 7.4], 150 mM NaCl, 1 mM EDTA, 1% Triton X-100) by triggering the LytA activity at 37°C for 5 minutes. The lysate was incubated with 40 µl ANTI-FLAG® M2 Affinity Gel at 4°C over-night with gentle mixing. The agarose beads were then washed 3 times in 500 µl TBS (50 mM Tris-HCl [pH 5 7.4], 150 mM NaCl) as described by the manufacturer, before 60 µl of SDS-sample buffer was added and the beads were heated to 95°C for 5 minutes. Eight µl samples were separated by SDS-PAGE using a 12% separation gel and the buffer conditions described by Laemmli (1970). The Flag-fused versions of StkP (Flag-StkP, Flag-StkP^{K42M}, and Flag-StkP$^{\Delta PASTA}$) were detected in the membranes from strain SPH453, SPH454 and SPH455 respectively. Flag-MltG was detected in membranes from strain SPH473 and SPH474. Membranes were isolated from 30 ml cell cultures at OD_{550}= 0.3 as described by Straume *et al.* (2017). The membranes were solubilized in 100 µl SDS-sample buffer, and the membrane proteins in 15 µl volumes were separated by SDS-PAGE. A 12% separation gel was used for the MltG fusions and a 10% separation gel for the StkP fusions.

After electrophoresis, the proteins were transferred to a PVDF membrane by electroblotting and both Flag-fused proteins and proteins containing phosphorylated threonines were detected as described previously by Stamsaås *et al.* (2017).

Microscopy techniques and construction of fluorescent fusion proteins

Phase contrast microscopy was used to analyze the morphology of different *S. pneumoniae* mutant strains. Pneumococcal strains were pre-grown to OD_{600}= 0.4, then diluted 100-fold and grown to OD_{600}= 0.1 prior to microscopy. Cells were spotted directly onto slide with a layer of 1.2% agarose in PBS. Images were acquired using a Zeiss AxioObserver with ZEN Blue software, and an ORCA-Flash 4.0 V2 Digital CMOS camera (Hamamatsu Photonics) using a 1003 phase-contrast objective. For cell detection and analysis of cell morphologies, the ImageJ plugin MicrobeJ (Ducret *et al.*, 2016) was used. Data analysis and plotting were performed using RStudio.

The subcellular localization of EloR and MltG was examined by fluorescence microscopy. Strains SPH468 and SPH469 express EloR fused C-terminally to the monomeric superfolder gfp, *m(sf)gfp* (Liu *et al.*, 2017) using a Zn^{21} inducible promoter. EloR-m(sf)gfp was constructed by ligation of the *eloR* gene into the plasmid pMK17 (van Raaphorst *et al.*, 2017) allowing *eloR* to be fused to *m(sf)gfp* via a flexible, domain breaking linker encoding sequence. The plasmid pMK17 contains homology regions for integration in the non-essential *bgaA* locus of *S. pneumoniae*, and pMK17-eloR was transformed into *S. pneumoniae* RH425 and D39. The *m(sf)gfp-mltG* fusion was constructed by overlap extension PCR as described above. Strain SPH468, SPH469 and SPH470 pre-grown to OD_{600}= 0.4 were diluted 100-fold and grown for 2 hours prior to imaging. For SPH468 and SPH469, 0.2/0.02 mM $ZnCl_2$/$MnCl_2$ was added to the growth medium to induce expression of the fluorescent fusions. Imaging was performed on a Zeiss AxioObserver with the same software, camera and objective as mentioned above. An HXP 120 Illuminator (Zeiss) was used as a fluorescence light source. ImageJ was used to prepare the images for publication.

BACTH-assay

The BACTH two-hybrid system is based on the complementation of the T18 and T25 domains of the adenylate cyclase derived from Bordetella pertussis (Karimova *et al.*, 1998). When the T18 and T25 domains are brought together, it will restore adenylate cyclase activity, leading to the synthesis of cAMP, which in turn results in the expression of β-galactosidase. Proteins of interest are fused to the T18 and T25 domain, co-expressed in a *cya⁻ E. coli* strain, and the β-galactosidase production is detected by growing the cells on LB plates containing X-Gal. A positive interaction between two proteins will result in blue colonies. A negative interaction will appear as white colonies. The BACTH assays were performed as described by the manufacturer (Euromedex). Our genes of interest were cloned in frame with either the T18 or T25 encoding sequences in specific plasmids supplied by the manufacturer, giving rise to either N-terminally or C-terminally T18/T25 fusions. All plasmids used in BACTH analysis are listed in Supporting Information Table S1. The plasmids were first transformed into *E. coli* XL1-Blue cells, from which they were purified. Then, two plasmids, one encoding a T18 fusion and the other encoding a T25 fusion, were co-transformed into *cya*- BTH101 cells. Transformants were selected on LB plates containing both ampicillin (100 μg/ml) and kanamycin (50 μg/ml). Five random colonies were grown in liquid LB at 37°C with shaking. When reaching OD_{600} 0.5, 2.5 μl cell culture were spotted onto LB plates containing ampicillin, kanamycin, 0.5 mM IPTG and 40 μg/ml X-gal. The plates were incubated at 30°C overnight. Bacterial spots that appeared blue were regarded as a positive interaction between the two proteins of interest. Each experiment was repeated at least three times.

Labelling of PBPs with bocillin FL

Fluorescent labelling of PBPs with Bocillin FL was carried according to the protocol of Rutschman *et al.* (2007). Exponentially growing *S. pneumoniae* cells from 10 ml cultures were harvested at 4000*g* when reaching OD_{550}= 0.3. The cells were resuspended in 100 μl sodium phosphate buffer (20 mM, pH 7.2) with 0.2% Triton X-100. The samples were incubated at 37°C for 5 minutes to allow LytA to completely lyse the cells. The PBPs were fluorescently labelled by adding Bocillin FL to a final concentration of 3.3 μM followed by incubation at 37°C for 30 minutes. The labelled PBPs were separated by SDS-PAGE as described by Rutschman *et al.* and visualized in an Azure C400 imaging system.

Acknowledgements

The authors would like to thank Zhian Salehian and Dr. Davide Porcellato for excellent technical assistance.

Author contributions

Conception or design of study: DS, GAS, MK, LSH

Acquisition, analysis or interpretation of data: DS, GAS, ARW, MK, CAF, LSH

Writing of the manuscript: DS, GAS, MK, LSH

References

Alyahya, S.A., Alexander, R., Costa, T., Henriques, A.O., Emonet, T., and Jacobs-Wagner, C. (2009) RodZ, a component of the bacterial core morphogenic apparatus. Proc Natl Acad Sci USA 106: 1239–1244.

Bankevich, A., Nurk, S., Antipov, D., Gurevich, A.A., Dvorkin, M., Kulikov, A.S., *et al.* (2012) SPAdes: a new genome assembly algorithm and its applications to single-cell sequencing. J Comput Biol 19: 455–477.

Beilharz, K., Novakov a, L., Fadda, D., Branny, P., Massidda, O., and Veening, J.W. (2012) Control of cell division in *Streptococcus pneumoniae* by the conserved Ser/Thr protein kinase StkP. Proc Natl Acad Sci USA 109: E905– E913.

Berg, K.H., Stamsås, G.A., Straume, D., and Håvarstein, L.S. (2013) Effects of low PBP2b levels on cell morphology and peptidoglycan composition in *Streptococcus pneumoniae*. J Bacteriol 195: 4342–4354.

Ducret, A., Quardokus, E.M., and Brun, Y.V. (2016) MicrobeJ, a tool for high throughput bacterial cell detection and quantitative analysis. Nat Microbiol 1: 16077.

Echenique, J., Kadioglu, A., Romao, S., Andrew, P.W., and Trombe, M.C. (2004) Protein serine/threonine kinase StkP positively controls virulence and competence in *Streptococcus pneumoniae*. Infect Immun 72: 2434– 2437.

Eldholm, V., Johnsborg, O., Straume, D., Ohnstad, H.S., Berg, K.H., Hermoso, J.A., and Håvarstein, L.S. (2010) Pneumococcal CbpD is a murein hydrolase that requires a dual cell envelope binding specificity to kill target cells during fratricide. Mol Microbiol 76: 905–917.

Errington, J., Appleby, L., Daniel, R.A., Goodfellow, H., Partridge, S.R., and Yudkin, M.D. (1992) Structure and function of the *spoIIIJ* gene of *Bacillus subtilis*: a vegetatively expressed gene that is essential for σ^G activity at an intermediate stage of sporulation. J Gen Microbiol 138: 2609–2618.

Falk, S.P., and Weisblum, B. (2012) Phosphorylation of the *Streptococcus pneumoniae* cell wall biosynthesis enzyme MurC by a eukaryotic-like Ser/Thr kinase. FEMS Microbiol Lett 340: 19–23.

Fenton, A.K., El Mortaji, L., Lau, D.T.C., Rudner, D.Z., and Bernhardt, T.G. (2016) CozE is a member of the MreCD complex that directs cell elongation in *Streptococcus pneumoniae*. Nat Microbiol 2: 237.

Fleurie, A., Cluzel, C., Guiral, S., Freton, C., Galisson, F., Zanella-Cleon, I., Di Guilmi, A.M., and Grangeasse, C. (2012) Mutational dissection of the S/T-kinase StkP reveals crucial roles in cell division of *Streptococcus pneumoniae*. Mol Microbiol 83: 746–758.

Fleurie, A., Lesterlin, C., Manuse, S., Zhao, C., Cluzel, C., Lavergne, J.P., *et al.* (2014a) MapZ marks the division sites and positions FtsZ rings in *Streptococcus pneumoniae*. Nature 516: 259–262.

Fleurie, A., Manuse, S., Zhao, C., Campo, N., Cluzel, C., Lavergne, J.P., *et al.* (2014b) Interplay of the serine/threonine-kinase StkP and the paralogs DivIVA and GpsB in pneumococcal cell elongation and division. PloS Genet 10: e1004275.

Grangeasse, C. (2016) Rewiring the pneumococcal cell cycle with serine/threonine- and tyrosine-kinases. Trends Microbiol 24: 713–724.

Grishin, N.V. (1998) The R3H motif: a domain that binds single-stranded nucleic acids. Trends Biochem Sci 23: 329–330.

Hakenbeck, R., and Kohiyama, M. (1982) Purification of penicillin-binding protein 3 from *Streptococcus pneumoniae*. Eur J Biochem 127: 231–236.

Hardt, P., Engels, I., Rausch, M., Gajdiss, M., Ulm, H., Sass, P., *et al.* (2017) The cell wall precursor lipid II acts as a molecular signal for the Ser/Thr kinase PknB of *Staphylococcus aureus*. Int J Med Microbiol 307: 1–10.

Higuchi, R., Krummel, B., and Saiki, R.K. (1988) A general method of *in vitro* preparation and specific mutagenesis of DNA fragments: study of protein and DNA interactions. Nucleic Acids Res 16: 7351–7367.

Holeckova, N., Doubravov a, L., Massidda, O., Molle, V., Buriankov a, K., Benada, O., *et al.* (2015) LocZ is a new cell division protein involved in proper septum placement in *Streptococcus pneumoniae*. mBio 6: e01700–e01714.

Hollingworth, D., Candel, A.M., Nicastro, G., Martin, S.R., Briata, P., Gherzi, R., and Ramos, A. (2012) KH domains with impaired nucleic acid binding as a tool for functional analysis. Nucl Acids Res 40: 6873–6886.

Jaudzems, K., Jia, X., Yagi, H., Zhulenkovs, D., Graham, B., Otting, G., and Liepinsh, E. (2012) Structural basis for 5′end-specific recognition of single-stranded DANN by the R3H domain from human Sμbp-2. J Mol Biol 424: 42–53.

Johnsborg, O., Eldholm, V., Bjørnstad, M.L., and Ha˚varstein, L.S. (2008) A predatory mechanism dramatically increases the efficiency of lateral gene transfer in *Streptococcus pneumoniae* and related commensal species. Mol Microbiol 69: 245–253.

Karimova, G., Pidoux, J., Ullmann, A., and Ladant, D. (1998) A bacterial two-hybrid system based on a reconstituted signal transduction pathway. Proc Natl Acad Sci USA 95: 5752–5756.

Kearse, M., Moir, R., Wilson, A., Stones-Havas, S., Cheung, M., Sturrock, S., *et al.* (2012) Geneious basic: an integrated and extendable desktop software platform for the organization and analysis of sequence data. Bioinformatics 28: 1647–1649.

Kell, C.M., Sharma, U.K., Dowson, C.G., Town, C., Balganesh, T.S., and Spratt, B. (1993) Deletion analysis of the essentiality of penicillin-binding proteins 1A, 2B, and 2X of *Streptococcus pneumoniae*. FEMS Microbiol Lett 106: 171–175.

Lacks, S., and Hotchkiss, R.D. (1960) A study of the genetic material determining an enzyme in pneumococcus. Biochem Biophys Acta 39: 508–518.

Laemmli, U.K. (1970) Cleavage of structural proteins during the assembly of the head of bacteriophage T4. Nature 227: 680–685.

Land, A.D., and Winkler, M.E. (2011) The requirement for pneumococcal MreC and MreD is relieved by inactivation of the gene encoding PBP1a. J Bacteriol 193: 4166– 4179.

Liu, X., Gallay, C., Kjos, M., Domenech, A., Slager, J., van Kessel, S.P., *et al.* (2017) High-throughput CRISPRi phenotyping identifies new essential genes in *Streptococcus pneumoniae*. Mol Syst Biol 13: 931.

Lovering, A.L., and Strynadka, C.J. (2007) High-resolution structure of the major periplasmic domain from the cell shape-determining filament MreC. J Mol Biol 372: 1034– 1044.

Maestro, B., Novakova, L., Hesek, D., Lee, M., Leyva, E., Mobashery, S., *et al.* (2011) Recognition of peptidoglycan and β-lactam antibiotics by the extracellular domain of the Ser/Thr protein kinase StkP from *Streptococcus pneumoniae*. FEBS Lett 585: 357–363.

Manuse, S., Fleurie, A., Zucchini, L., Lesterlin, C., and Grangeasse, C. (2016) Role of eukaryotic-like serine/threonine kinases in bacterial cell division and morphogenesis. FEMS Microbiol Rev 40: 41–56.

Massidda, O., Novakova, L., and Vollmer, W. (2013) From models to pathogens: how much have we learned about *Streptococcus pneumoniae* cell division?. Environ Microbiol 15: 3133–3157.

Meeske, A.J., Riley, E.P., Robins, W.P., Uehara, T., Mekelanos, J.J., Kahne, D., *et al.* (2016) SEDS proteins are a widespread family of bacterial cell wall polymerases. Nature 537: 634–638.

Mir, M., Asong, J., Li, X., Cardot, J., Boons, G.J., and Husson, R.N. (2011) The extracytoplasmic domain of the *Mycobacterium tuberculosis* Ser/Thr kinase PknB binds specific muropeptides and is required for PknB localization. PLoS Pathog 7: e1002182.

Morlot, C., Bayle, L., Jacq, M., Fleurie, A., Tourcier, G., Galisson, F., *et al.* (2013) Interaction of penicillin-binding protein 2x and Ser/Thr protein kinase StkP, two key players in *Streptococcus pneumoniae* R6 morphogenesis. Mol Microbiol 90: 88–102.

Novakov a, L., Saskova, L., Pallova, P., Janecek, J., Novotna, J., Ulrych, A., *et al.* (2005) Characterization of a eukaryotic type serine/threonine protein kinase and protein phosphatase of *Streptococcus pneumoniae* and identification of kinase substrates. FEBS J 272: 1243–1254.

Philippe, J., Vernet, T., and Zapun, A. (2014) The elongation of ovococci. Microb Drug Resist 20: 215–221.

Rutschman, J., Maurer, P., and Hakenbeck, R. (2007) Detection of penicillin-binding proteins. In Molecular Biology of Streptococci. Hakenbeck, R., and Chhatwal, S. (eds). Norfolk: Horizon Bioscience, pp. 537–542.

Sauvage, E., Kerff, F., Terrak, M., Ayala, J.A., and Charlier, P. (2008) The penicillin-binding proteins: structure and role in peptidoglycan biosynthesis. FEMS Microbiol Rev 32: 234–258.

Seemann, T. (2014) Prokka: rapid prokaryotic genome annotation. Bioinformatics 30: 2068–2069.

Shah, I.M., Laaberki, M.H., Popham, D.L., and Dworkin, J. (2008) A eukaryotic-like Ser/Thr kinase signals bacteria to exit dormancy in response to peptidoglycan fragments. Cell 135: 486–496.

Stamsås, G.A., Straume, D., Salehian, Z., and Håvarstein, L.S. (2017) Evidence that pneumococcal WalK is regulated by StkP through protein-protein interaction. Microbiology 163: 383–399.

Straume, D., Stamsås, G.A., Berg, K.H., Salehian, Z., and Håvarstein, L.S. (2017) Identification of pneumococcal proteins that are functionally linked to penicillin-binding protein 2b (PBP2b). Mol Microbiol 103: 99–116.

Sun, X., Ge, F., Xiao, C.L., Yin, X.F., Ge, R., Zhang, L.H., and He, Q.Y. (2010) Phosphoproteomic analysis reveals the multiple roles of phosphorylation in pathogenic bacterium *Streptococcus pneumoniae*. J Proteome Res 9: 275–282.

Sung, C.K., Li, H., Claverys, J.P., and Morrison, D.A. (2001) An *rpsL* cassette, Janus, for gene replacement through negative selection in *Streptococcus pneumoniae*. Appl Environ Microbiol 67: 5190–5196.

Tsui, H.C.T., Zheng, J.J., Magallon, A.N., Ryan, J.D., Yunck, R., Rued, B.E., *et al.* (2016) Suppression of a deletion mutation in the gene

encoding essential PBP2b reveals a new lytic transglycosylase involved in peripheral peptidoglycan synthesis in *Streptococcus pneumoniae* D39. Mol Microbiol 100: 1039–1065.

Ulrych, A., Holecˇkova, N., Goldova, J., Doubravova, L., Benada, O., Kofronov a, O., *et al.* (2016) Characterization of pneumococcal Ser/Thr protein phosphatase *phpP* mutant and identification of a novel PhpP substrate, putative RNA binding protein JAG. BMC Microbiol 16: 6.

Valverde, R., Edwards, L., and Regan, L. (2008) Structure and function of KH domains. FEBS J 275: 2712–2726.

van den Ent, F., Leaver, M., Bendezu, F., Errington, J., de Boer, P., and Lowe, J. (2006) Dimeric structure of the cell shape protein MreC and its functional implications. Mol Microbiol 62: 1631–1642.

van Raaphorst, R., Kjos, M., and Veening, J.W. (2017) Chromosome segregation drives division site selection in *Streptococcus pneumoniae*. Proc Natl Acad Sci U S A. pii: 201620608. doi: 10.1073/pnas.1620608114.

Vollmer, W., Blanot, D., and de Pedro, M.A. (2008) Peptidoglycan structure and architecture. FEMS Microbiol Rev 32: 149–167.

Yunck, R., Cho, H., and Bernhardt, T.G. (2016) Identification of MltG as a potential terminase for peptidoglycan polymerization in bacteria. Mol Microbiol 99: 700–718.

Zapun, A., Vernet, T., and Pinho, M.G. (2008) The different shapes of cocci. FEMS Microbiol Rev 32: 345–360.

Suppressor mutations found in the *eloR* gene in Δ*pbp2b* mutants.

GTGGTAGTATTTACAGGTTCAACTGTTGAAGAAGCAATCCAGAAAGGATTGAAAGAATTA
GATATTCCAAGAATGAAGGCTCATATCAAAGTCATTTCTAGGGAGAAAAAAGGCTTTCTT
GGTCTATTTGGTAAAAAACCAGCCCAAGTGGATATTGAAGCGATTAGTGAAACGACTGTT
GTCAAAGCAAATCAACAGGTAGTAAAAGGCGTTCCGAAAAAAATCAATGATTTGAACGAG

GS6-strain ccgaaaaaa-tcaatgatttga

CCTGTGAAGACGGTTAGTGAAGAAACCGTTGACCTTGGTCATGTGGTTGATGCTATTAAA
AAAATAGAGGAAGAAGGTCAAGGTATTTCTGATGAAGTCAAGGCTGAAATCTTAAAACAT

aaa-tagaggaagaagg GS4-strain

GAAAGACATGCCAGCACTATCTTAGAAGAAACTGGTCACATTGAGATTTTAAATGAACTT
CAAATCGAGGAAGCGATGAGGGAAGAAGCAGGCGCTGATGACCTTGAAACTGAGCAAGAC

GS3-strain ttgaaagtgaaaacgaa

CAAGCTGAAAGTCAAGAACTAGAAGACTTGGGCTTGAAAGTTGAAACGAACTTTGATATT

ctttga

GAACAAGTAGCTACGGAAGTAATGGCTTATGTTCAAACGATTATTGATGACATGGATGTT
GAGGCTACACTTTCAAATGATTATAACCGTCGTAGCATCAATCTACAAATTGACACCAAC
GAACCAGGTCGTATTATCGGCTACCATGGTAAAGTCTTGAAGGCCTTGCAACTGTTGGCT
CAAAATTATCTTTACAACCGCTATTCCAGAACCTTCTACGTTACAATCAATGTCAATGAT
TATGTCGAACACCGTGCAGAAGTCTTGCAGACCTATGCGCAAAAATTGGCGACTCGTGTT
TTGGAAGAAGGGCGCAGTCATAAAACAGATCCAATGTCAAATAGCGAACGCAAGATTATC
CATCGTATTATTTCACGTATGGATGGCGTGACTAGTTACTCTGAAGGTGATGAGCCAAAT
CGCTATGTTGTTGTAGATACAGAATAA

Fig. S1. Nucleic acid sequence of the *eloR* (*spr1851*) gene. The illustration shows positions of mutations leading to truncated *eloR* genes in the GS3, GS4 and GS6 suppressor strains. Premature stop codons are shown in a yellow background.

Labelling of PBPs with Bocillin FL.

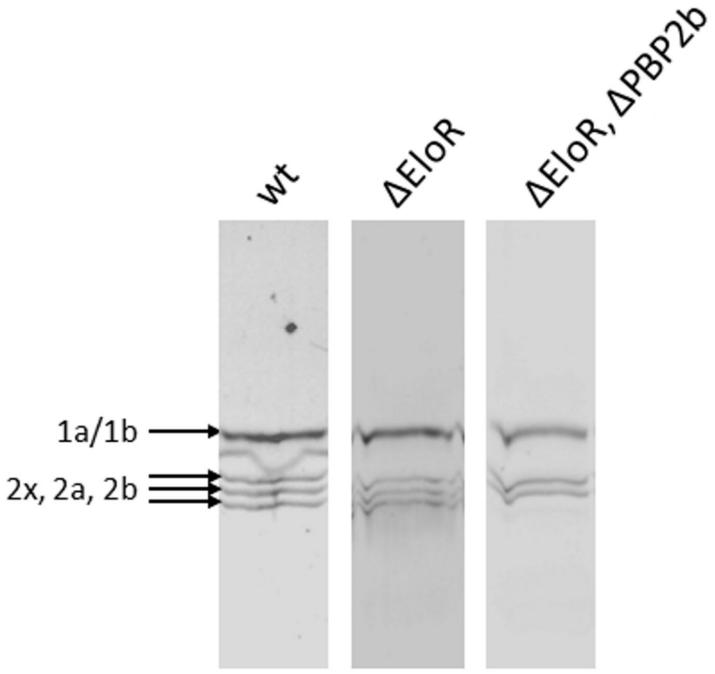

Fig. S2. Visualization of PBPs in strain RH425 (wt), SPH445 (Δ*eloR*) and SPH446 (Δ*eloR*, Δ*pbp2b*) after labelling with Bocillin FL and separation by SDS-PAGE.

Localization of EloR.

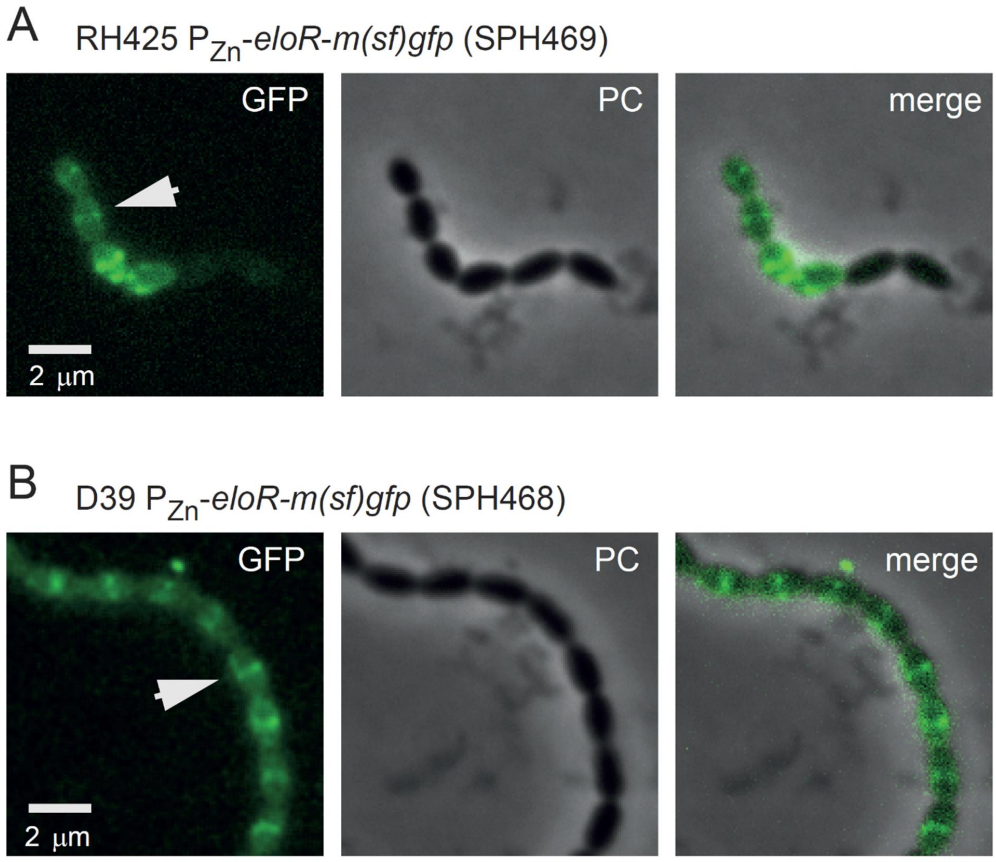

Fig. S3. A. Localization of EloR-m(sf)GFP in a *S. pneumoniae* RH425 (A) and D39 (B). The fusion gene was expressed from an ectopic locus and gene expression was induced by addition of $ZnCl_2/MnCl_2$ to the growth medium. The arrows points to cells were EloR-m(sf)GFP clearly localizes to mid-cell. Phase contrast and GFP images are shown individually and merged. The scale bar is 2 μm.

Immunodetection of Flag-StkP, Flag-StkP^{K42M} and Flag-StkP$^{\Delta PASTA}$ in cell membranes.

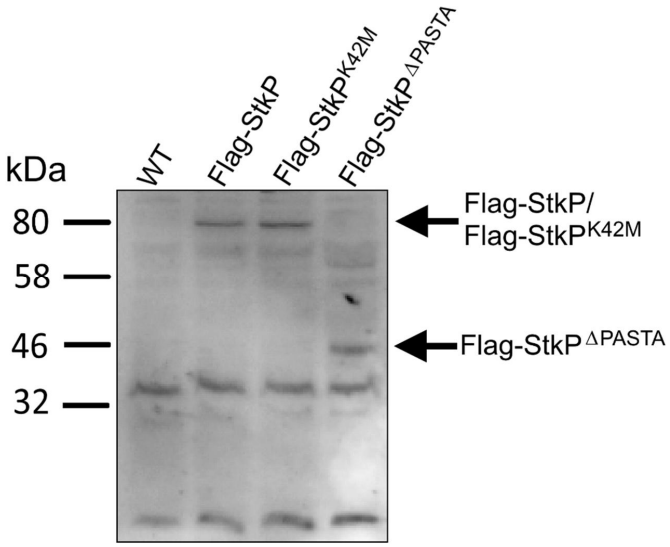

Fig. S4. Detection of Flag-StkP, Flag-StkP^{K42M} and Flag-StkP$^{\Delta PASTA}$ in cell membranes derived from strain SPH453, SPH454 and SPH455, respectively. Both Flag-StkP^{K42M} and StkP$^{\Delta PASTA}$ were found in the membrane fraction. Membranes isolated from wild type cells (RH425) was used as a Flag-negative control.

Cell morphology.

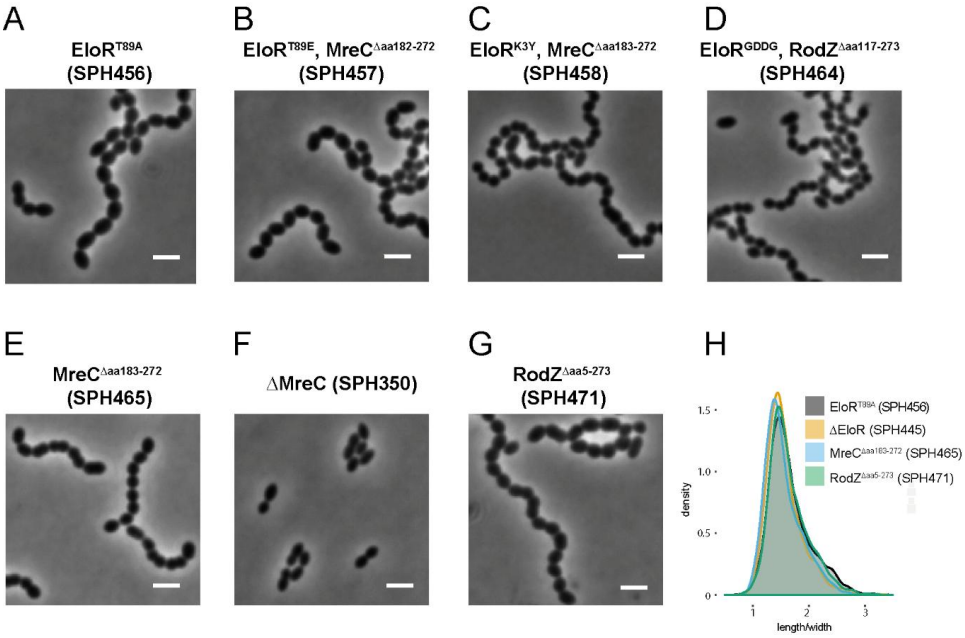

Fig. S5. Representative phase contrast images of strains EloR^{T89A} (A), EloR^{T89E} with suppressor mutation MreC$^{\Delta aa182-272}$ (B), ElorR^{K3Y} with suppressor mutation MreC$^{\Delta aa183-272}$ (C), EloR^{GDDG} with suppressor mutation RodZ$^{\Delta aa117-273}$ (D), MreC$^{\Delta aa183-272}$ (E), ΔMreC (F), RodZ$^{\Delta aa5-273}$ (G). The scale bars are 2 μm. (H) Density plots of cell shape distributions for mutant strains EloR^{T89A}, ΔEloR, MreC$^{\Delta aa183-272}$, RodZ$^{\Delta aa5-273}$ and ΔEloR. Density plots were used instead of histogram for easier comparison of four different distributions.

Suppressor mutations found in the *mreC* gene in strains expressing EloR^{T89E} or EloR^{K3Y}.

ATGAACCGTTTTAAAAAATCAAAATATGTCATTATTGTTTTTGTCACTGTTCTGCTTGTGTCAGCT
CTCTTAGCGACGACTTATTCAAGTACAATTGTGACAAAATTAGGAGATGGAATCTCATTGGTTGAT
AGAGTTGTACAAAAACCTTTTCAGTGGTTTGATTCTGTCAAATCAGATTTGGCTCATTTGACACGA
ACATATAATGAAAATGAAAGTTTGAAGAAACAGCTTTACCAATTAGAAGTTAAATCAAATGAGGTG
GAAAGTTTAAAGACAGAAAATGAACAACTGCGCCAATTGCTTGATATGAAGTCTAAATTGCAAGCC
ACAAAGACTTTAGCAGCAGATGTTATTATGCGTTCTCCGGTATCTTGGAAGCAGGAGTTGACCTTA
GATGCAGGTAGATCAAAAGGTGCTTCTGAGAACATGTTAGCTATTGCAAATGGTGGCTTGATTGGG
AGTGTTTCAAAAGTAGAGGAGAACTCTACTATAGTCAACCTTCTGACAAATACGGAAAATGCTGAT
AAGATTTCTGTTAAAATTCAACATGGCTCTACTACAATTTATGGAATT

tt-aaa taa

ATTATTGGCTATGACAAGGAAAATGACGTTCTTAAAATTAGCCAATTAAATAGTAATAGCGATATT
AGTGCGGGAGATAAGGTGACTACTGGTGGATTAGGAAACTTTAACGTTGCTGATATTCCTGTTGGT
GAAGTGGTTGCCACAACGCATAGTACAGACTATTTGACACGAGAAGTAACTGTTAAATTGAGTGCA
GATACTCATAATGTAGATGTGATAGAATTAGTGGGGAATTCATAA

Fig. S6. Nucleic acid sequence of the *mreC* (*spr2023*) gene. Deletion of an adenosine at position 541 (red) leading to a frame shift was found in strains SPH457. Substitution of the cytosine to an adenosine at position 547 (green) introducing the stop codon TAA was found in strains SPH458, SPH459, SPH460 and SPH461.

Suppressor mutations found in the *rodZ* gene in strains expressing EloR^{T89E} or EloR^{GDDG}.

ATGAGAAAAAAAACAATTGGAGAGGTTTTACGATTAGCTAGAATCAATCAGGGATTGAGTTTAG

gag-aaaaaaacaa

ATGAATTGCAGAAAAAGACAGAAATCCAGTTAGATATGTTGGAAGCAATGGAAGCAGACGATTTCG
ATCAACTTCCAAGTCCTTTTTACACGCGTTCTTTCTTGAAAAAATATGCATGGGCTGTTGAGTTAG
ATGACCAAATTGTTTTGGATGCTTATGATTCTGGGAGTATGATTACTTATGAGGAAGTAGATGTTG
ATGAAGATGAGTTGACAGGTCGTAGACGTTCAAGTAAGAAAAAGAAGAAAAAAACATCATTTTTAC
CTTTTATTTTATTTTATCCTTTTTGCTTTATCGATTTTAATTTTTGTGACTTATTAT

acc-----tttattt

GTTTGGAACTATATTCAAACTCAACCAGAGGAGCCTTCTCTTTCTAATTACAGTGTGGTTCAATCA
ACAAGTTCAACTAGCTCTGTTCCCCACTCCTCAAGTAGTAGTTCTTCTAGTATAGAATCAGCTATA
AGTGTATCAGGCGAAGGAAATCATGTAGAAATCGCTTATAAGACAAGTAAGGAAACAGTTAAATTG
CAATTGGCAGTTTCAGATGTTACAAGTTGGGTCAGTGTTTCAGAAAGCGAACTTGAGGGCGGTGTA
ACCTTATCGCCAAAGAAGAAAAGTGCAGAAGCAACAGTTGCAACTAAAAGTCCTGTAACAATTACG
TTAGGTGTTGTAAAAGGTGTTGATTTGACAGTAGATAATCAGACTGTTGATTTATCGAAATTAACA
GCTCAGACTGGACAAATCACTGTAACCTTTACTAAAAATTAA

Fig. S7. Nucleic acid sequence of the *rodZ* (*spr2028*) gene. Deletion of one of the adenosine (red) in adenosine stretch of after position five leads to a frame shift and premature termination of protein translation. This suppressor mutation was found in strains SPH462 and SPH463. Deletion of TTTAT after position 330 (green) leading to a frame-shift and premature termination of translation was found in strain SPH464.

Deletion of *pbp2b* or *rodA* does not affect the growth rate in an MreC$^{\Delta aa183\text{-}272}$ background.

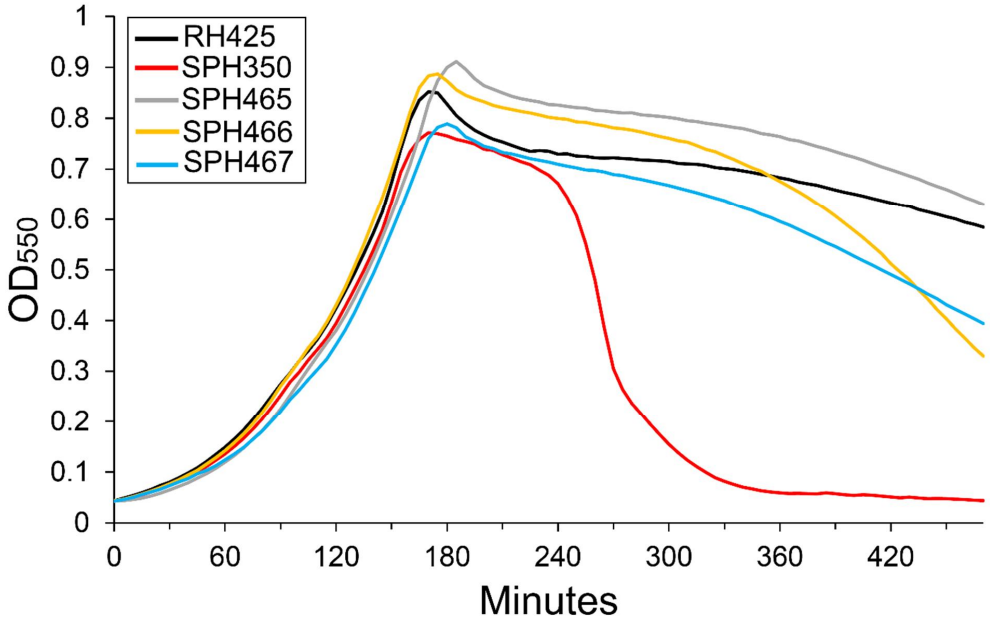

Fig. S8. The strains SPH350 (Δ*mreC*), SPH465 (*mreC*$^{\Delta aa183\text{-}272}$), SPH466 (*mreC*$^{\Delta aa183\text{-}272}$, Δ*pbp2b*) and SPH467 (*mreC*$^{\Delta aa183\text{-}272}$, Δ*rodA*) displayed similar growth rates as wild type *S. pneumoniae* (RH425). Noteworthy, the Δ*mreC* strain entered autolysis earlier than the other mutants.

The expression level and localization of MltG in a Δ*eloR* mutant.

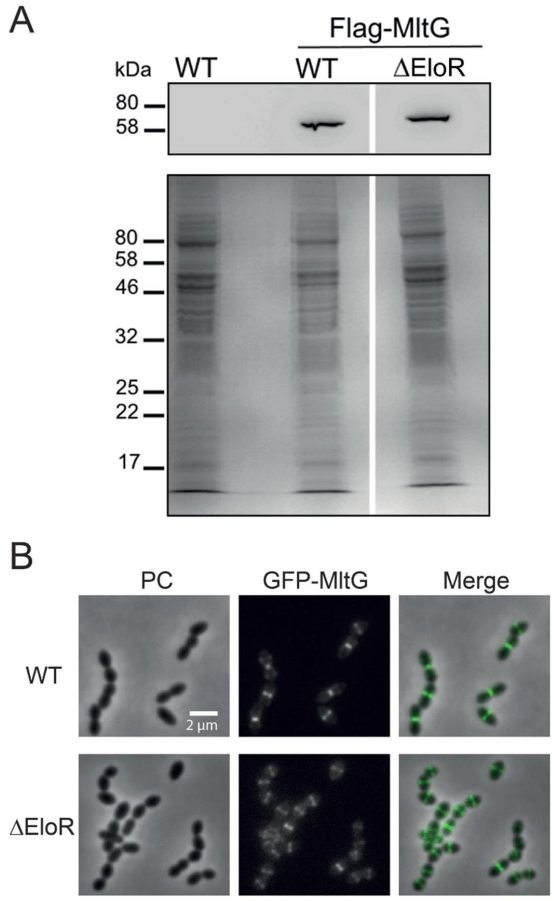

Fig. S9. A. Immunodetection of Flag-MltG in membrane fractions derived from strain SPH473 (WT) and SPH474 (Δ*eloR*) are shown in the upper panel. Membranes isolated from strain RH425 was used as wild type Flag-negative control. The lower panel shows a coomassie blue stained gel as loading control. B. Localization of m(sf)GFP-MltG in wild-type cells (SPH470) and ΔEloR (SPH472). Phase contrast (PC) and GFP images are shown individually and merged. The scale bar is 2 µm.

Experimental Procedures

Bacterial strains, cultivation and transformation.

Bacterial strains used in this study are listed in Table S1. Strains of *Escherichia coli* were grown in Luria Bertani broth with shaking or on LB agar plates at 30 or 37°C. When appropriate, the following antibiotic concentrations were used in the growth medium: ampicillin = 100 μg/ml and kanamycin = 50 μg/ml. Chemically competent *E. coli* was transformed by typical heat-shock at 42°C for 30 seconds. *S. pneumoniae* was grown in C medium (Lacks and Hotchkiss, 1960) at 37°C without shaking. When selecting for *S. pneumoniae* transformants, the pneumococcus was grown on Todd-Hewitt agar plates in an oxygen-depleted chamber using AnaeroGen™ bags from Oxoid. Gene knockouts or introduction of point mutations in the *S. pneumoniae* genome were performed by natural transformation. Pneumococcal cultures growing exponentially at OD_{550} = 0.05-0.1 were mixed with 100-200 ng of the transforming DNA and CSP to a final concentration of 250 ng/ml. After 2 hours of incubation at 37°C, transformants were selected on TH-agar containing the appropriate antibiotic (kanamycin = 400 μg/ml, streptomycin = 200 μg/ml and tetracycline = 1 μg/ml).

When following the growth of *S. pneumoniae* over time, pneumococcal strains where grown in 96-well Corning NBS clear-bottom plates at 37°C. First, cells were grown to exponential growth phase (OD_{550} = 0.2 – 0.3) in 5 ml volumes, collected by centrifugation at 4000 x *g* and resuspended in fresh C medium to OD_{550} = 0.05. Then 300 μl cell culture were transferred to the wells in a microtiter plate, and OD_{550} was measured automatically every 5 minutes using a Synergy H1 Hybrid Reader (BioTek).

Construction of DNA amplicons

DNA amplicons used to transform *S. pneumoniae* were constructed by overlap extension PCR based on the principle of Higuchi *et al.* (1988). Most gene knockouts created in this study were made by using the Janus cassette (Sung *et al*., 2001), or in some cases a tetracycline resistance cassette. Basically, a ~1000 bp region upstream and downstream of a desired target gene were fused the 5' and 3' end of the knockout cassette as described in previous works (Johnsborg *et al*., 2008; Eldholm *et al*., 2010). By using a streptomycin resistant strain, the Janus cassette can be deleted by replacing it with a DNA fragment containing flanking sequences that are homologous to the corresponding regions flanking the Janus cassette in the genome. All primers used to create DNA amplicons in the present work are listed in Table S2.

Construction of PBP2b suppressor mutants

Based on our previous work with PBP2b, which showed that cells depleted for PBP2b becomes very sensitive towards LytA (Berg *et al*., 2013), we chose to knock out *pbp2b* in both a LytA+ and a LytA- background. A fragment carrying the Janus cassette fused to the flanking regions of *pbp2b* was transformed into strain RH4 (LytA+) and RH6 (LytA-). After 24 hours of incubation at 37°C, three colonies had appeared on the plate carrying the LytA+ strain. PCR confirmed that two of the three transformants were *bona fide* Δ*pbp2b* knockouts. Of the two correct Δ*pbp2b* mutants, one was genome sequenced and named G1 (Table S1). The plate with the LytA- strain also contained 3 colonies after 24 hours of incubation, 5 colonies after 48 hours and ~20 new colonies after 6 days of incubation. PCR screening identified five transformants to be *bona fide* Δ*pbp2b* mutants (GS2-GS6). Strain GS1-GS6 were genome sequenced to look for suppressor mutations.

Whole genome sequencing

The strains RH425, GS1-GS6, SPH445 and SPH456 – SPH464 were grown in 10 ml C medium and collected at 4000 x *g* when reaching OD_{550} = 0.4. Genomic DNA was isolated by using the NucleoBond® AXG 100 kit from Macherey-Nagel according to the manufacturer's protocol. DNA library was created by using the Nextera XT DNA Library Preparation Kit (Illumina) by following the protocol of the manufacturer, and genome sequencing was done by using an Illumina MiSeq. The RH425 raw sequences were assembled to the reference genome *S. pneumoniae* R6 (NC_003098.1) using SPAdes v3.10.0 (Bankevich *et al*., 2012) and annotated using the Prokka pipeline (Seemann, 2014). Genomic analysis of the GS1-GS6, SPH445 and SPH456-464 sequences, including sequence mapping, coverage calculation, variant calling and visualization, was performed using Geneious v8.1.9 (Kearse *et al*., 2012).

SDS-PAGE and immunoblotting

To detect Flag-EloR and its phosphorylated form, Flag-EloR was first isolated from a 50 ml cell culture by performing an immunoprecipitation assay using Anti-Flag antibodies conjugated to agarose beads (ANTI-FLAG® M2 Affinity Gel, Sigma). RH425 (WT) and pneumococci expressing Flag-EloR in different genetic backgrounds (SPH448 – SPH452) were harvested at OD_{550} = 0.3, and auto-lysed in 1 ml of binding buffer (50 mM Tris-HCl [pH = 7.4], 150 mM NaCl, 1 mM EDTA, 1% Triton X-100) by triggering the LytA activity at 37°C for 5 minutes. The lysate was incubated with 40 µl ANTI-FLAG® M2 Affinity Gel at 4°C over-night with gentle mixing. The agarose beads were then washed 3 times in 500 µl TBS (50 mM Tris-HCl [pH = 7.4], 150 mM NaCl) as described by the manufacturer, before 60 µl of SDS-sample buffer was added and the beads were heated to 95°C for 5 minutes. Eight µl samples were separated by SDS-PAGE using a 12% separation gel and the buffer conditions described by Laemmli (1970). The Flag-fused versions of StkP (Flag-StkP, Flag-$StkP^{K42M}$, and Flag-$StkP^{\Delta PASTA}$) were detected in the membranes from strain SPH453, SPH454 and

SPH455, respectively. Flag-MltG was detected in membranes from strain SPH473 and SPH474. Membranes were isolated from 30 ml cell cultures at OD_{550} = 0.3 as described by Straume *et al*. (2017b). The membranes were solubilized in 100 µl SDS-sample buffer, and the membrane proteins in 15 µl volumes were separated by SDS-PAGE. A 12% separation gel was used for the MltG fusions and a 10% separation gel for the StkP fusions.

After electrophoresis, the proteins were transferred to a PVDF membrane by electroblotting and both Flag-fused proteins and proteins containing phosphorylated threonines were detected as described previously by Stamsås *et al*. (2017).

Microscopy techniques and construction of fluorescent fusion proteins

Phase contrast microscopy was used to analyze the morphology of different *S. pneumoniae* mutant strains. Pneumococcal strains were pre-grown to OD_{600} = 0.4, then diluted 100-fold and grown to OD_{600} = 0.1 prior to microscopy. Cells were spotted directly onto slide with a layer of 1.2 % agarose in PBS. Images were acquired using a Zeiss AxioObserver with ZEN Blue software, and an ORCA-Flash 4.0 V2 Digital CMOS camera (Hamamatsu Photonics) using a 100x phase-contrast objective. For cell detection and analysis of cell morphologies, the ImageJ plugin MicrobeJ (Ducret *et al*., 2016) was used. Data analysis and plotting was performed using RStudio.

The subcellular localization of EloR and MltG was examined by fluorescence microscopy. Strains SPH468 and SPH469 express EloR fused C-terminally to the monomeric superfolder gfp, m(sf)gfp (Liu *et al*., 2016) using a Zn^{2+} inducible promoter. EloR-m(sf)gfp was constructed by ligation of the *eloR* gene into the plasmid pMK17 (van Raaphorst *et al*., 2016) allowing *eloR* to be fused to *m(sf)gfp* via a flexible, domain breaking linker encoding sequence. The plasmid pMK17 contains homology regions for integration in the non-essential *bgaA* locus of *S. pneumoniae*, and pMK17-eloR was transformed into *S. pneumoniae* RH425 and D39. The *m(sf)gfp-mltG* fusion was

constructed by overlap extension PCR as described above. Strain SPH468, SPH469 and SPH470 pre-grown to OD_{600} = 0.4 were diluted 100-fold and grown for 2 hours prior to imaging. For SPH468 and SPH469, 0.2/0.02 mM $ZnCl_2$/$MnCl_2$ was added to the growth medium to induce expression of the fluorescent fusions. Imaging was performed on a Zeiss AxioObserver with the same software, camera and objective as mentioned above. An HXP 120 Illuminator (Zeiss) was used as a fluorescence light source. ImageJ was used to prepare the images for publication.

BACTH-assay

The BACTH two-hybrid system is based on the complementation of the T18 and T25 domains of the adenylate cyclase derived from *Bordetella pertussis* (Karimova *et al.*, 1998). When the T18 and T25 domains are brought together, it will restore adenylate cyclase activity, leading to the synthesis of cAMP, which in turn results in the expression of β-galactosidase. Proteins of interest are fused to the T18 and T25 domain, co-expressed in a *cya- E. coli* strain, and the β-galactosidase production is detected by growing the cells on LB plates containing X-Gal. A positive interaction between two proteins will result in blue colonies. A negative interaction will appear as white colonies. The BACTH assays were performed as described by the manufacturer (Euromedex). Our genes of interest were cloned in frame with either the T18 or T25 encoding sequences in specific plasmids supplied by the manufacturer, giving rise to either N-terminally or C-terminally T18/T25 fusions. All plasmids used in BACTH analysis are listed in Table S1. The plasmids were first transformed into *E. coli* XL1-Blue cells, from which they were purified. Then, two plasmids, one encoding a T18 fusion and the other encoding a T25 fusion, were co-transformed into *cya-* BTH101 cells. Transformants were selected on LB plates containing both ampicillin (100 µg/ml) and kanamycin (50 µg/ml). Five random colonies were grown in liquid LB at 37°C with shaking. When reaching OD_{600} ~0.5, 2.5 µl cell culture were spotted onto LB plates containing ampicillin, kanamycin, 0.5

mM IPTG and 40 µg/ml X-gal. The plates were incubated at 30°C overnight. Bacterial spots that appeared blue were regarded as a positive interaction between the two proteins of interest. Each experiment was repeated at least three times.

Labelling of PBPs with Bocillin FL

Fluorescent labelling of PBPs with Bocillin FL was carried according to the protocol of Rutchman *et al*. (Rutschman *et al*., 2007). Exponentially growing *S. pneumoniae* cells from 10 ml cultures were harvested at 4000 x *g* when reaching OD_{550} = 0.3. The cells were resuspended in 100 µl sodium phosphate buffer (20 mM, pH 7.2) with 0.2 % Triton X-100. The samples were incubated at 37°C for 5 minutes to allow LytA to completely lyse the cells. The PBPs were fluorescently labeled by adding Bocillin FL to a final concentration of 3.3 µM followed by incubation at 37°C for 30 minutes. The labelled PBPs were separated by SDS-PAGE as described by Rutchman *et al.* (2007) and visualized in a Azure C400 imaging system.

Table S1. Strains and plasmids used in this study.

Name	Relevant characteristics	Source
***S. pneumoniae* strains**		
R704	R6 derivative, *comA*::*ermAM*; Ery^R	JP. Claverys*
RH425	R704, but streptomycin resistant; Ery^R, Sm^R	(Johnsborg *et al.*, 2009)
D39	wild-type, serotype 2	(Avery *et al*., 1944)
RH1	R704 derivative; Δ*comA* Δ*ebg*; Ery^R Spc^R	(Johnsborg *et al.*, 2008)
RH4	Δ*comA*, Δ*ebg*, Δ*hirL*::*lacZ*; Ery^R, Spc^R,Cm^R, Sm^R	(Eldholm *et al.*, 2009)

RH6	Δ*comA*, Δ*ebg*, Δ*hirL*::*lacZ*, Δ*lytA*; Ery^R, Spc^R, Cm^R, Sm^R	(Eldholm *et al.*, 2009)
GS1	Δ*comA*, Δ*pbp2b*::janus, *mltG*^{A505V}; Ery^R, Kan^R	This work
GS2	Δ*comA*, Δ*lytA*, Δ*pbp2b*::janus, *mltG*^{mut}; Ery^R, Kan^R	This work
GS3	Δ*comA*, Δ*lytA*, Δ*pbp2b*::janus, *eloR*^{mut}; Ery^R, Kan^R	This work
GS4	Δ*comA*, Δ*lytA*, Δ*pbp2b*::janus, *eloR*^{mut}; Ery^R, Kan^R	This work
GS5	Δ*comA*, Δ*lytA*, Δ*pbp2b*::janus, *mltG*$^{\Delta aa169\text{-}551}$; Ery^R, Kan^R	This work
GS6	Δ*comA*, Δ*lytA*, Δ*pbp2b*::janus, *eloR*^{mut}; Ery^R, Kan^R	This work
SPH156	Δ*comA*, P_{comX}-*pbp2b*, Δ*pbp2b*$_{wt}$::Janus; Ery^R, Kan^R	(Berg *et al.*, 2013)
SPH317	Δ*comA,* P_{pcsB}::*luc*, *stkP*^{K42M}; Ery^R, Sm^R	(Stamsås *et al.*, 2017)
SPH350	Δ*comA*, Δ*mreC*; Ery^R, Sm^R	(Straume *et al.*, 2017a)
SPH445	Δ*comA*, Δ*eloR*; Ery^R, Sm^R	This work
SPH446	Δ*comA*, Δ*eloR,* Δ*pbp2b*::janus; Ery^R, Kan^R	This work
SPH447	Δ*comA*, Δ*eloR*, Δ*rodA*::janus; Ery^R, Kan^R	This work
SPH448	Δ*comA*, *flag-eloR*; Ery^R, Sm^R	This work
SPH449	Δ*comA*, *flag-eloR*^{T89A}; Ery^R, Sm^R	This work
SPH450	Δ*comA*, *flag-eloR*, Δ*stkP*::janus; Ery^R, Kan^R	This work
SPH451	Δ*comA*, *flag-eloR*, *stkP*^{K42M}; Ery^R, Sm^R	This work
SPH452	Δ*comA*, *flag-eloR*, *stkP*$^{\Delta PASTA}$; Ery^R, Sm^R	This work
SPH453	Δ*comA*, *flag-stkP*; Ery^R, Sm^R	This work
SPH454	Δ*comA*, *flag-stkP*^{K42M}; Ery^R, Sm^R	This work
SPH455	Δ*comA*, *flag-stkP*$^{\Delta PASTA}$; Ery^R, Sm^R	This work
SPH456	Δ*comA*, *eloR*^{T89A}; Ery^R, Sm^R	This work
SPH457	Δ*comA*, *eloR*^{T89E}, *mreC*$^{\Delta aa182\text{-}272}$; Ery^R, Sm^R	This work
SPH458	Δ*comA*, *eloR*^{K3Y}, *mreC*$^{\Delta aa183\text{-}272}$; Ery^R, Sm^R	This work
SPH459	Δ*comA*, *eloR*^{T89E}, *mreC*$^{\Delta aa183\text{-}272}$; Ery^R, Sm^R	This work
SPH460	Δ*comA*, *eloR*^{T89E}, *mreC*$^{\Delta aa183\text{-}272}$; Ery^R, Sm^R	This work

SPH461	Δ*comA*, *eloR*^{T89E}, *mreC*$^{\Delta aa183-272}$; Ery^R, Sm^R	This work
SPH462	Δ*comA*, *eloR*^{T89E}, *rodZ*$^{\Delta aa5-273}$; Ery^R, Sm^R	This work
SPH463	Δ*comA*, *eloR*^{T89E}, *rodZ*$^{\Delta aa5-273}$; Ery^R, Sm^R	This work
SPH464	Δ*comA*, *eloR*^{GDDG}, *rodZ*$^{\Delta aa117-273}$; Ery^R, Sm^R	This work
SPH465	Δ*comA*, *mreC*$^{\Delta aa183-272}$; Ery^R, Sm^R	This work
SPH466	Δ*comA*, *mreC*$^{\Delta aa183-272}$, Δ*pbp2b*::janus; Ery^R, Kan^R	This work
SPH467	Δ*comA*, *mreC*$^{\Delta aa183-272}$, Δ*rodA*::janus; Ery^R, Kan^R	This work
SPH468	D39, *bgaA*::P$_{Zn}$-*eloR*-linker-*m(sf)gfp*; Tet^R	This work
SPH469	Δ*comA*, *bgaA::*P$_{Zn}$-*eloR*-linker-*m(sf)gfp*; Ery^R, Sm^R,Tet^R	This work
SPH470	Δ*comA, m(sf)GFP-mltG*; Ery^R, Sm^R	This work
SPH471	Δ*comA*, *rodZ*$^{\Delta aa5-273}$; Ery^R, Sm^R	This work
SPH472	Δ*comA,* Δ*eloR*::janus, *m(sf)GFP-mltG*; Ery^R, Kan^R	This work
SPH473	Δ*comA, flag-mltG*; Ery^R, Sm^R	This work
SPH474	Δ*comA,* Δ*eloR*, *flag-mltG*; Ery^R, Sm^R	This work
SPH475	Δ*comA*, *flag-eloR*, *mreC*$^{aa183-272}$; Ery^R, Sm^R	This work
***E. coli* strains**		
XL1-Blue	Host strain	Agilent Technologies
BTH101	BACTH expression strain, *cya-*	Euromedex
Plasmids		
pMK17	*bgaA*' TetR P$_{Zn}$-MCS-linker-*m(sf)gfp* '*bgaA*	(van Raaphorst *et al.*, 2017)
pMK17-eloR	*bgaA*' TetR P$_{Zn}$-*eloR*-linker-*m(sf)gfp* '*bgaA*	This work
pUT18C	Plasmid used in BACTH analyses	Euromedex
pKT25	Plasmid used in BACTH analyses	Euromedex
pKNT25	Plasmid used in BACTH analyses	Euromedex
pKT25-zip	T25 fused to a leucine zipper domain	Euromedex
pUT18C-zip	T18 fused to a leucine zipper domain	Euromedex
pUT18C-mreC	T18 domain fused to the N-terminus of MreC	This work

pUT18C-mreC^{N182}	T18 domain fused to the N-terminus of the N-terminal 182 aa of MreC	This work
pKT25-mreC	T25 domain fused to the N-terminus of MreC	This work
pKT25-mreC^{N182}	T25 domain fused to the N-terminus of the N-terminal 182 aa of MreC	This work
pUT18C-eloR	T18 domain fused to the N-terminus of EloR	This work
pKT25-pbp1a	T25 domain fused to the N-terminus of PBP1a	This work
pKT25-pbp1b	T25 domain fused to the N-terminus of PBP1b	This work
pKT25-pbp2a	T25 domain fused to the N-terminus of PBP2a	This work
pKT25-stkP	T25 domain fused to the N-terminus of StkP	(Stamsås *et al.*, 2017)
pKNT25-mreD	T25 domain fused to the C-terminus of MreD	(Straume *et al.*, 2017a)
pKT25-cozE	T25 domain fused to the N-terminus of CozE	(Straume *et al.*, 2017a)
pKT25-pbp2b	T25 domain fused to the N-terminus of PBP2b	(Straume *et al.*, 2017a)
pKT25-rodZ	T25 domain fused to the N-terminus of RodZ	This work
pUT18C-rodZ	T18 domain fused to the N-terminus of RodZ	This work
pKT25-mltG	T25 domain fused to the N-terminus of MltG	This work
pUT18C-mltG	T18 domain fused to the N-terminus of MltG	This work

*Gift from Professor Jean-Pierre Claverys, CNRS, Toulouse, France.

Table S2. Primers used in the study.

Primer	Sequence (5` → 3`)	Reference
Primers used to create the Δ*pbp2b*::janus amplicon and screening for the *pbp2b* gene		
khb129	CGATAAAGAAGAGCATAGGAAG	(Berg *et al.*, 2013)
khb132	TCCCAATCAATGGTTTCATTGG	(Berg *et al.*, 2013)
gs407	AGGTCCTACACCATTTGTTAG	This work
khb443	CCGATATGAGCATCTTGCAC	This work

khb427	TACGGAATTCCTAATTCATTGGATGGTATTTTTG	This work
Kan484F	GTTTGATTTTTAATGGATAATGTG	(Johnsborg *et al*., 2008)
Primers used to create the Δ*eloR*::janus amplicon		
ds374	CGAAACCTTGGGATACGCAG	This work
ds375	CACATTATCCATTAAAAATCAAACTACCAGATTCC TCCTTATTTATTTC	This work
ds376	TTAAATGTGCTATAATACTAGAAAATACTTGTAAA ATCAGGTTTATCCTGATTTT	This work
ds377	CAGCACCCACGTTAAGCAAC	This work
Primers used for fusion of FLAG-tag to EloR		
gs515	CCATCATGATCTTTATAATCCACTACCAGATTCCTC CTTATTTATTTC	This work
gs516	GTGGATTATAAAGATCATGATGGTGATTATAAAGA TCATGATATTGATTATAAAGATGATGATGATAAAG TGGTAGTATTTACAGGTTCAA	This work
Primers used for pMK17-eloR		
mk76	GCTCGGATCCAGGAGGAATCTGGTAaTGGTAG	This work
mk77	CGTAGCGGCCGCTTCTGTATCTACAACAACATAGC	This work
Primers used for fusion of *m(sf)gfp and flag-tag to mltG*		
ds391	TTGGATTATAAAGATCATGATGGTGATTATAAAGA TCATGATATTGATTATAAAGATGATGATGATAAAA GTGAAAAGTCAAGAGAAGAAG	This work
ds392	CCATCATGATCTTTATAATCCAAAAGTTTTTCCTCC TTGTTGATAATC	This work
ds361	AAACTAGCCGCAGGTTGCTC	(Straume *et al.*, 2017a)
ds362	AATTAAGATCATTCAGGCAAGC	(Straume *et al*., 2017a)
ds401	GCTAGTTCCAGCTTTAGCTGC	This work
mk48	ATGTCAAAAGGAGAAGAGCTGTTCAC	This work
mk49	AACAGCTCTTCTCCTTTTGACATAAGTTTTTCCTCCT TGTTGATAA	This work
mk50	GCAGCTAAAGCTGGAACTAGCAGTGAAAAGTCAAG AGAAGAAG	This work
mk52	GAGAGTCCTGATGAGCTGCT	This work
mk53	TGAAACTGACAAAGTCAGTAAC	This work
Primers used to create N-terminally flag-fused versions of StkP		
ds434	ATGGATTATAAAGATCATGATGGTGATTATAAAGA TCATGATATTGATTATAAAGATGATGATGATAAAA TCCAAATCGGCAAGATTTTTG	This work

ds435	CCATCATGATCTTTATAATCCATTCATTCTGCATCC TCCTCGTTC	This work
ds436	CTCATTTTGATTATCCATCTGCTTTTAGGCAATGGT TGCAGGAGTTC	This work
ds437	AAGCAGATGGATAATCAAAATGAG	This work
khb410	AGAAATATTAGGTAGTGTTTGTC	(Straume *et al.*, 2017a)
khb411	CCAGACAGTCATGCCCAAAATC	(Straume *et al.*, 2017a)

Primers used to create the Δ*mreC*::janus amplicon, *mreC*$^{\Delta aa183\text{-}272}$ and *mreC*^{bpC547A}

gs223	ATGGATAGTATGATTTTGGGG	(Straume *et al*., 2017a)
gs224	CTACGAGCTTGTTTTTCCAAC	(Straume *et al*., 2017a)
gs225	CACATTATCCATTAAAAATCAAACATCCCTACCTTT ATATCAAAAAC	(Straume *et al*., 2017a)
gs226	AAATACTTGTGGAGGTTCCATTAATTAGTGGGGAA TTCATAATG	(Straume *et al*., 2017a)
gs229	ATCCCTACCTTTATATCAAAAAC	(Straume *et al*., 2017a)
ds453	GTTTTTGATATAAAGGTAGGGATATGAACCGTTTT AAAAAATCAAAATATG	This work
ds454	CTCATTATGAATTCCCCACTAATTTTAAATTTTAAC AGAAATCTTATCAGC	This work
ds455	AATTAGTGGGGAATTCATAATGAG	This work

Primers used for BACTH analysis

khb475	TACGGCTGCAGGG	This work
khb477	AACAAACCAACGATTCTGCGCTACGGGATCCTTAT GGTTGTGCTGGTTGAGG	This work
khb488	TACGGGATCCCCAAAATCAATTAAATGAATTAAAA C	This work
gs330	TACGGAATTCTTATCGTCTCGCCCTTGAAG	This work
khb451	TACGGGATCCCAGAAAAAAAACAATTGGAGAGGT	This work
khb452	TACGGAATTCTTAATTTTTAGTAAAGGTTACAGTG	This work
khb491	TACGTCTAGAGAAATTAGATAAATTATTTGAGAAA TTT	This work
khb490	TACGCCCGGGTTAGCGAAATAGATTGACTATCG	This work
khb492	TACGACTCTAGAGAACCGTTTTAAAAAATCAAAAT ATG	This work
khb493	TACGCCCCGGGTATTATGAATTCCCCACTAATTCTA	This work
gs624	GATCGAATTCTTAAATTTTAACAGAAATCTTATCAG	This work

gs633	GATCTCTAGAGATGAGTGAAAAGTCAAGAGAAGAAGAG	This work
gs634	GATCCCCGGGGTTAGTTTAATTTGCTGTTGACATGT	This work
mk17	GAGCGGATCCCGTGGTAGTATTTACAGGTTCAAC	This work
mk18	GCATGAATTCGAACCAGAACCACCTTCTGTATCTACAACAACATAGC	This work
Primers used to create the *eloR*^{T89A} amplicon		
aw19	GCCGTTGACCTTGGTCATGTGGT	This work
aw20	ACCACATGACCAAGGTCAACGGCTTCTTCACTAACCGTCTTCACA	This work
ds374	CGAAACCTTGGGATACGCAG	This work
ds377	CAGCACCCACGTTAAGCAAC	This work
Primers used to create the *eloR*^{T89E} amplicon		
aw21	GAAGTTGACCTTGGTCATGTGGT	This work
aw22	ACCACATGACCAAGGTCAACTTCTTCTTCACTAACCGTCTTCACA	This work
ds374	CGAAACCTTGGGATACGCAG	This work
ds377	CAGCACCCACGTTAAGCAAC	This work
Primers used to create the *eloR*^{K3Y} amplicon		
aw35	AAAAAGATTATCTATCGTATTATTTCACGTATGGATGG	This work
aw36	ATAGATAATCTTTTTTTCGCTATTTGACATTGGATCTG	This work
ds374	CGAAACCTTGGGATACGCAG	This work
ds377	CAGCACCCACGTTAAGCAAC	This work
Primers used to create the *eloR*^{GDDG} amplicon		
aw33	GATGATGGTAAAGTCTTGAAGGCCTTG	This work
aw34	CAAGGCCTTCAAGACTTTACCATCATCGCCGATAATACGACCTGGTT	This work
ds374	CGAAACCTTGGGATACGCAG	This work
ds377	CAGCACCCACGTTAAGCAAC	This work
Primers used to create the *rodZ*$^{\Delta aa5\text{-}273}$ amplicon		
khb445	TAGATTTACTTGATGAATTGGTAA	(Straume *et al*., 2017a)
khb448	CCACACGTTGCTTTTGGCC	(Straume *et al*., 2017a)

References.

1. Avery, O.T., Macleod, C.M., and McCarty, M. (1944) Studies on the chemical nature of the substance inducing transformation of pneumococcal types : Induction of

transformation by a desoxyribonucleic acid fraction isolated from pneumococcus type III. *J Exp Med* **79:** 137-158.
2. Bankevich, A., Nurk, S., Antipov, D., Gurevich, A.A., Dvorkin, M., Kulikov, A.S., *et al.* (2012) SPAdes: a new genome assembly algorithm and its applications to single-cell sequencing. *J Comput Biol* **19:** 455-477.
3. Berg, K.H., Stamsås, G.A., Straume, D., and Håvarstein, L.S. (2013) Effects of low PBP2b levels on cell morphology and peptidoglycan composition in *Streptococcus pneumoniae* R6. *J Bacteriol* **195:** 4342-4354.
4. Ducret, A., Quardokus, E.M., and Brun, Y.V. (2016) MicrobeJ, a tool for high throughput bacterial cell detection and quantitative analysis. *Nat Microbiol* **1:** 16077.
5. Eldholm, V., Johnsborg, O., Haugen, K., Ohnstad, H.S., and Håvarstein, L.S. (2009) Fratricide in *Streptococcus pneumoniae*: contributions and role of the cell wall hydrolases CbpD, LytA and LytC. *Microbiology* **155:** 2223-2234.
6. Eldholm, V., Johnsborg, O., Straume, D., Ohnstad, H.S., Berg, K.H., Hermoso, J.A., and Håvarstein, L.S. (2010) Pneumococcal CbpD is a murein hydrolase that requires a dual cell envelope binding specificity to kill target cells during fratricide. *Mol Microbiol* **76:** 905-917.
7. Higuchi, R., Krummel, B., and Saiki, R.K. (1988) A general method of in vitro preparation and specific mutagenesis of DNA fragments: study of protein and DNA interactions. *Nucleic Acids Res* **16:** 7351-7367.
8. Johnsborg, O., Eldholm, V., Bjørnstad, M.L., and Håvarstein, L.S. (2008) A predatory mechanism dramatically increases the efficiency of lateral gene transfer in *Streptococcus pneumoniae* and related commensal species. *Mol Microbiol* **69:** 245-253.
9. Johnsborg, O., and Havarstein, L.S. (2009) Pneumococcal LytR, a protein from the LytR-CpsA-Psr family, is essential for normal septum formation in *Streptococcus pneumoniae*. *J Bacteriol* **191:** 5859-5864.
10. Karimova, G., Pidoux, J., Ullmann, A., and Ladant, D. (1998) A bacterial two-hybrid system based on a reconstituted signal transduction pathway. *Proc Natl Acad Sci U S A* **95:** 5752-5756.
11. Kearse, M., Moir, R., Wilson, A., Stones-Havas, S., Cheung, M., Sturrock, S., *et al.* (2012) Geneious basic: an integrated and extendable desktop software platform for the organization and analysis of sequence data. *Bioinformatics* **28:** 1647-1649.
12. Lacks, S., and Hotchkiss, R.D. (1960) A study of the genetic material determining an enzyme in Pneumococcus. *Biochim Biophys Acta* **39:**508-518.
13. Laemmli, U.K. (1970) Cleavage of structural proteins during the assembly of the head of bacteriophage T4. *Nature* **227:** 680-685.
14. Liu, X., Gallay, C., Kjos, M., Domenech, A., Slager, J., van Kessel, S.P., *et al*. (2016) High- througput CRISPRi phenotyping in *Streptococcus pneumoniae* identifies new essential genes involved in cell wall synthesis and competence development. *bioRxiv* doi: http://dx.doi.org/10.1101/088336.
15. Rutschman, J., Maurer, P., and Hakenbeck, R. (2007) Detection of penicillin-binding proteins. In *Molecular Biology of Streptococci.* Hakenbeck, R., and Chhatwal, S. (eds). Norfolk: Horizon Bioscience, pp. 537-542.
16. Seemann, T. (2014) Prokka: rapid prokaryotic genome annotation. *Bioinformatics* **30:** 2068-2069.

17. Stamsås, G.A., Straume, D., Salehian, Z., and Håvarstein, L.S. (2017) Evidence that pneumococcal WalK is regulated by StkP through protein-protein interaction. *Microbiology* **163:** 383-399.
18. Straume, D., Stamsås, G.A., Berg, K.H., Salehian, Z., and Håvarstein, L.S. (2017a) Identification of pneumococcal proteins that are functionally linked to penicillin-binding protein 2b (PBP2b). *Mol Microbiol* **103:** 99-116.
19. Straume, D., Stamsås, G.A., Salehian, Z., and Håvarstein, L.S. (2017b) Overexpression of the fratricide immunity protein ComM leads to growth inhibition and morphological abnormalities in *Streptococcus pneumoniae*. *Microbiology* **163:** 9-21.
20. Sung, C.K., Li, H., Claverys, J.P., and Morrison, D.A. (2001) An *rpsL* cassette, janus, for gene replacement through negative selection in *Streptococcus pneumoniae*. *Appl Environ Microbiol* **67:** 5190-5196.
21. van Raaphorst, R., Kjos, M., and Veening, J.W. (2016) Chromosome segregation drives division site selection in *Streptococcus pneumoniae*. *bioRxiv* doi: https://doi.org/10.1101/087627.

PAPER II

SCIENTIFIC REPORTS

OPEN

Prevention of EloR/KhpA heterodimerization by introduction of site-specific amino acid substitutions renders the essential elongasome protein PBP2b redundant in *Streptococcus pneumoniae*

Received: 18 October 2018
Accepted: 27 December 2018
Published online: 06 March 2019

Anja Ruud Winther, Morten Kjos, Gro Anita Stamsås, Leiv Sigve Håvarstein & Daniel Straume

The RNA binding proteins EloR and KhpA are important components of the regulatory network that controls and coordinates cell elongation and division in *S. pneumoniae*. Loss of either protein reduces cell length, and makes the essential elongasome proteins PBP2b and RodA dispensable. It has been shown previously in formaldehyde crosslinking experiments that EloR co-precipitates with KhpA, indicating that they form a complex *in vivo*. In the present study, we used 3D modeling and site directed mutagenesis in combination with protein crosslinking to further study the relationship between EloR and KhpA. Protein-protein interaction studies demonstrated that KhpA forms homodimers and that KhpA in addition binds to the KH-II domain of EloR. Site directed mutagenesis identified isoleucine 61 (I61) as crucial for KhpA homodimerization. When substituting I61 with phenylalanine, KhpA lost the ability to homodimerize, while it still interacted clearly with EloR. In contrast, both homo- and heterodimerization were lost when I61 was substituted with tyrosine. By expressing these KhpA versions in *S. pneumoniae*, we were able to show that disruption of EloR/KhpA heterodimerization makes the elongasome redundant in *S. pneumoniae*. Of note, loss of KhpA homodimerization did not give rise to this phenotype, demonstrating that the EloR/KhpA complex is crucial for regulating the activity of the elongasome. In support of this conclusion, we found that localization of KhpA to the pneumococcal mid-cell region depends on its interaction with EloR. Furthermore, we found that the EloR/KhpA complex co-localizes with FtsZ throughout the cell cycle.

In most bacteria, the cytoplasmic membrane is surrounded by a peptidoglycan layer, which gives the cell its shape and provides resistance to internal turgor pressure[1]. The peptidoglycan sacculus also serves as an anchoring device for surface proteins and other cell wall components such as teichoic acids and extracellular polysaccharides[2–5]. During cell division and growth, the peptidoglycan synthesis machineries add new material into the existing cell wall. In ovoid bacteria, such as the important human pathogen *Streptococcus pneumoniae*, two modes of cell wall synthesis occur. The divisome synthesizes the septal crosswall, while extension of the lateral cell body is carried out by the elongasome[6,7]. The cell wall synthesis machineries of *S. pneumoniae* contain six penicillin binding proteins (PBPs), five of which participate in building the cell wall via transglycosylase and transpeptidase reactions. The class A PBPs, PBP1a, PBP2a, PBP1b, perform both reactions, while the class B PBPs,

The Norwegian University of Life Sciences, Faculty of Chemistry, Biotechnology and Food Science, Christian Magnus Falsens vei 1, 1430, Ås, Norway. Correspondence and requests for materials should be addressed to D.S. (email: daniel.straume@nmbu.no)

PBP2b and PBP2x, only have transpeptidase activity. Recently, it was discovered that the monofunctional class B enzymes PBP2x and PBP2b operate in conjunction with FtsW and RodA, two newly discovered transglycosylases belonging to the SEDS family proteins (shape, elongation, division and sporulation)[8,9]. The sixth PBP, PBP3, is a D,D-carboxypeptidase that reduces the level of inter peptide cross-bridges in the peptidoglycan by cleaving off the C-terminal D-Ala residue in stem pentapeptides[10]. PBP2b and RodA have been found to be essential for cell elongation, while PBP2x and FtsW are essential for synthesis of the septal disc. Functional studies and subcellular localizations suggest that PBP2b/RodA and PBP2x/FtsW are key components of the elongasome and the divisome, respectively[11–14]. It is not clear whether the elongasome- and divisome activities alternate or if these machineries work simultaneously during cell division[6,15]. However, some data suggest a short period of cell elongation before the onset of septal peptidoglycan synthesis[12,16].

In contrast to rod-shaped bacteria, *S. pneumoniae* lacks MreB, a cytoskeleton-like protein that moves with the cell wall synthesis machinery in helical patterns perpendicular to the cell length axis[17]. Instead, pneumococci elongate by inserting new peptidoglycan into the existing cell wall between the future cell equator and the septum in a circumferentially motion guided by the FtsZ/FtsA division ring[6,18–21]. At some point during cell elongation, the divisome initiates septal cross wall synthesis. If the coordinated activities of the elongasome and the divisome get out of control, it leads to severe growth defects and development of morphological abnormalities[11,13,22]. The cells have therefore developed sophisticated systems to monitor cell cycle progression in order to fine-tune the activity of the elongasome and divisome during cell division. One of these systems includes the membrane-spanning eukaryotic-like serine/threonine kinase StkP. It has four extracellular cell-wall-binding PASTA domains, which are believed to monitor the status of the cell wall during division and activate the appropriate cell division proteins through phosphorylation[23–26].

In a recent study we found that EloR, which is phosphorylated by StkP on threonine 89[27], is a key regulator of cell elongation in *S. pneumoniae*[28]. Our results indicated that EloR stimulates cell elongation when phosphorylated, while being inactive or preventing elongation in its non-phosphorylated form. Moreover, we found that Δ*eloR* cells can survive without PBP2b and its cognate SEDS transglycosylase RodA, demonstrating that deletion of *eloR* supresses the need for a functional elongasome in *S. pneumoniae*. Cells lacking EloR displayed a significant reduction in growth rate and became short and round[28,29]. EloR is a cytoplasmic protein of 37 kDa comprising three different domains: an N-terminal jag-domain of unknown function followed by two RNA-binding domains, a type II KH domain (KH-II) and R3H, at the C-terminal end [30,31]. In a recent study Zheng *et al.*[32] showed that EloR co-precipitates with a protein called KhpA after treating cells with formaldehyde cross linker. KhpA is a small (8.9 kDa) RNA-binding protein that consists only of a type II KH domain. Similar to EloR, deletion of the *khpA* gene supresses the need for a fully functional elongasome, as *pbp2b* as well as *rodA* can be deleted in a Δ*khpA* mutant[32]. EloR and KhpA must bind specific target RNAs probably resulting in modulated expression of cell division proteins during different stages of the cell cycle. In support of this hypothesis Zheng *et al.*[32] reported that the absence of EloR or KhpA results in higher cellular levels of the cell division protein FtsA, and that this increase compensates for the loss of PBP2b[32]. Homologs of EloR and KhpA appear to be widespread in many Gram-positive bacteria, and are found in genera such as *Streptococcus*, *Bacillus*, *Clostridium*, *Listeria*, *Enterococcus*, *Lactobacillus* and *Lactococcus*. The conservation of these proteins across large phylogenetic distances indicates that they are central players in the cell elongation and division machineries of low G + C Gram-positive bacteria.

In the present study, we show that KhpA homodimerizes, and that it in addition interacts with the KH-II domain of EloR forming an EloR/KhpA heterodimer. Furthermore, we identified amino acids critical for these interactions. We successfully constructed a single amino acid mutant of KhpA that fails to homodimerize but still interacts with EloR, and a single amino acid mutant that neither self-interacts nor heterodimerizes. The unique properties of these KhpA versions were used to demonstrate that the function of EloR is compromised when it is no longer able to interact with KhpA, resulting in cells phenocopying Δ*eloR* and Δ*khpA* mutants (reduced cell elongation). Finally, *in vivo* localization studies showed that KhpA co-localizes with FtsZ throughout the cell cycle, and that this localization pattern depends on its interaction with EloR.

Results

KhpA interacts with itself and the KH-II-domain of EloR. In a recent study we showed that the loss of EloR suppresses the need of a functional elongasome in *S. pneumoniae* since *pbp2b* and *rodA* could be deleted[28]. Soon after this, Zheng and co-workers published that EloR co-precipitated with a small protein (8.9 kDa) called KhpA in formaldehyde crosslinking experiments. In addition, they found that a Δ*khpA* mutant phenocopies a Δ*eloR* mutant and that both proteins bound to a similar set of RNA molecules in pulldown experiments[32]. In the present work, we utilized a bacterial two-hybrid system (BACTH assay) to further study the interaction between EloR and KhpA. The BACTH system is based on interaction-mediated reconstitution of the *Bordetella pertussis* adenylate cyclase CyaA, which consists of two domains (T18 or T25). When brought together through interaction of the proteins tested, the active T18-T25 reconstitution produces cAMP, which ultimately results in measurable β-galactosidase production in the *E. coli* host[33]. When testing full-length EloR against KhpA in the BACTH assay, we observed a clear positive interaction (Fig. 1), confirming the crosslinking results of Zheng and co-workers[32]. Next, we wanted to identify the part of EloR that interacts with KhpA. To do so, each of the three domains of EloR (Jag, KH-II and R3H) was tested individually against KhpA (Fig. 1). The results clearly showed that KhpA specifically interacts with the KH-II-domain of EloR (KH-II^{EloR}).

Since KH-domains recognize on average up to four nucleotides, they have a tendency to interact with each other to bind longer sequences and thereby increase their target specificity[31,34]. We therefore suspected that KhpA self-interacts and forms homodimers. BACTH assays using KhpA fused to T18 and T25 resulted in a positive signal (Fig. 1), suggesting that KhpA, in addition to interacting with EloR, also forms homodimers.

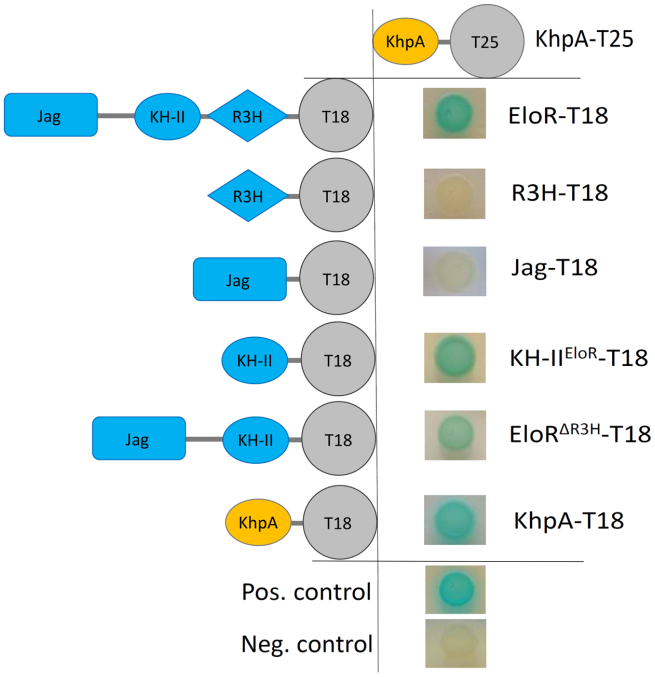

Figure 1. BACTH-assay showing that KhpA interacts directly with EloR and with itself. KhpA (orange shape) was probed against full-length EloR, the R3H domain, the KH-II^{EloR} domain, the Jag domain and EloR missing the C-terminal R3H domain (EloR$^{\Delta R3H}$) (blue shapes). Positive interactions (blue spots) were only seen between KhpA and parts of EloR having the KH-II^{EloR} domain. The positive self-interaction of KhpA is shown at the bottom.

Identification of amino acid residues crucial for KhpA homo- and EloR/KhpA heterodimerization. We reasoned that a 3D model of KhpA might help us identify amino acids that are crucial for homodimerization and heterodimerization with EloR. KH-domains have a highly conserved fold and many 3D-structures are available in the databases[31,34]. To predict the 3D structure of KhpA, we used the online structure prediction tool iTasser. As expected, the predicted structure shows a typical KH-II domain (C-score = −0.36) consisting of three α-helices packed against a three-stranded β-sheet (α-β-β-α-α-β) (Fig. 2A). The conserved RNA binding cleft is made up of the third α-helix and the third β-strand. The typical GxxG loop that interacts with the phosphate backbone of the ssRNA (or in some cases ssDNA) is located between the α2- and α3-helices (marked in green in Fig. 2A). Introduction of two aspartates in this loop (GDDG) abolishes binding of target RNA[35]. To predict the interaction surface between two KhpA molecules, we did protein docking using ZDOCK with the 3D-model of KhpA as input. According to the model (ZDOCK score = 895.421), the α3-helix creates an anti-parallel interaction surface between two KhpA proteins, resulting in a homodimeric structure where the GxxG loops of the two proteins point in opposite directions (Fig. 2B). Based on this structure, we made four different mutant versions of KhpA in which single amino acids predicted to protrude from the α3-helix was altered (R53K, R59K, T60Q and I61F). The point mutated versions of KhpA were then tested for their ability to homodimerize by performing BACTH assays. The changes in position 53, 59 or 60 did not dramatically reduce homodimerization, but changing I61 to the bulkier phenylalanine abolished the interaction between KhpA monomers (Fig. 2C). In our 3D model, a bulky phenylalanine in position 61 cannot fit in a dimeric structure due to steric hindrance (Fig. 2B), complying with the loss of homodimerization. The model also shows that R53 locates on opposite sides in a KhpA dimer, while R59 sticks into the RNA binding cavity (see supplemental Fig. S1), which might explain why changing these residues did not give any dramatic effect on dimerization. The T60, on the other hand, appears to be in close contact in a KhpA dimer (Fig. S1), but it seems to be less important for dimerization than I61.

To get more accurate data on the effect of the I61F mutation, we chose to measure the β-galactosidase production when performing BACTH (see Materials and Methods). Indeed, the KhpA^{I61F} mutant protein has completely lost the ability to self-interact, but can still form heterodimers with EloR (Fig. 3A). In an attempt to create a KhpA mutant that does not form homodimers nor EloR/KhpA heterodimers, I61 was changed to tyrosine, which adds a polar hydroxyl group to the bulky phenyl ring. When tested in BACTH assays, our results showed that the KhpA^{I61Y} mutant has lost the ability to interact with itself and the interaction with EloR was dramatically reduced (Fig. 3A).

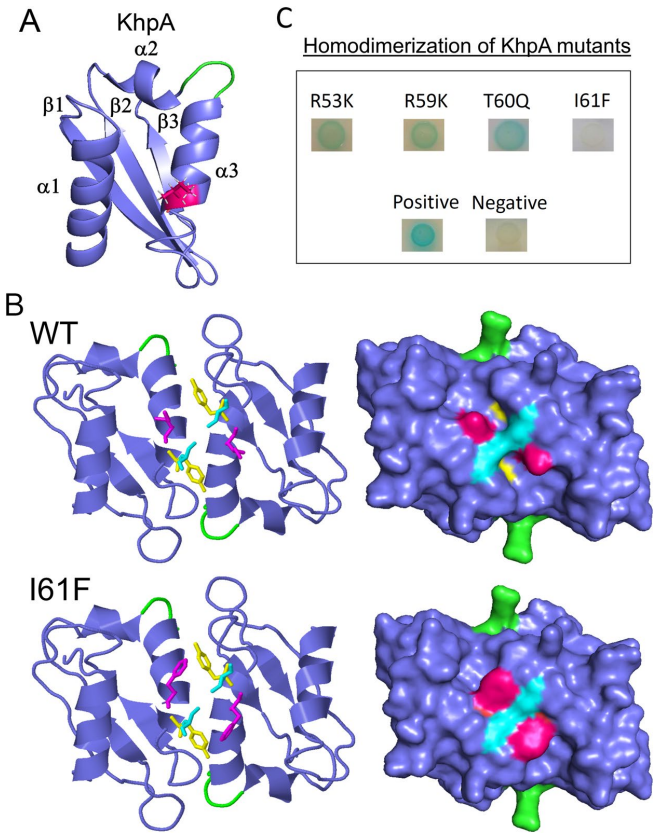

Figure 2. Structure prediction of KhpA using iTasser and ZDOCK. (**A**) KhpA was predicted to have the typical α-β-α-α-β fold of KH-II domains, with the I61 (shown in magenta) protruding from the α3-helix. (**B**) (upper) Protein-protein docking of KhpA homodimers using ZDOCK. The α3-helix of two KhpA molecules are predicted to make contact anti-parallel of each other forming a homodimer where the GXXG RNA-binding loops (shown in green) point in opposite directions. The I61 (magenta) of two KhpA monomers are brought in close proximity in the dimeric structure, facilitating a hydrophobic contact surface. (lower) The dimeric model of the I61F substitution suggests that the phenyl ring does not fit properly into the space between the two KhpA molecules probably because this space is occupied by Tyr63 (yellow) and Ser64 (cyan) of the other KhpA molecule. (**C**) BACTH assay showing KhpA's ability to form homodimers when selected amino acids in the α3-helix were changed (R53K, R59K, T60Q and I61F). Positive interactions appear as blue spots.

Amino acid sequence alignment of the KH-II^{EloR} domain and KhpA, suggests that leucine 239 (L239) in EloR corresponds to I61 in KhpA (see supplemental Fig. S2). Accordingly, when L239 in EloR was substituted with a tyrosine, KhpA could no longer interact with EloR^{L239Y}, showing that this residue is indeed important for EloR/KhpA heterodimerization (Fig. 3A). To prove that L239 and I61 are in close proximity in the EloR/KhpA heterodimer, we replaced these two amino acids with cysteins to determine whether this would result in a disulfide bridge between the two proteins *in vivo*. A pneumococcal strain expressing the mutant proteins EloR^{L239C} and KhpA^{I61C} was therefore constructed (strain AW336). EloR^{L239C} contained an N-terminal 3xflag-tag to allow detection with α-flag antibodies. Strain AW336 was grown to exponential phase, harvested, and lysed using SDS loading buffer with or without the reducing agent β-mercaptoethanol (see Material and Methods). Next, samples were analyzed by SDS-PAGE followed by immunoblotting. In non-reduced cell lysates, we detected a shift in band size corresponding to the complex between EloR and KhpA (Fig. 3B). This shift was not present in samples where β-mercaptoethanol had been added to break the disulfide bond, or in any of the samples containing wild type 3xflag-EloR or 3xflag-EloR^{L239C} only. This confirms the interaction between KhpA and the KH-II domain of EloR *in vivo*, and that I61 in the α3-helix of KhpA interacts directly with L239 in the α3-helix of the KH-II^{EloR} domain.

Prevention of EloR/KhpA heterodimerization relieves the requirement of *pbp2b*. A Δ*khpA* mutant phenocopies a Δ*eloR* mutant[32]. Both mutants have reduced growth rates, form shorter cells and are

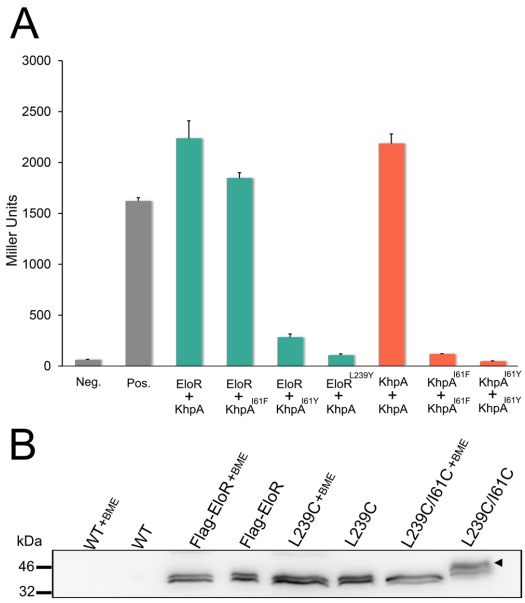

Figure 3. The α3-helix of KhpA is critical for self-dimerization and for EloR/KhpA complex formation. (**A**) Measurements of β-galactosidase production in BACTH assays testing the interaction between EloR and KhpA, KhpA^{I61F} or KhpA^{I61Y} in addition to EloR^{L239Y} against KhpA (green bars). β-galactosidase production resulting from homodimerization of KhpA, KhpA^{I61F} and KhpA^{I61Y} is represented by orange bars, while negative and positive controls are shown in grey. (**B**) Immunoblot detection of 3xflag-EloR in strain RH425, SPH448, AW334 and AW336. A Crosslinked EloR/KhpA complex was observed in strain AW336 under non-reducing conditions, but not after reduction with β-mercaptoethanol (+BME). The image is cropped from the full-length immunoblot, which is shown in Fig. S3.

viable without a functional elongasome (i.e. without a *pbp2b* or *rodA* gene)[28,32]. We hypothesized that the reason why Δ*khpA* cells phenocopies Δ*eloR* cells is because deletion of either will prevent the formation of the EloR/KhpA complex. In other words, the elongasome only becomes essential when the EloR/KhpA complex is able to form and carry out its normal biological function. To test this hypothesis we exploited the unique properties of KhpA^{I61F} and KhpA^{I61Y}. KhpA^{I61F} does not form homodimers, but form heterodimers with EloR, while KhpA^{I61Y} is unable to form either. First, we examined if expression of KhpA^{I61F} or KhpA^{I61Y} generated cells with reduced growth rate similar to a Δ*khpA* mutant. Deletion of *khpA* (strain DS420) increased the doubling time with approximately 15 minutes, which complies with previous findings (15–30 minutes)[32], while strains expressing KhpA^{I61F} or KhpA^{I61Y} (AW212 and AW275) had growth rates similar to the wild type strain (data not shown). Microscopic examination of KhpA^{I61F} or KhpA^{I61Y} cells showed that the KhpA^{I61Y} strain grew in short chains similar to KhpA deficient cells. The KhpA^{I61F} strain on the other hand grew mainly as diplococci similar to the wild type strain (Fig. 4A). By measuring cell lengths and widths, it became evident that KhpA^{I61Y} cells, in which KhpA is unable to form a complex with EloR, have a rounder cell morphology with reduced cell elongation similar to Δ*khpA* cells (Fig. 4B). This phenotype is also characteristic for Δ*eloR* cells[28,29,32]. In contrast, cells expressing the monomeric version of KhpA (I61F) that can still form a complex with EloR, displayed a normal length/width distribution (Fig. 4B).

To further test our hypothesis that EloR/KhpA heterodimerization is required for normal elongasome function, we compared pneumococcal mutants expressing KhpA^{I61F}, KhpA^{I61Y} and EloR^{L239Y} (AW279) with respect to the essentiality of their *pbp2b* gene. Indeed, *pbp2b* could be deleted in KhpA^{I61Y} and EloR^{L239Y} cells with normal transformation frequencies, but not in KhpA^{I61F} cells (see Table S1). Deletion of *pbp2b* in these strains could not be attributed to decreased stability of the mutated EloR and KhpA version since immunodetection of Flag-tagged EloR^{L239Y}, KhpA^{I61F} and KhpA^{I61Y} showed that they were expressed at similar levels as the wild type proteins (see Fig. S4). Since it has been shown that mutants expressing a KhpA are unable to bind ssRNA (changing the ssRNA-binding motif GxxG to GDDG) have a Δ*khpA*/Δ*eloR* phenotype[32], we wondered whether this was because KhpA^{GDDG} had reduced interaction with EloR. However, our BACTH assay showed that KhpA^{GDDG} successfully formed a complex with EloR (Fig. 4C), and we confirmed that *pbp2b* could be deleted in pneumococci expressing KhpA^{GDDG}, as also reported by Zheng *et al.*[32]. This demonstrates that PBP2b becomes redundant in cells having an EloR/KhpA complex in which KhpA no longer binds RNA or when KhpA no longer interacts with EloR.

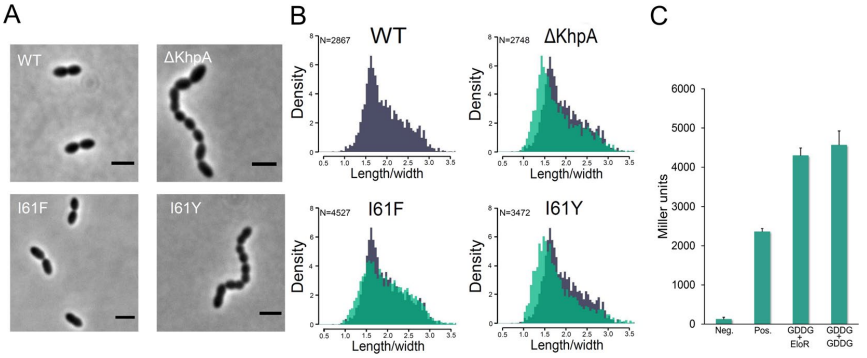

Figure 4. (**A**) Comparison of the morphology of strain RH425 (wt), DS420 (Δ*khpA*), AW212 (I61F) and AW275 (I61Y). Loss of KhpA homodimerization ($KhpA^{I61F}$) produced cells with morphology similar to wild type. Cells in which KhpA no longer interacts with EloR ($KhpA^{I61Y}$) had morphologies resembling the Δ*khpA* mutant. The microscopy images are representatives of whole cell populations. Scale bars are 2 µm. (**B**) Comparison of the cell-shape distribution (length/width) of Δ*khpA*-, $KhpA^{I61F}$- and $KhpA^{I61Y}$-cells (in green) with wild type cells (in grey). $KhpA^{I61Y}$ and Δ*khpA* cells were both significantly different from wild type ($p < 0.05$, two-sample t-test), while the shape distribution of $KhpA^{I61F}$ cells was similar to wild type. C. Quantitative BACTH assay showing that $KhpA^{GDDG}$ self-dimerizes and forms complex with EloR.

EloR recruits KhpA to the division site. KhpA and EloR have been shown to co-localize to the septal region of dividing cells[28,32]. Since they form heterodimers *in vivo*, we wondered if KhpA is recruited to mid-cell through its interaction with EloR. To explore this, the subcellular localization of sfGFP-fused KhpA (KhpA-sfGFP was functional since *pbp2b* could not be deleted in strain AW5, see Table S1) was determined in wild type cells and in a Δ*eloR* mutant (Fig. 5). A subtle mid-cell enrichment of KhpA-sfGFP was found in 73.2% of wild type cells, confirming previous findings[32]. In contrast, KhpA-sfGFP was found at mid-cell in only 0.5% of the Δ*eloR* mutant cells. To show that it is the direct interaction between KhpA and EloR that localizes KhpA to the division site and not some indirect effect of deleting the *eloR* gene, we fused sfGFP to $KhpA^{I61F}$ and $KhpA^{I61Y}$. As expected, $KhpA^{I61Y}$-sfGFP, which does not bind EloR, lost its localization to mid-cell (found at mid-cell in only 2% of the cells). The monomeric $KhpA^{I61F}$-sfGFP are still able to interact with EloR and displayed significantly higher degree of mid-cell enrichment (found at mid-cell in 19% of the cells). In accordance with these results, expression of $EloR^{L239Y}$, which cannot interact with KhpA, resulted in mislocalization of KhpA-sfGFP (Fig. 5). Together, these results show that KhpA is recruited to mid-cell through complex formation with EloR.

To determine whether the EloR/KhpA complex is recruited to the division zone during early, late or all stages of cell division, we compared the localization patterns of KhpA and FtsZ. FtsZ forms the division ring, which functions as a scaffold for a number of proteins found in the elongasome and divisome. FtsZ is therefore present at the division zone during initiation of new septa, cell elongation and cross wall synthesis, but it is not required for the final stage of daughter cell separation[12,18]. KhpA-sfGFP and FtsZ fused to the fluorescent marker mKate2 were co-expressed in *S. pneumoniae* (strain AW198), and fluorescence microscopy images demonstrate that KhpA-sfGFP enriched at mid-cell follows the same localization pattern as FtsZ (Fig. 6). This shows that the EloR/KhpA complex is recruited to the division zone at the very early stage, and that it remains co-localized with the cell division machineries throughout the cell cycle. Note, however, that KhpA is not exclusively co-localized with FtsZ as it is also found throughout the cytoplasm.

Discussion

It has been shown previously that Δ*khpA* and Δ*eloR* mutant strains are similar in several respects. They both exhibit reduced cell lengths, and are able to survive without PBP2b and other essential components of the elongasome[28,32]. The fact that Δ*khpA* and Δ*eloR* mutants have similar phenotypes could suggest that KhpA and EloR are acting at different steps in the same regulatory pathway. However, the finding that KhpA co-precipitates with EloR after formaldehyde crosslinking[32] suggests an alternative model, namely that they function as a single unit and that disruption of this complex gives rise to the phenotypes described above. The results presented in the present work prove that the latter model is correct. Disruption of the EloR/KhpA complex by introduction of site-specific amino acid substitutions, gives rise to shorter cells and renders the elongasome redundant (Fig. 7). It is therefore likely that its role is to stimulate or control elongasome-mediated lateral cell wall synthesis. To do this, our results show that KhpA must be able to bind its target nucleic acid, which is most likely ssRNA. The typical binding surface of KH-domains can only accommodate four unpaired bases[31,34], and consequently has low binding specificity. It is reasonable to assume that the RNA sequence motifs recognized by KhpA and the KH-II domain of EloR are different. Hence, by combining the two domains in a heterodimer the binding specificity and affinity for its target ssRNA(s) are substantially increased. Another possible role for the interaction between EloR and KhpA could be to bridge two segments on an RNA molecule by binding two distant motifs, inducing a loop formation. Such loops are proposed to facilitate binding of posttranscriptional regulatory protein

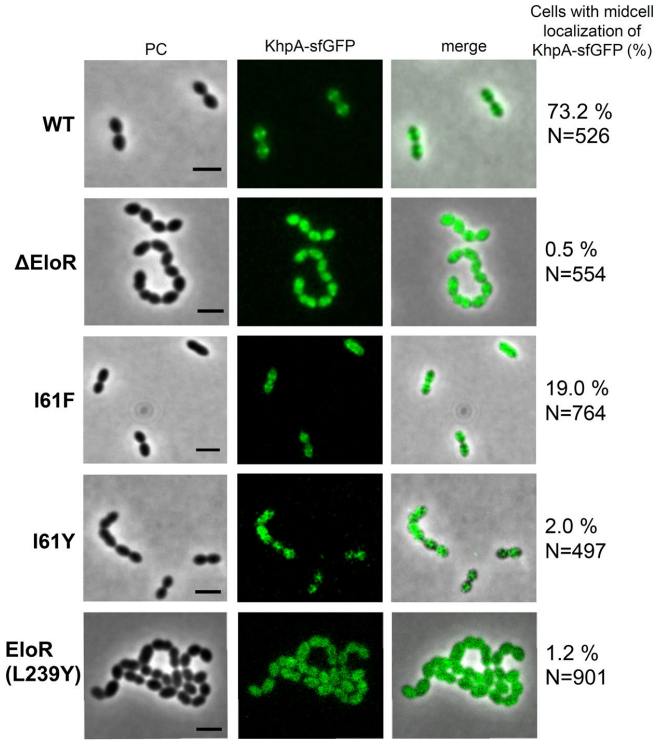

Figure 5. Micrographs showing the localization of KhpA-sfGFP in strain AW5 (wt), AW238 (Δ*eloR*), AW267 (KhpA^{I61F}-sfGFP), AW321 (KhpA^{I61Y}-sfGFP) and AW353 (EloR^{L239Y}). The percent of cells having KhpA-sfGFP enriched to mid-cell are indicated. Scale bars are 2 µm.

complexes[34,36,37]. Identification of the EloR/KhpA RNA target(s) will be an important goal for future research seeking to understand the function of the EloR/KhpA system.

Our results show that KhpA also forms homodimers, which might have their own distinct biological function (see Figs 1 and 3A). However, our preliminary studies did not detect any obvious functional deficits or major phenotypic changes associated with the KhpA^{I61F} mutation, i.e. the mutation disrupting the formation of KhpA homodimers without preventing the formation of EloR/KhpA heterodimers. As the docking model shows, the KhpA monomers are likely arranged in an antiparallel orientation in the dimer so that they will be able bind two successive sequence motifs on the same RNA strand. The binding of two motifs will increase the target sequence specificity considerably, and will make the RNA sequence motif recognized by the homodimer different from that recognized by the EloR/KhpA heterodimer. Considering this, and that the KhpA^{I61F} and KhpA^{I61Y} mutations give rise to completely different phenotypes, it is likely that the KhpA homodimers and EloR/KhpA heterodimers serve different biological functions.

The EloR/KhpA heterodimer contains three RNA-binding domains, i.e two domains from EloR (KH-II and R3H) and one from KhpA. The presence of several RNA-binding domains is a common feature of proteins containing KH-domains. As mentioned above, this increases target specificity and is also believed to have an important role in the folding of ssRNA sequences[34]. Based on the present and previous studies[28,29,32], we know that the EloR/KhpA complex requires the combined action of all three RNA-binding domains to regulate cell elongation. However, it is not known whether all three domains bind to the same RNA strand, or if the KH-II^{EloR}/KhpA complex binds one strand while the R3H domain binds another. The crystal structure of an EloR homolog from *Clostridium symbosium* (PDB 3GKU) suggests a dimeric structure[38], which in principle could bind two KhpA molecules resulting in a complex with a total of six RNA-binding domains. To test this possibility we used the BACTH system to determine if EloR from *S. pneumoniae* forms homodimers. The results were inconclusive as we obtained just a weak positive signal (data not shown). Hence, we cannot conclude whether the biologically active complex between EloR and KhpA is dimeric (EloR/KhpA) or tetrameric (KhpA/EloR/EloR/KhpA).

Synthesis of the lateral cell wall takes place in an area close to the division septum, possibly where the division septum meets the periphery of the cell. Previous studies show that EloR and KhpA localize to the septal region[28,32]. Here, we show that KhpA homodimers are found throughout the cytoplasm (strain AW353) (Fig. 5), while KhpA/EloR heterodimers localize together with FtsZ to the division site (AW198) (Fig. 6). This finding

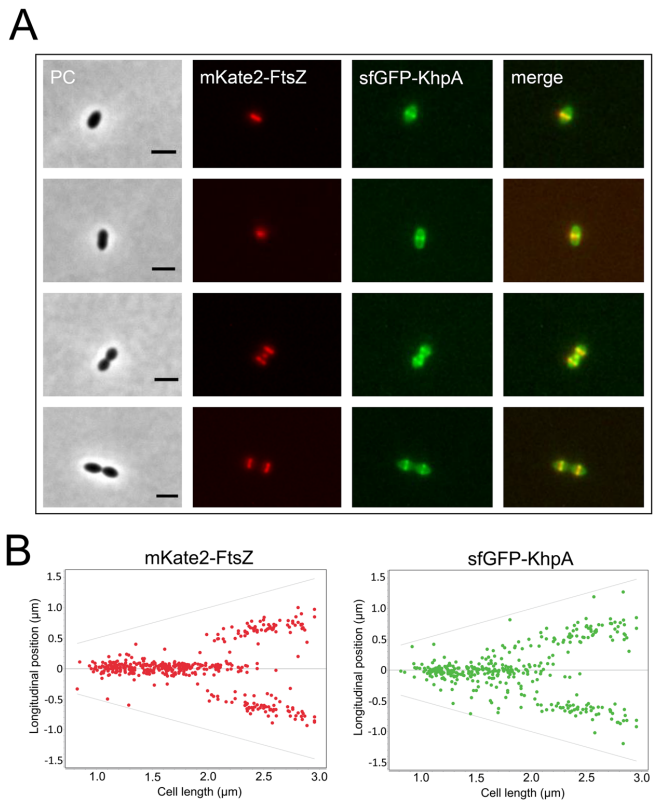

Figure 6. Localization of KhpA-sfGFP and mKate2-FtsZ at different stages of cell division. (**A**) Microscopic examination of strain AW198 showed that KhpA-sfGFP co-localizes to the division site with FtsZ-mKate2 during cell division. Scale bars are 2 µm. (**B**) The fluorescence maximum signals of FtsZ-mKate2 and KhpA-sfGFP plotted relative to cell length. 437 cells were analyzed.

support the notion that these homo- and heterodimers serve different functions. Of note, FtsZ has been reported to disappear from the septum prior to both essential cell division proteins PBP2x (divisome) and PBP2b (elongasome)[12]. Since KhpA co-localizes with the FtsZ-ring throughout the cell cycle, it suggests that a functional EloR/KhpA complex is important during the stages of cell division, which involves active peptidoglycan synthesis during cell elongation and early to mid crosswall synthesis, but not during the final stage of cell division.

Zheng and co-workers report that the levels of FtsA, which together with FtsZ assembles into the division ring[6,18,39,40], were elevated two- to threefold in Δ*eloR* and Δ*khpA* mutants. Their results suggest that EloR and KhpA bind 5′ untranslated regions of mRNAs, including the *ftsA* transcript, resulting in altered translation rates[32]. In support of this hypothesis they found that *pbp2b* could be deleted in wild type D39 cells overexpressing FtsA, although overexpression of FtsA could not fully restore the wild type phenotype of Δ*eloR*/Δ*khpA* cells[32]. We attempted to reproduce the described effect of elevated FtsA levels in our D39 strain. However, despite using the exact same expression conditions, i.e. overexpression of *ftsA* and its 24 nt upstream region from a P_{Zn} zinc-inducible promoter, we were not successful. Nevertheless, translational control of specific mRNAs seems to be the most probable mode of action for the EloR/KhpA complex.

Interestingly, the *eloR* gene is co-transcribed with a gene called *yidC* in *S. pneumoniae*[41] and most likely in several other bacteria including *S. thermophilus*, *L. monocytogenes*, *B. subtilis*, *L. lactis*, *E. faecium* and *L. plantarum*. Such conserved co-transcription could indicate a functional relationship between the genes. YidC is an insertase that assists in co-translational insertion of membrane proteins into the lipid bilayer. It functions together with the SecYEG translocon, the signal recognition particle (SRP) and the SRP-receptor FtsY. During co-translational protein targeting to the SecYEG translocon, the SRP-ribosome-nascent protein chain complex is first targeted to FtsY, which delivers the chain to the SecYEG translocon channel. The function of YidC is to facilitate the release of the transmembrane domains of inner membrane proteins from the channel into the lipid bilayer[42,43]. Having this in mind, it is tempting to speculate that the EloR/KhpA complex could be involved in regulating the expression and insertion of specific membrane proteins involved in cell elongation through translational control.

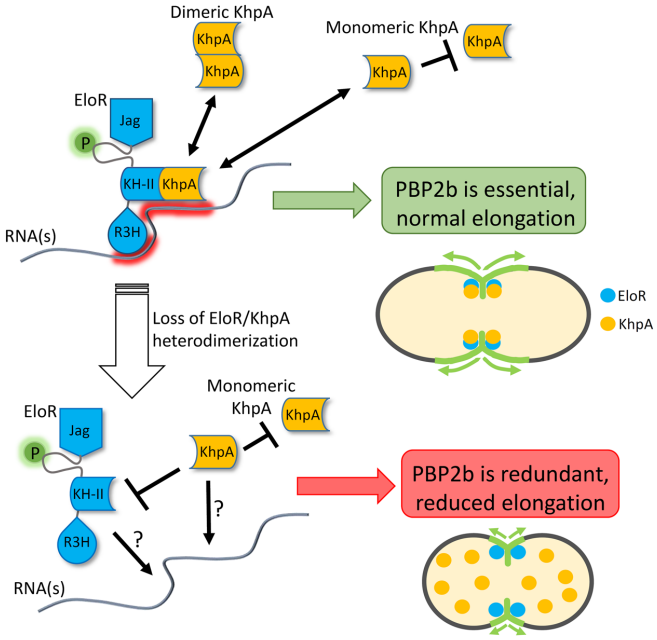

Figure 7. Model depicting EloR- and KhpA dependent cell elongation. KhpA binds the KH-II domain of EloR, which recruits KhpA to the division zone where new cell wall is synthesized. At the division zone the EloR/KhpA complex regulates cell elongation by binding RNA. Whether EloR/KhpA binds one or more specific sequence motifs or specific RNA secondary structures, and how binding of RNA regulates cell division are still not settled. A monomeric KhpA does not render cells independent on PBP2b as long as it still forms a complex with EloR. If the interaction between EloR and KhpA is broken, KhpA loses its mid-cell localization and binding to the target RNA(s) is most probably reduced or lost. Since EloR requires the RNA binding activity of KhpA to function, preventing EloR/KhpA complex formation results in compromised cell elongation.

Methods

Bacterial strains, cultivation and transformation. All strains used in this work are listed in Table 1. *E. coli* strains were grown in LB broth at 37 °C with shaking (200 rpm), or on LB plates at 37 °C unless otherwise indicated. When necessary the following antibiotics were used: kanamycin (50 µg/ml) and ampicillin (100 µg/ml). Transformation experiments were performed with chemically competent cells using the heat shock method at 42 °C for 45 seconds. *S. pneumoniae* were grown in C medium[44] or on Todd Hewitt-agar plates at 37 °C. Agar plates were incubated in anaerobic chambers using AnaeroGen™ bags from Oxoid. When necessary, kanamycin (400 µg/ml) and streptomycin (200 µg/ml) were employed for selection of transformants. In order to knock out genes or introduce mutations, natural genetic transformation was employed. For transformation experiments, the culture was grown to an OD_{550} of 0.05–0.1 and mixed with the transforming DNA (100–200 ng) and CSP1, which was added to a final concentration of 250 ng/ml. After 2 hours of incubation at 37 °C, 30 µl of the culture was plated on TH-agar containing the appropriate antibiotic followed by incubation at 37 °C over night. To investigate growth rates of different mutants, cultures were grown to an OD_{550} of 0.2, diluted to $OD_{550} = 0.05$, and grown in 96-well Corning NBS clear-bottom plates in a Synergy H1 Hybrid Reader (BioTek). The OD_{550} was measured automatically every 5 minutes for 20 hours.

Construction of genetic mutants, gene fusions and point mutations. DNA amplicons used in transformation experiments were created with overlap extension PCR as previously described[45]. Genes were knocked out using a Janus cassette[46]. The cassettes were created with sequences of ~1000 bp homologous to the flanking sequences of the insertion site in the genome. The same technique was employed when introducing point mutations or fusion genes. Primers used to create these amplicons are listed in Table S2. The ftsZ-mKate2 fusion gene together with a kanamycin resistance cassette was amplified from genomic DNA of strain RR66[47]. All constructs were verified with PCR and Sanger Sequencing.

SDS-PAGE and immunoblotting. The strains RH425, SPH448, AW334 and AW336 were grown to an OD_{550} of 0.3 in a culture volume of 45 ml. The cells were harvested at 4000 × *g*, and resuspended in 200 µl 1 × SDS sample buffer not containing any reducing agents. The samples were then split in two, and β-mercaptoethanol

Name	Relevant characteristics	Reference
R704	R6 derivative, *comA::ermAM*; Ery^R	JP. Claverys*
RH425	R704, but streptomycin resistant; Ery^R, Sm^R	[54]
DS420	Δ*comA*, Δ*khpA*; Ery^R, Sm^R	This work
DS428	Δ*comA*, Δ*khpA*, Δ*pbp2b::janus*; Ery^R, Kan^R	This work
DS764	Δ*comA*, *flag-khpA*^{I61F}; Ery^R, Sm^R	This work
DS765	Δ*comA*, *flag-khpA*^{I61Y}; Ery^R, Sm^R	This work
DS766	Δ*comA*, *flag-eloR*^{L239Y}; Ery^R, Sm^R	This work
AW5	Δ*comA*, *khpA-sfgfp*; Ery^R, Sm^R	This work
AW9	Δ*comA*, *flag-khpA*; Ery^R, Sm^R	This work
AW24	Δ*comA*, *khpA*^{GDDG}; Ery^R, Sm^R	This work
AW27	Δ*comA*, *khpA*^{GDDG}, Δ*pbp2b::janus*; Ery^R, Kan^R	This work
AW198	Δ*comA*, *khpA-sfgfp*, *ftsZ-mKate2-Km*; Ery^R, Km^R, Sm^R	This work
AW212	Δ*comA*, *khpA*^{I61F}; Ery^R, Sm^R	This work
AW238	Δ*comA*, *khpA-sfgfp*, Δ*eloR*; Ery^R, Sm^R	This work
AW267	Δ*comA*, *khpA*^{I61F}*-sfgfp*; Ery^R, Sm^R	This work
AW275	Δ*comA*, *khpA*^{I61Y}; Ery^R, Sm^R	This work
AW279	Δ*comA*, *eloR*^{L239Y}; Ery^R, Sm^R	This work
AW313	Δ*comA*, *khpA*^{I61Y}, Δ*pbp2b::janus*; Ery^R, Kan^R	This work
AW314	Δ*comA*, *eloR*^{L239Y}, Δ*pbp2b::janus*; Ery^R, Kan^R	This work
AW321	Δ*comA*, *khpA*^{I61Y}*-sfgfp*; Ery^R, Sm^R	This work
AW334	Δ*comA*, *flag-eloR*^{L239C}; Ery^R, Sm^R	This work
AW336	Δ*comA*, *flag-eloR*^{L239C}, *khpA*^{I61C}; Ery^R, Sm^R	This work
AW353	Δ*comA*, *khpA-sfgfp*, *eloR*^{L239Y}; Ery^R, Sm^R	This work
SPH445	Δ*comA*, Δ*eloR*, Ery^R, Sm^R	[28]
SPH446	Δ*comA*, Δ*eloR*, Δ*pbp2b::janus*; Ery^R, Kan^R	[28]
SPH448	Δ*comA*, *flag-eloR*; Ery^R, Sm^R	[28]
RR66	D39 derivative, *ftsZ-mKate2*, Kan^R	[47]

Table 1. *S. pneumoniae* strains used in the present study. *Gift from Professor Jean-Pierre Claverys, CNRS, Toulouse, France.

was added to one parallel half of the samples to a final concentration of 100 mM. All the samples (including the non-reduced) were heated at 100 °C for 10 minutes. The cell lysates were separated on a 15% polyacrylamide gel with buffer conditions as previously described[48]. For immunodetection purposes, the separated proteins were electroblotted onto a PVDF membrane (BioRad), and flag-EloR was detected with α-flag antibodies as previously described[49]. To detect the expression of Flag-EloR, Flag-EloR^{L239Y}, Flag-KhpA, Flag-KhpA^{I61F} and Flag-KhpA^{I61Y}, strain SPH448, DS766, AW9, DS764 and DS765 were grown to $OD_{550} = 0.3$ in 10 ml C medium. Flag-tagged proteins were then detected in whole cell lysates as described above.

BACTH-assay. The bacterial adenylate cyclase two hybrid (BACTH) assay, is based on the functional complementation of T18 and T25, two domains of the *B. pertussis* adenylate cyclase (CyaA)[33]. When these domains are brought in close proximity to each other, they can actively produce cAMP. The production of cAMP leads to activation of the catabolite activator protein CAP, which in a complex with cAMP activates expression of a reporter gene placed behind the cAMP/CAP promoter. The reporter gene used in this system encodes the β-galactosidase enzyme. In order to investigate the interaction between two proteins, we cloned genes encoding the proteins of interest in frame with either the T25 -or the T18-encoding sequences in plasmids provided by the manufacturer (Euromedex). The plasmids used in this study are listed in Table S3. Next, two plasmids, each expressing one protein fused to either T18 or T25 were transformed into *E. coli* BTH101 cells (a *cya*$^-$ strain). After overnight incubation on LB plates containing kanamycin (50 µg/ml) and ampicillin (100 µg/ml), five colonies from each transformation were grown in LB containing the appropriate antibiotics. When reaching an OD_{600} of 0.2, three µl of the cell cultures were spotted onto LB plates containing 0.5 mM IPTG (to induce expression of the fusion genes), X-gal (40 µg/ml), kanamycin (50 µg/ml) and ampicillin (100 µg/ml). After an overnight incubation at 30 °C, results were interpreted as positive or negative based on the color of the spot. A positive interaction between the proteins of interest will result in blue spots on a plate. In addition, the production of β-galactosidase reporter was measured by performing β-galactosidase assays using ortho-nitrophenyl-β-galactoside (ONPG) as substrate. *E. coli* BTH101 containing plasmids with T18 and T25-fused genes were grown in the presence of kanamycin (50 µg/ml) and ampicillin (100 µg/ml) to $OD_{600} = 0.4–0.5$. Then the cells were diluted to $OD_{600} = 0.05$ in similar medium also containing 0.5 mM IPTG. The cells were incubated at 30 °C with shaking for 4 hours. Cells from one ml culture were lysed using 0.5 g of ≤106 µm glass beads (Sigma) and bead beating at 6.5 m/s for 3 × 20 seconds. Then the β-galactosidase activity in 100 µl cell lysate was determined following the protocol of Steinmoen *et al.*[50].

Microscopy and cell shape distribution analyses. The subcellular localization of different point mutated versions of the KhpA proteins was examined by fluorescence microscopy. The mutated proteins in question were fused to sfGFP[47] via a short glycine-linker (GGGGG). sfGFP fusions were expressed in the native *khpA* locus in the *S. pneumoniae* genome (strains AW5, AW198, AW238, AW267, AW321 and AW353).

The cell morphology and cell shape distributions were examined by phase contrast microscopy. Microscopy experiments were performed by growing the strains to an OD_{550} of 0.1 before immobilizing the cells on a microscopy slide using 1.2% low melting agarose (Biorad) in PBS. Phase contrast images and GFP fluorescence images were obtained using a Zeiss AxioObserver with ZEN Blue software, and an ORCA-Flash 4.0 V2 Digital CMOS camera (Hamamatsu Photonics) using a 1003 phase-contrast objective. The ImageJ plugin MicrobeJ[51] was used to analyze the cell shape and the subcellular localization of KhpA-sfGFP and FtsZ-mKate2. Cells were segmented using the phase contrast images. Cell shape distributions were made by calculating length/width for the individual cell and the significance of the differences between distributions were determined using a two-sample t-test. To determine the percentage of cells having KhpA-sfGFP enriched at mid-cell, the GFP fluorescence profiles were plotted for the individual cells. KhpA-sfGFP was scored as mid-cell localized when a fluorescence maximum peak was found in the mid-cell area (between 40–60% of the cell length), and the percentage of cells with KhpA-sfGFP enriched at mid-cell was calculated. To analyze the subcellular localization of FtsZ-mKate2 and KhpA-sfGFP, the Maxima-option in MicrobeJ was used.

3D-modelling. The online structure determination tool iTasser was used to predict the 3D-structure of KhpA. It uses algorithms to predict protein 3D structure based on the amino acid sequence and known, published structures[52]. KhpA was modeled based on the solved structure of the KH-II domain of PDB entry 3gku (21% sequence identity and 60% similarity with KhpA). The ZDOCK server was used to predict the interaction surface in a KhpA homodimer[53]. Based on the predicted interaction surface in a KhpA homodimer, we created point mutated versions of KhpA, introduced these into the BACTH system, and tested interactions between mutated KhpA proteins and between mutated KhpA and wild type EloR.

References

1. Vollmer, W., Blanot, D. & de Pedro, M. A. Peptidoglycan structure and architecture. *FEMS Microbiol Rev* **32**, 149–167, https://doi.org/10.1111/j.1574-6976.2007.00094.x (2008).
2. Dramsi, S., Magnet, S., Davison, S. & Arthur, M. Covalent attachment of proteins to peptidoglycan. *FEMS Microbiol Rev* **32**, 307–320, https://doi.org/10.1111/j.1574-6976.2008.00102.x (2008).
3. Brown, S., Santa Maria, J. P. Jr. & Walker, S. Wall teichoic acids of gram-positive bacteria. *Annu Rev Microbiol* **67**, 313–336, https://doi.org/10.1146/annurev-micro-092412-155620 (2013).
4. Bazaka, K., Crawford, R. J., Nazarenko, E. L. & Ivanova, E. P. Bacterial extracellular polysaccharides. *Adv Exp Med Biol* **715**, 213–226, https://doi.org/10.1007/978-94-007-0940-9_13 (2011).
5. Sørensen, U. B., Henrichsen, J., Chen, H. C. & Szu, S. C. Covalent linkage between the capsular polysaccharide and the cell wall peptidoglycan of *Streptococcus pneumoniae* revealed by immunochemical methods. *Microb Pathog* **8**, 325–334 (1990).
6. Pinho, M. G., Kjos, M. & Veening, J. W. How to get (a)round: mechanisms controlling growth and division of coccoid bacteria. *Nature reviews. Microbiology* **11**, 601–614, https://doi.org/10.1038/nrmicro3088 (2013).
7. Zapun, A., Vernet, T. & Pinho, M. G. The different shapes of cocci. *FEMS Microbiol Rev* **32**, 345–360, https://doi.org/10.1111/j.1574-6976.2007.00098.x (2008).
8. Cho, H. *et al*. Bacterial cell wall biogenesis is mediated by SEDS and PBP polymerase families functioning semi-autonomously. *Nat Microbiol*, 16172, https://doi.org/10.1038/nmicrobiol.2016.172 (2016).
9. Meeske, A. J. *et al*. SEDS proteins are a widespread family of bacterial cell wall polymerases. *Nature* **537**, 634–638, https://doi.org/10.1038/nature19331 (2016).
10. Morlot, C. *et al*. Crystal structure of a peptidoglycan synthesis regulatory factor (PBP3) from *Streptococcus pneumoniae*. *J Biol Chem* **280**, 15984–15991, https://doi.org/10.1074/jbc.M408446200 (2005).
11. Berg, K. H., Stamsås, G. A., Straume, D. & Håvarstein, L. S. Effects of low PBP2b levels on cell morphology and peptidoglycan composition in *Streptococcus pneumoniae* R6. *J Bacteriol* **195**, 4342–4354, https://doi.org/10.1128/JB.00184-13 (2013).
12. Tsui, H. C. *et al*. Pbp2x localizes separately from Pbp2b and other peptidoglycan synthesis proteins during later stages of cell division of *Streptococcus pneumoniae* D39. *Mol Microbiol* **94**, 21–40, https://doi.org/10.1111/mmi.12745 (2014).
13. Land, A. D. *et al*. Requirement of essential Pbp2x and GpsB for septal ring closure in *Streptococcus pneumoniae* D39. *Mol Microbiol* **90**, 939–955, https://doi.org/10.1111/mmi.12408 (2013).
14. Perez-Nunez, D. *et al*. A new morphogenesis pathway in bacteria: unbalanced activity of cell wall synthesis machineries leads to coccus-to-rod transition and filamentation in ovococci. *Mol Microbiol* **79**, 759–771, https://doi.org/10.1111/j.1365-2958.2010.07483.x (2011).
15. Sham, L. T., Tsui, H. C., Land, A. D., Barendt, S. M. & Winkler, M. E. Recent advances in pneumococcal peptidoglycan biosynthesis suggest new vaccine and antimicrobial targets. *Curr Opin Microbiol* **15**, 194–203, https://doi.org/10.1016/j.mib.2011.12.013 (2012).
16. Wheeler, R., Mesnage, S., Boneca, I. G., Hobbs, J. K. & Foster, S. J. Super-resolution microscopy reveals cell wall dynamics and peptidoglycan architecture in ovococcal bacteria. *Mol Microbiol* **82**, 1096–1109, https://doi.org/10.1111/j.1365-2958.2011.07871.x (2011).
17. Garner, E. C. *et al*. Coupled, circumferential motions of the cell wall synthesis machinery and MreB filaments in *B. subtilis*. *Science* **333**, 222–225, https://doi.org/10.1126/science.1203285 (2011).
18. Mura, A. *et al*. Roles of the essential protein FtsA in cell growth and division in *Streptococcus pneumoniae*. *J Bacteriol*. https://doi.org/10.1128/JB.00608-16 (2016).
19. Jacq, M. *et al*. Remodeling of the Z-Ring Nanostructure during the *Streptococcus pneumoniae* cell cycle revealed by photoactivated localization microscopy. *MBio* **6**, https://doi.org/10.1128/mBio.01108-15 (2015).
20. Fleurie, A. *et al*. Interplay of the serine/threonine-kinase StkP and the paralogs DivIVA and GpsB in pneumococcal cell elongation and division. *PLoS Genet* **10**, e1004275, https://doi.org/10.1371/journal.pgen.1004275 (2014).
21. Li, Y. *et al*. MapZ forms a stable ring structure that acts as a nanotrack for FtsZ treadmilling in *Streptococcus mutans*. *ACS Nano*, https://doi.org/10.1021/acsnano.8b02469 (2018).
22. Straume, D., Stamsås, G. A., Berg, K. H., Salehian, Z. & Håvarstein, L. S. Identification of pneumococcal proteins that are functionally linked to penicillin-binding protein 2b (PBP2b). *Mol Microbiol* **103**, 99–116, https://doi.org/10.1111/mmi.13543 (2017).
23. Fleurie, A. *et al*. Mutational dissection of the S/T-kinase StkP reveals crucial roles in cell division of *Streptococcus pneumoniae*. *Mol Microbiol* **83**, 746–758, https://doi.org/10.1111/j.1365-2958.2011.07962.x (2012).

24. Novakova, L. *et al*. Identification of multiple substrates of the StkP Ser/Thr protein kinase in *Streptococcus pneumoniae*. *J Bacteriol* **192**, 3629–3638, https://doi.org/10.1128/JB.01564-09 (2010).
25. Beilharz, K. *et al*. Control of cell division in *Streptococcus pneumoniae* by the conserved Ser/Thr protein kinase StkP. *Proc Natl Acad Sci USA* **109**, E905–913, https://doi.org/10.1073/pnas.1119172109 (2012).
26. Zucchini, L. *et al*. PASTA repeats of the protein kinase StkP interconnect cell constriction and separation of *Streptococcus pneumoniae*. *Nat Microbiol* **3**, 197–209, https://doi.org/10.1038/s41564-017-0069-3 (2018).
27. Sun, X. *et al*. Phosphoproteomic analysis reveals the multiple roles of phosphorylation in pathogenic bacterium *Streptococcus pneumoniae*. *J Proteome Res* **9**, 275–282, https://doi.org/10.1021/pr900612v (2010).
28. Stamsås, G. A. *et al*. Identification of EloR (Spr1851) as a regulator of cell elongation in *Streptococcus pneumoniae*. *Mol Microbiol* **105**, 954–967, https://doi.org/10.1111/mmi.13748 (2017).
29. Ulrych, A. *et al*. Characterization of pneumococcal Ser/Thr protein phosphatase *phpP* mutant and identification of a novel PhpP substrate, putative RNA binding protein Jag. *BMC Microbiol* **16**, 247, https://doi.org/10.1186/s12866-016-0865-6 (2016).
30. Grishin, N. V. The R3H motif: a domain that binds single-stranded nucleic acids. *Trends Biochem Sci* **23**, 329–330 (1998).
31. Valverde, R., Edwards, L. & Regan, L. Structure and function of KH domains. *FEBS J* **275**, 2712–2726, https://doi.org/10.1111/j.1742-4658.2008.06411.x (2008).
32. Zheng, J. J., Perez, A. J., Tsui, H. T., Massidda, O. & Winkler, M. E. Absence of the KhpA and KhpB (JAG/EloR) RNA-binding proteins suppresses the requirement for PBP2b by overproduction of FtsA in *Streptococcus pneumoniae* D39. *Mol Microbiol* **106**, 793–814, https://doi.org/10.1111/mmi.13847 (2017).
33. Karimova, G., Pidoux, J., Ullmann, A. & Ladant, D. A bacterial two-hybrid system based on a reconstituted signal transduction pathway. *Proceedings of the National Academy of Sciences* **95**, 5752–5756 (1998).
34. Nicastro, G., Taylor, I. A. & Ramos, A. KH-RNA interactions: back in the groove. *Curr Opin Struct Biol* **30**, 63–70, https://doi.org/10.1016/j.sbi.2015.01.002 (2015).
35. Hollingworth, D. *et al*. KH domains with impaired nucleic acid binding as a tool for functional analysis. *Nucleic acids research* **40**, 6873–6886 (2012).
36. Chao, J. A. *et al*. ZBP1 recognition of beta-actin zipcode induces RNA looping. *Genes Dev* **24**, 148–158, https://doi.org/10.1101/gad.1862910 (2010).
37. Patel, V. L. *et al*. Spatial arrangement of an RNA zipcode identifies mRNAs under post-transcriptional control. *Genes Dev* **26**, 43–53, https://doi.org/10.1101/gad.177428.111 (2012).
38. Tan, K., Keigher, L., Jedrzejczak, R., Babnigg, G. & Joachimiak, A. (http://www.rcsb.org/structure/3GKU).
39. Bisson-Filho, A. W. *et al*. Treadmilling by FtsZ filaments drives peptidoglycan synthesis and bacterial cell division. *Science* **355**, 739–743, https://doi.org/10.1126/science.aak9973 (2017).
40. Yang, X. *et al*. GTPase activity-coupled treadmilling of the bacterial tubulin FtsZ organizes septal cell wall synthesis. *Science* **355**, 744–747, https://doi.org/10.1126/science.aak9995 (2017).
41. Slager, J., Aprianto, R. & Veening, J. W. Deep genome annotation of the opportunistic human pathogen *Streptococcus pneumoniae* D39. *Nucleic Acids Res* https://doi.org/10.1093/nar/gky725 (2018).
42. Wu, Z. C., de Keyzer, J., Berrelkamp-Lahpor, G. A. & Driessen, A. J. Interaction of *Streptococcus mutans* YidC1 and YidC2 with translating and nontranslating ribosomes. *J Bacteriol* **195**, 4545–4551, https://doi.org/10.1128/JB.00792-13 (2013).
43. Steinberg, R., Knupffer, L., Origi, A., Asti, R. & Koch, H. G. Co-translational protein targeting in bacteria. *FEMS Microbiol Lett* **365**, https://doi.org/10.1093/femsle/fny095 (2018).
44. Lacks, S. & Hotchkiss, R. D. A study of the genetic material determining an enzyme activity in pneumococcus. *Biochimica et biophysica acta* **39**, 508–518 (1960).
45. Higuchi, R., Krummel, B. & Saiki, R. A general method of *in vitro* preparation and specific mutagenesis of DNA fragments: study of protein and DNA interactions. *Nucleic acids research* **16**, 7351–7367 (1988).
46. Sung, C., Li, H., Claverys, J. & Morrison, D. An *rpsL* cassette, janus, for gene replacement through negative selection in *Streptococcus pneumoniae*. *Applied and environmental microbiology* **67**, 5190–5196 (2001).
47. van Raaphorst, R., Kjos, M. & Veening, J. W. Chromosome segregation drives division site selection in *Streptococcus pneumoniae*. *Proc Natl Acad Sci USA* **114**, E5959–E5968, https://doi.org/10.1073/pnas.1620608114 (2017).
48. Laemmli, U. K. Cleavage of structural proteins during the assembly of the head of bacteriophage T4. *nature* **227**, 680 (1970).
49. Stamsås, G. A., Straume, D., Salehian, Z. & Håvarstein, L. S. Evidence that pneumococcal WalK is regulated by StkP through protein–protein interaction. *Microbiology* **163**, 383–399 (2017).
50. Steinmoen, H., Knutsen, E. & Håvarstein, L. S. Induction of natural competence in *Streptococcus pneumoniae* triggers lysis and DNA release from a subfraction of the cell population. *Proceedings of the National Academy of Sciences* **99**, 7681–7686 (2002).
51. Ducret, A., Quardokus, E. M. & Brun, Y. V. MicrobeJ, a tool for high throughput bacterial cell detection and quantitative analysis. *Nature microbiology* **1**, 16077 (2016).
52. Roy, A., Kucukural, A. & Zhang, Y. I-TASSER: a unified platform for automated protein structure and function prediction. *Nature protocols* **5**, 725 (2010).
53. Pierce, B. G. *et al*. ZDOCK server: interactive docking prediction of protein–protein complexes and symmetric multimers. *Bioinformatics* **30**, 1771–1773 (2014).
54. Johnsborg, O. & Håvarstein, L. S. Pneumococcal LytR, a protein from the LytR-CpsA-Psr family, is essential for normal septum formation in *Streptococcus pneumoniae*. *J Bacteriol* **191**, 5859–5864, https://doi.org/10.1128/JB.00724-09 (2009).

Acknowledgements

This work was partly funded by a grant given by the Research Council of Norway.

Author Contributions

A.R.W. made mutants strains, performed BACTH assays, microscopy and immunoblots. M.K. performed microscopy, cell shape measurements and revised the manuscript. G.A.S. helped with constructing mutant strains, interpreting results and revising the manuscript. L.S.H. contributed with experimental design, 3D-modelling, interpreting results and revising the manuscript. D.S. contributed with experimental design, BACTH assays, interpreting results and writing of the manuscript.

Additional Information

Supplementary information accompanies this paper at https://doi.org/10.1038/s41598-018-38386-6.

Competing Interests: The authors declare no competing interests.

Publisher's note: Springer Nature remains neutral with regard to jurisdictional claims in published maps and institutional affiliations.

Supplemental Material.

Prevention of EloR/KhpA heterodimerization by introduction of site-specific amino acid substitutions renders the essential elongasome protein PBP2b redundant in *Streptococcus pneumoniae*.

Anja Ruud Winther, Morten Kjos, Gro Anita Stamsås, Leiv Sigve Håvarstein and Daniel Straume.

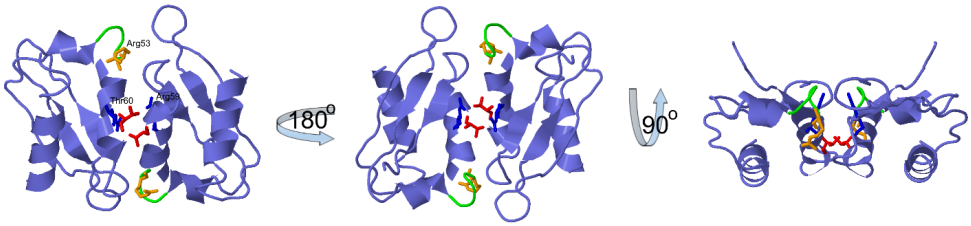

Fig. S1. Model of the KhpA homodimer. The residues R53 (orange), R59 (Blue) and T60 (red) are shown as sticks.

```
KhpA        MDTIENLIIAIVKPLISQPDALTIKIEDTPEFLEYHLNLDQSDVGRVIGRKGRTISAIRT 60
KH-II       --------MAYVQTIIDDMDV-EATLSNDYNRRSINLQIDTNEPGRIIGYHGKVLKALQL 51
                    :* *: :*.: *.   .:.:  :  . :*::* .: **:** :*:.:.*::

KhpA        IVYSVPT-EYKK-VRIVIDEK    79
KH-II       LAQNYLYNRYSRTFYVTI---    69
            :. .    .*.: . :.*
```

Fig. S2. Alignment of the amino acid sequences of KhpA and KH-II^{EloR} using Clustal Omega[1]. The RNA-binding GXXG loop, and I61 and L239 in KhpA and EloR, respectively, are boxed.

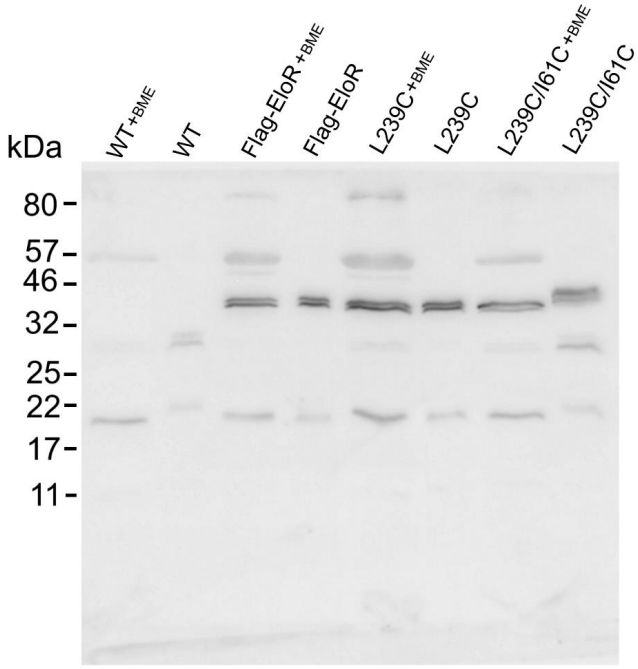

Fig. S3. Full-length image of the immunoblot shown in Fig. 3B.

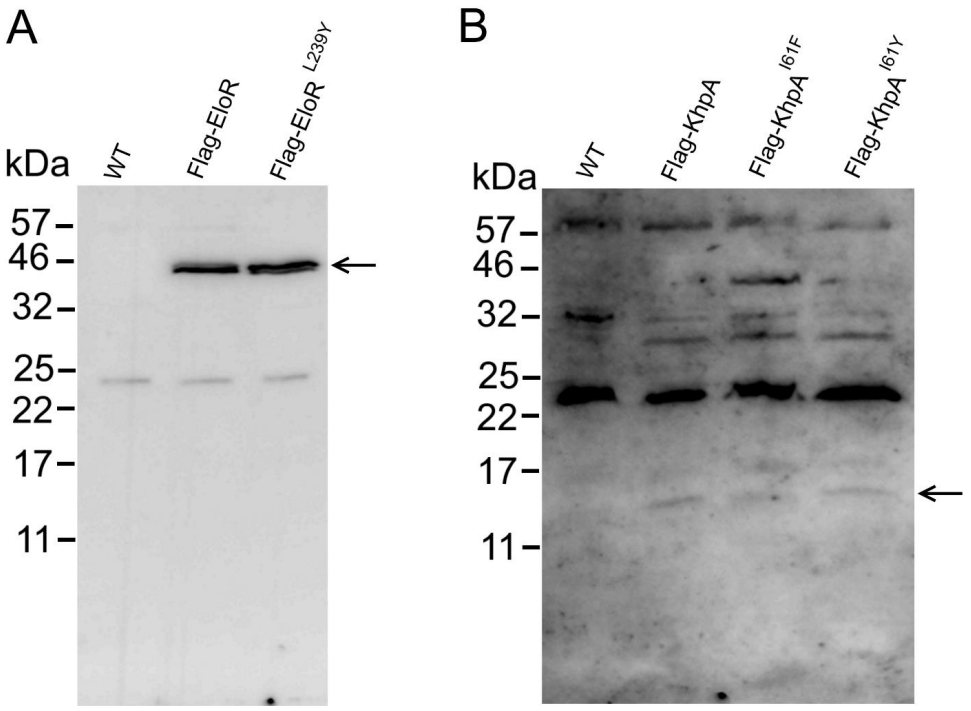

Figure S4. Immunodetection of Flag-EloR and Flag-EloR^{L239Y} is shown in panel A, while detection of Flag-KhpA, Flag-KhpA^{I61F} and Flag-KhpA^{I61Y} is shown in panel B. The arrows indicate Flag-tagged proteins.

Table S1. Suppression of Δ*pbp2b* phenotype when the EloR/KhpA interaction is broken.

Strains[a]	Genotype	Number of normal sized colonies after 18-20 hours of incubation
RH425	R6 derivative, but Sm^R	0
DS420	Δ*comA*, Δ*khpA*; Ery^R, Sm^R	>500
SPH445	Δ*comA*, Δ*eloR*; Ery^R, Sm^R	>500
AW5	Δ*comA, sfgfp-khpA*; Ery^R, Sm^R	0
AW24	Δ*comA, khpA^{GDDG}*; Ery^R, Sm^R	>500
AW212	Δ*comA, khpA^{I61F}*; Ery^R, Sm^R	0
AW275	Δ*comA, khpA^{I61Y}*; Ery^R, Sm^R	>500
AW279	Δ*comA, eloR^{L239Y}*; Ery^R, Sm^R	>500

[a]The strains listed were transformed with a Δ*pbp2b*::janus amplicon as described in materials and methods. The transformations were done at least three times with similar results.

Table S2. Primers used in the present study.

Primer	Sequence (5` → 3`)	Reference
Primers used to create the Δ*khpA*::janus amplicon		
ds382	ATTTAGGGAACCAGATCTTAAG	This work
ds383	CACATTATCCATTAAAAATCAAACCTGTCAACCTACT TTAAACTTATTTTG	This work
ds384	GTCCAAAAGCATAAGGAAAGGAAGGGCGGGACGGAT GTC	This work
ds385	CAGGACCACACTCGTCAATC	This work
Kan484F	GTTTGATTTTTAATGGATAATGTG	[2]
RpsL41R	CTTTCCTTATGCTTTTGGAC	[2]
Primers used to create the Δ*pbp2b*::janus amplicon		
khb129	CGATAAAGAAGAGCATAGGAAG	[3]
khb132	TCCCAATCAATGGTTTCATTGG	[3]
Primers used to create the Δ*rodA*::janus amplicon		
ds342	AGAAAGTATTCGCTTTGAGTGC	[4]
ds343	TCCAAAACCTGATCATTTCGATG	[4]
Primers used to create the Δ*eloR*::janus amplicon		
ds374	CGAAACCTTGGGATACGCAG	[5]
ds377	CAGCACCCACGTTAAGCAAC	[5]
Primers used to create the *khpA*^{I61F} amplicon		
aw130	TTTGTCTACTCTGTCCCAACTGA	This work
aw131	TCAGTTGGGACAGAGTAGACTTTCGTTCTTATCGCAGA AATAGTG	This work
ds382	ATTTAGGGAACCAGATCTTAAG	This work
ds385	CAGGACCACACTCGTCAATC	This work
Primers used to create the *khpA*^{I61Y} amplicon		
aw147	TACGTCTACTCTGTCCCAACTGA	This work
aw148	TCAGTTGGGACAGAGTAGACGTACGTTCTTATCGCAGA AATAGTG	This work
ds382	ATTTAGGGAACCAGATCTTAAG	This work
ds385	CAGGACCACACTCGTCAATC	This work
Primers used to create the *khpA*^{I61C} amplicon		
aw189	TGTGTCTACTCTGTCCCAACTGA	This work
aw190	TCAGTTGGGACAGAGTAGACACACGTTCTTATCGCAGAA A TAGTG	This work
ds382	ATTTAGGGAACCAGATCTTAAG	This work
ds385	CAGGACCACACTCGTCAATC	This work
Primers used to create the *eloR*^{L239Y} amplicon		
aw158	CGGTTGTAAAGATAATTTTGAGCATACAGTTGCAAGGCCT TCAAGA	This work
aw157	TATGCTCAAAATTATCTTTACAACCG	This work
ds374	CGAAACCTTGGGATACGCAG	[5]
ds377	CAGCACCCACGTTAAGCAAC	[5]
Primers used to create the *eloR*^{L239C} amplicon		

aw191	TGTGCTCAAAATTATCTTTACAACCGC	This work
aw192	GCGGTTGTAAAGATAATTTTGAGCACACAGTTGCAAGGCC TTCAAGA	This work
ds374	CGAAACCTTGGGATACGCAG	[5]
ds377	CAGCACCCACGTTAAGCAAC	[5]
Primers used for fusion of 3xflag-tag to EloR		
gs515	CCATCATGATCTTTATAATCCACTACCAGATTCCTCCTTAT TTATTTC	[5]
gs516	GTGGATTATAAAGATCATGATGGTGATTATAAAGATC ATGATATTGATTATAAAGATGATGATGATAAAGTGGT AGTATTTACAGGTTCAA	[5]
Primers used for fusion of 3xflag-tag to KhpA		
gs517	CCATCATGATCTTTATAATCCATCTGTCAACCTACTTTAAA CTTATTTTG	This work
gs518	ATGGATTATAAAGATCATGATGGTGATTATAAAGATCATG ATATTGATTATAAAGATGATGATGATAAAATGGATACGAT TGAAAATCTCAT	This work
Primers used to create the *khpA-sfgfp* fusion		
ds382	ATTTAGGGAACCAGATCTTAAG	This work
aw5	TTTTTCGTCAATAACGATTCTTACTTT	This work
aw9	AAAGTAAGAATCGTTATTGACGAAAAAGGCGGCGGCG GCGGCAAACATCTTACCGGTTCTAAAGG	This work
ds233	TTATGCGGCCGCTCCACTAG	[4]
aw12	GTACAAAACTAGTGGAGCGGCCGCATAAGAAGGGCGG GACGGATG	This work
ds385	CAGGACCACACTCGTCAATC	This work
Primers used to create the *ftsZ-mKate-Km* fusion		
aw93	CCTGTTATTGCTCGTATCGC	This work
aw94	AGATACTTTCGTTTCCTGCCAA	This work
Primers used to construct T18 and T25 fusions for BACTH analysis		
mk17[a]	GAGCGGATCCCGTGGTAGTATTTACAGGTTCAAC	[5]
mk18	GCATGAATTCGAACCAGAACCACCTTCTGTATCT ACAACAACATAGC	[5]
aw90	GATCTCTAGAGATGGATACGATTGAAAATCTCATTAT	This work
aw92	GATCGAATTCGATTTTTCGTCAATAACGATTCTTACTT	This work
aw113	GATCTCTAGAGGTAGTATTTACAGGTTCAACTGTT	This work
aw116	GATCGAATTCGATTCAATATCCACTTGGGCTGG	This work
aw119	GATCGAATTCGAATTGACATTGATTGTAACGTAGAAG	This work
aw120	GATCTCTAGAGCACCGTGCAGAAGTCTTGC	This work
aw114	GATCGAATTCGATTCTGTATCTACAACAACATAGCG	This work
aw121	GATCTCTAGAGGTAGCTACGGAAGTAATGGC	This work
aw122	GATCGAATTCGAATCATTGACATTGATTGTAACGTAG	This work

[a] Restriction sites are underlined.

Table S3. *E. coli* strains and plasmids used in BACTH assays.

Name	Relevant characteristics	Reference
XL1Blue	Host strain	Aligent technologies
BTH101	BACTH expression strain, *cya*$^{-}$	Euromedex
Plasmids		
pUT18	Plasmid used in BATCH analysis	Euromedex
pKNT25	Plasmid used in BATCH analysis	Euromedex
pUT18-khpA	T18 fused to the C-terminus of KhpA	This work
pKNT25-khpA	T25 fused to the C-terminus of KhpA	This work
pUT18-khpA^{I61F}	T18 fused to the C-terminus of KhpA ^{I61F}	This work
pKNT25-khpA^{I61F}	T25 fused to the C-terminus of KhpA ^{I61F}	This work
pUT18-khpA^{I61Y}	T18 fused to the C-terminus of KhpA ^{I61Y}	This work
pKNT25-khpA^{I61Y}	T25 fused to the C-terminus of KhpA ^{I61Y}	This work
pUT18-khpA^{R53K}	T18 fused to the C-terminus of khpA^{R53K}	This work
pKNT25-khpA^{R53K}	T25 fused to the C-terminus of khpA^{R53K}	This work
pUT18-khpA^{R59K}	T18 fused to the C-terminus of khpA^{R59K}	This work
pKNT25-khpA^{R59K}	T25 fused to the C-terminus of khpA^{R59K}	This work
pUT18-khpA^{T60Q}	T18 fused to the C-terminus of khpA^{T60Q}	This work
pKNT25-khpA^{T60Q}	T25 fused to the C-terminus of khpA^{T60Q}	This work
pUT18-khpA^{GDDG}	T18 fused to the C-terminus of khpA^{GDDG}	This work
pKNT25- khpA^{GDDG}	T25 fused to the C-terminus of khpA^{GDDG}	This work
pUT18-eloR	T25 fused to the C-terminus of EloR	[5]
pUT18-eloR$^{\Delta R3H}$	T18 fused to the C-terminus of EloR$^{\Delta R3H}$	This work
pUT18-eloR^{R3H}	T18 fused to the C-terminus of EloR^{R3H}	This work
pUT18-KH-II^{EloR}	T18 fused to the C-terminus of KH-II^{EloR}	This work
pUT18-eloR^{Jag}	T18 fused to the C-terminus of EloR^{Jag}	This work
pUT18-eloR^{L239Y}	T18 fused to the C-terminus of EloR^{L239Y}	This work

References.

1 Sievers, F. *et al.* Fast, scalable generation of high-quality protein multiple sequence alignments using Clustal Omega. *Mol Syst Biol* **7**, 539, doi:10.1038/msb.2011.75 (2011).

2 Johnsborg, O., Eldholm, V., Bjørnstad, M. L. & Håvarstein, L. S. A predatory mechanism dramatically increases the efficiency of lateral gene transfer in *Streptococcus pneumoniae* and related commensal species. *Molecular microbiology* **69**, 245-253 (2008).

3 Berg, K. H., Stamsås, G. A., Straume, D. & Håvarstein, L. S. Effects of low PBP2b levels on cell morphology and peptidoglycan composition in *Streptococcus pneumoniae* R6. *Journal of bacteriology* **195**, 4342-4354 (2013).

4 Straume, D., Stamsås, G. A., Berg, K. H., Salehian, Z. & Håvarstein, L. S. Identification of pneumococcal proteins that are functionally linked to penicillin-binding protein 2b (PBP2b). *Molecular microbiology* **103**, 99-116 (2017).

5 Stamsås, G. A. *et al.* Identification of EloR (Spr1851) as a regulator of cell elongation in *Streptococcus pneumoniae*. *Mol Microbiol* **105**, 954-967, doi:10.1111/mmi.13748 (2017).

PAPER III

EloR interacts with the lytic transglycosylase MltG at midcell in *Streptococcus pneumoniae* R6

Anja Ruud Winther, Leiv Sigve Håvarstein, Morten Kjos, Daniel Straume

The Norwegian University of Life Sciences, Faculty of Chemistry, Biotechnology and Food Science, Christian Magnus Falsens vei 1, 1430 Ås, Norway

Abstract

The oval shape of *Streptococcus pneumoniae* is determined by the synchronized actions of the elongasome and the divisome. These machineries have the tasks of creating peptidoglycan (PG) that is necessary to elongate the cells and the PG that divides one cell into two, respectively. There is little knowledge about what coordinates these two modes of PG synthesis. Over the last years, a novel regulatory mechanism regarding elongation in *S. pneumoniae* has emerged – the EloR/KhpA complex. Previous investigations by us and others have showed that this complex is vital in regulating cell elongation, working closely with the Ser/Thr kinase StkP [1-5]. Here, we have further explored how this regulation occur. Through fluorescent microscopy we found that EloR is dependent upon its Jag domain in order to localize to midcell. We found that EloR interacts with several elongasome proteins, one of these being MltG. We also show that the Jag domain of EloR is necessary for the MltG interaction, and we consider MltG to be a good candidate to direct EloR to its midcell localization

Introduction

In order to multiply, a bacterial cell splits into two daughter cells in an intricate process involving chromosome replication and segregation, production of new cell membrane, and synthesis of new cell wall. *Streptococcus pneumoniae* is a Gram-positive species, meaning it produces a thick cell wall that surrounds and protects the cell.

The major component of the cell wall is peptidoglycan (PG) which is made up of chains of polysaccharides that are cross linked with short peptide bridges. The polysaccharides consist of alternating molecules of N-acetylglucosamine (GlcNAc) and N-acetylmuramic acid (MurNAc). The

cross links are made between pentapeptides attached to MurNAc [6].

S. pneumoniae has an ellipsoid shape resulting from synthesis of the PG layer by two protein complexes – the elongasome and the divisome [7, 8]. As the name suggests, the elongasome is responsible for producing PG in the peripheral direction, creating the elongated shape of pneumococci. The divisome, on the other hand, is responsible for synthesizing the septal disc that divides one cell into two. The precursor for PG is made inside the pneumococcal cell, transported to the outside and incorporated into the growing PG through transglycosylation (TG) and transpeptidation (TP) reactions [6, 9]. One group of enzymes performing this incorporation are the penicillin binding proteins known as PBPs. *S. pneumoniae* has six PBPs, three class A PBPs (PBP1a, PBP1b, PBP2a) that harbor TG and TP activity, two class B PBPs (PBP2b, PBP2x) that only harbor TP activity, and PBP3, a D,D-carboxypeptidase whose activity affects the amount of cross linking in PG by removing the terminal D-Ala residues of pentapeptides [10-12]. It is widely acknowledged that PBP2b is an essential part of the elongasome and PBP2x is an essential part of the divisome [13-15]. The Shape Elongation Division and Sporulation (SEDS) proteins RodA and FtsW have emerged as the main TG enzymes during PG production, working alongside the TP enzymes PBP2b and PBP2x, respectively. These essential protein pairs (PBP2b/RodA and PBP2x/FtsW) are the main PG polymerizing units in *S. pneumoniae* [8, 16]. The discovery that SEDS proteins are the primary TG enzymes in PG synthesis, prompted researchers to reassess the role class A PBPs have in PG synthesis. Rather than being essential in building the primary PG, recent data strongly indicate that the class A PBPs are essential for maturation of newly synthesized PG, e.g. filling in gaps or mistakes left by the divisome and possibly the elongasome [17, 18]. Other proteins considered to be part of the elongasome and divisome are found to be important for scaffolding, localization and regulation of PG production. One newly emerged member of the elongasome is the membrane bound lytic transglycosylase MltG [19]. MltG is a membrane protein consisting of a cytosolic domain, a transmembrane α-helix, and an extracellular catalytic domain. Cells depleted of MltG decrease in length, and MltG localizes with elongasome proteins throughout the cell cycle, indicating that the protein is part of the elongasome [20]. The specific role of MltG in PG synthesis is

unknown, but Tsui et al., 2016 hypothesize that MltG releases PG strands synthesized by PBP1a for cross-linking by RodA/PBP2b. Interestingly, suppressor mutations of MltG allows deletion of the essential elongasome protein PBP2b [20].

A particularly interesting aspect of cell wall synthesis is how PG production is regulated. By tracking the incorporation of new PG material using super-resolution fluorescence microscopy, pneumococci have been shown to elongate a short time period before septal PG synthesis is initiated [14, 21]. Although several proteins have been shown to be involved in regulation of cell elongation and septation, there is little knowledge about how they make up regulatory systems controlling the timed activities between elongation and division. The eukaryotic-type Ser/Thr kinase StkP appears to play a key role in coordinating these two events [22, 23]. StkP phosphorylates and thereby modulates the activity of several cell division proteins, i.e. DivIVA, GpsB, MapZ, MurC, MacP and EloR (also known as Jag/KhpB) [3, 5, 24-28]. It has been shown that DivIVA and its paralogue GpsB together with StkP are important for proper cell wall synthesis, and a phosphorylated MacP is important for the PBP2a function. Phosphorylation of MapZ (scaffolding protein for FtsZ) has been shown to be important for FtsZ ring constriction and splitting, while the effect of MurC (UDP-N-acetylmuramoyl L-alanine ligase) phosphorylation is still unclear. StkP is also important for the localization of PBP2x through interaction between StkP's PASTA domains and the pedestal and/or the transpeptidase domain of PBP2x [29]. Phosphorylation of EloR has been shown to be essential in regulation of cell elongation in *S. pneumoniae* [1, 5]. EloR is conserved in a range of Gram-positive genera such as Streptococcus, Bacillus, Clostridium, Listeria, Enterococcus, Lactobacillus and Lactococcus. It is composed of three domains: (i) an N-terminal Jag domain, (ii) a KH-II domain and (iii) an R3H domain at its C-terminal end. The KH-II and R3H are both RNA binding domains (possibly single stranded DNA) while the Jag domain has an unknown function. EloR interacts with another RNA binding protein called KhpA (composed of one KH-II domain). If the EloR/KhpA complex is broken, cells become shorter, consistent with loss of elongasome function, and are no longer dependent upon the essential PBP2b/RodA pair [1, 5]. Point mutations inactivating the RNA binding domains of EloR suggest that phosphorylation of EloR by StkP leads to release of bound RNA. This stimulates cell

elongation in an unknown fashion [1]. EloR and KhpA localize to the division zone of *S. pneumoniae* to regulate cell elongation along with lateral PG synthesis. While midcell localization of KhpA depends on its interaction with the KH-II domain of EloR, it is not known what directs EloR to midcell.

In this study, we employed fluorescence microscopy to explore which part of EloR that is important for its midcell localization. We show that any construct containing the Jag-domain is targeted to midcell. Furthermore, we used a large bacterial two-hybrid screen to identify possible interaction partners for EloR at the division zone. EloR was shown to interact with the elongasome protein MltG via its Jag domain. This interaction was further confirmed by pull-down assay

Results and discussion

The Jag domain is essential for recruiting EloR to septum.

EloR consists of an N-terminal Jag domain and two C-terminal RNA binding domains, KH-II and R3H (Figure 1A). We and others have previously shown that EloR localizes to the division zone where it creates a complex with KhpA [4, 5]. While KhpA depends on its interaction with EloR in order to localize to the division zone, it is not known how EloR finds the midcell. We hypothesized that EloR must form interaction(s) with other elongasome proteins in order to localize correctly. The Jag domain is connected to the KH-II domain by a large linker region (134 amino acids long) with an unknown structure and function. Since the KH-II and R3H domains bind RNA, our rationale was that the Jag-linker part of EloR would be important for its subcellular localization. We tested this by fusing full length EloR, the Jag domain, the linker region, and the Jag-linker domains to the fluorescent protein mKate, creating the strains AW407, AW408, AW410, and AW409, respectively. These fusions were expressed ectopically from an inducible promoter using the ComRS system [30]. The native *eloR* gene was kept unchanged in the genome. When inducer (ComS) was supplied to the growth medium, we saw as expected that full length EloR fused with mKate (EloR-mKate) was concentrated at midcell (Figure 1B). We also found that both the Jag-mKate and the Jag-linker-mKate fusions concentrated at midcell, although the Jag-mKate had a somewhat more diffuse localization. The linker-mKate fusion on the other hand did not localize to midcell (Figure 1B).

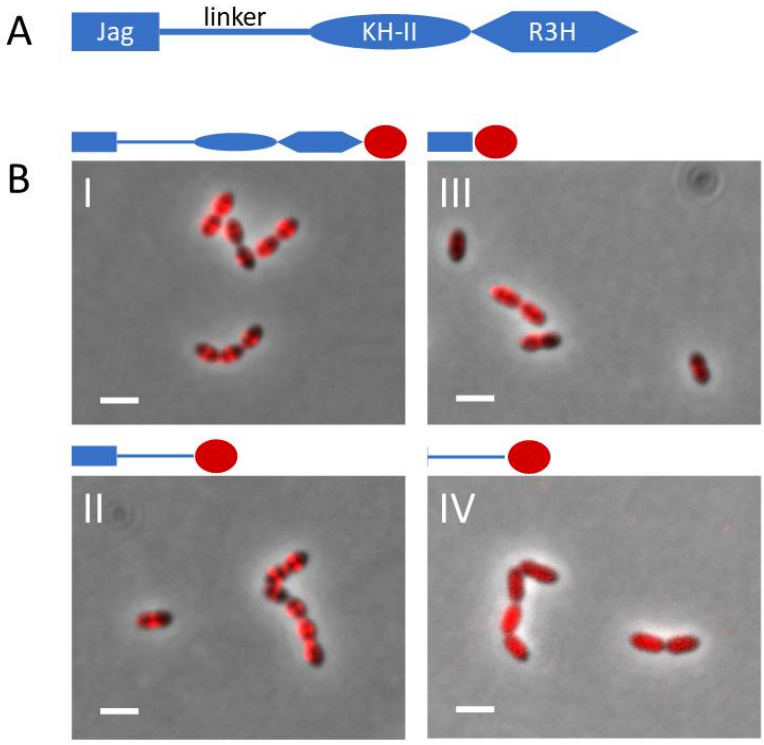

Figure 1. The Jag domain directs EloR to midcell. A) Schematic representation of EloR. B) Micrographs showing the localization of I) EloR-mKate (AW407), II) Jag-linker-mKate (AW409), III) Jag-mKate (AW408), and IV) linker-mKate (AW410). The full-length protein and the Jag-linker domains are located at midcell. The Jag domain alone localizes at midcell, but more diffuse then the full length EloR. The linker domain alone does not localize at midcell but is dispersed throughout the cytosol. Red circle in schematic drawings represents mKate. Scale bars are 2 μm.

Since the mKate fused with the linker domain alone did not localize to midcell, but a major bulk of Jag-mKate did, we concluded that the Jag domain targets EloR to the division zone, most probably by interacting with other cell division proteins. One such candidate is StkP as the kinase is located at midcell and is shown to phosphorylate EloR on two threonine residues (T89 and T126) found in the linker region [2, 31]. StkP is, however, not the reason why EloR-mKate can be found concentrated at midcell. In a genetic background lacking *stkP,* EloR-mKate can

still be seen at midcell (supplemental figure S1). The linker region seams necessary to obtain full midcell localization. Possibly the structure of the Jag domain is stabilized if it has the linker domain at the C-terminal end. The structure of the linker region is not known, whereas the 3D structure of the Jag domain has been solved for EloR in *Clostridium symbiosum* (PDB number 3GKU). It has a β-α-β-β fold with the α-helix laying on top of a three-stranded β-sheet. The conserved motif KKGFLG (supplemental figure S2) is found in the loop connecting the β2 and β3-strands. The same is true for the predicted structure of EloR from *S. pneumoniae* (supplemental Figure S3). We hypothesized that the conserved region (KKGFLG) could be involved in a protein-protein interaction possibly important for EloR localization. However, point mutations of several residues (K36A, K37A, F39A, and L40M) in this motif did not abrogate the midcell localization of EloR (supplemental Figure S4).

When aligning the amino acid sequences of EloR homologues from different Gram-positive species, the length of the linker region varies from approximately 135 amino acid residues in *S. pneumoniae* to approximately 10 residues in *Bacillus subtilis* (Supplemental Figure S5). Based on our results, the linker region is not crucial for recruiting EloR to midcell. The fact that the conserved threonine (T89 in *S. pneumoniae*) phosphorylated by StkP to modulate EloR activity is in the linker domain suggests that the linker could be involved in conformational rearrangements of the EloR protein between the active and inactive form. This, however, needs to be explored by structural studies comparing phosphorylated EloR with the non-phosphorylated form. It is also possible that the linker domain is involved in protein-protein interactions. The larger linker region in the pneumococcal EloR could accommodate for more interaction partners and hence more regulatory possibilities. Why pneumococci would need this is not clear.

EloR interacts with MltG through its Jag domain

We wanted to explore what other interactions EloR forms in addition to the one with KhpA. This might give an indication as to how EloR localizes at midcell and to its regulatory function in cell elongation. In order to investigate this, we screened our Bacterial Two-Hybrid (BACTH) assay library in *Escherichia coli* for possible interaction partners for EloR. The assay is based on blue (positive) and white (negative) color

selection, where the blue color comes from cleavage of X-gal in the medium by β-galactosidase. Briefly, the two proteins that are tested for interaction are fused to either the T18 or T25 domain. If an interaction between the two proteins occurs, T18 and T25 reconstitute an adenylate cyclase producing cAMP which induces expression of β-galactosidase [32]. EloR was probed against a range of known cell division proteins, namely PBP2b, RodA, RodZ, MreC, MreD, CozE, and MltG (Figure 2A). We also tested YidC2, a ribosome interacting membrane insertase sharing operon with *eloR* [33]. The presence of *yidC2* and *eloR* in one operon seems to be conserved in several species, e.g. *S. pneumoniae*, *S. mitis*, *S. oralis*, *B. subtilis*, and *Listeria monocytogenes*, to mention some), indicating a functional link between the two. Of all the proteins tested using BACTH, the positive hits were RodZ, YidC2 and MltG. MltG is a membrane protein predicted to be a lytic transglycosylase and is essential in *S. pneumoniae* [19]. RodZ is, similar to EloR, considered to be part of the elongasome and studies in *E. coli* indicate that RodZ is important for the elongated cell shape [34]. To test if RodZ or YidC2 were important for EloR localization, we imaged EloR-mKate in cells devoid of either *rodZ* or *yidC2* (Supplemental Figure S6). The midcell localization of EloR-mKate was not dramatically affected in these mutants, although somewhat higher signals of EloR-mKate were found in the cytosol. This does not mean that the interactions found with BACTH are not relevant in dissecting the function of EloR. If EloR is part of a larger complex regulating the expression of one or several elongasome proteins, it is possible that it has a connection to YidC2 and possibly ribosomes. To unravel this requires additional research.

Since deletion of *rodZ* or *yidC2* had little effect on EloR localization, we hypothesized that the EloR/MltG interaction could be important for this matter. However, MltG is essential in wild type cells making it impossible to track EloR-mKate in a Δ*mltG* mutant. Furthermore, we did not succeed in making an *mltG* depletion strain having EloR-mKate in the native *eloR* locus. Instead, we performed BACTH assays with the Jag domain of EloR (which is targeted to midcell) and the cytoplasmic domain of MltG. Indeed, the Jag-linker domains and the sole Jag domain interacted with the cytosolic domain of MltG (Figure 2B). MltG is therefore a candidate as to why EloR displays midcell localization.

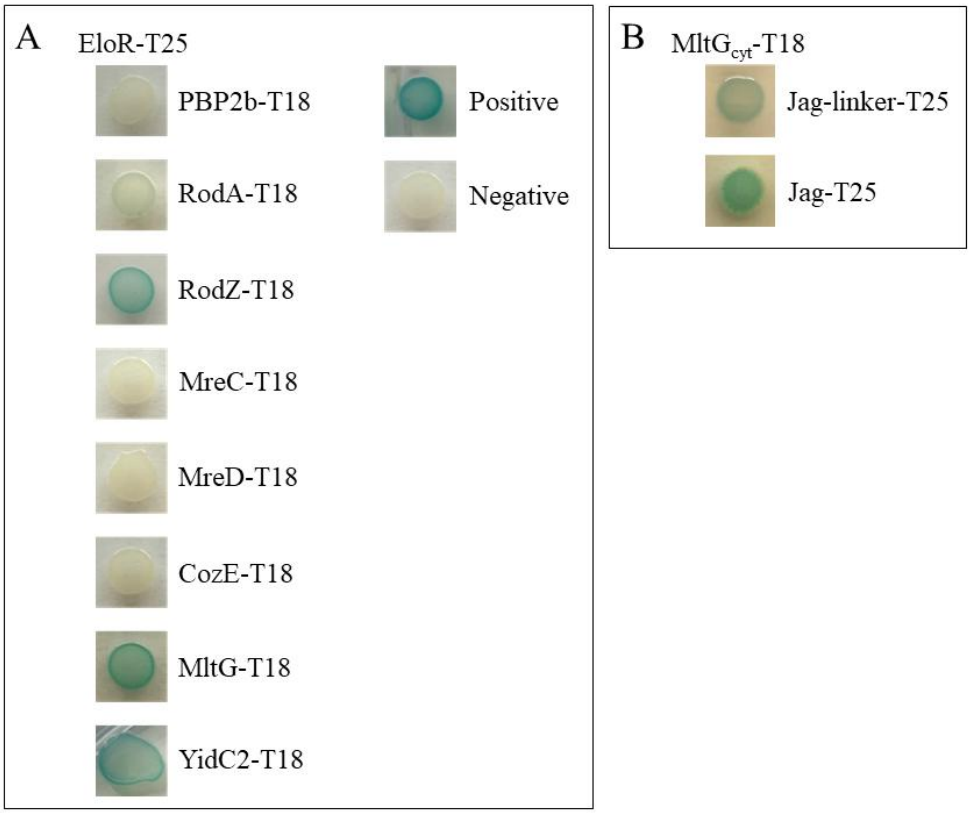

Figure 2. Bacterial two hybrid assay probing EloR against other elongasome proteins. A) PBP2b, RodA, MreC, MreD, and CozE probed against EloR gave colorless spots of bacteria complying with no interaction between the two proteins. RodZ, MltG and YidC2 on the other hand gave blue bacteria when probed against EloR, suggesting that an interaction occurs. Positive and negative controls were supplied by the manufacturer (Euromedex) and are included in panel A. B) The Jag-linker domains and the Jag domain of EloR were tested against the cytosolic domain of MltG. Both spots are positive, indicating that it is the Jag domain of EloR that interacts with the cytosolic domain of MltG.

EloR and MltG are part of the same complex

To confirm the interaction between EloR and MltG *in vivo* in *S. pneumoniae* we attempted to use EloR as bait to pull down MltG. In order to do so, we constructed a strain expressing a Flag-tagged EloR and a GFP-tagged MltG (strain AW447). By using resin beads tethered with α-Flag antibodies we

pulled out Flag-EloR from the cell lysate as previously described by Stamsås et al., 2017. Then we looked for both Flag-EloR and GFP-MltG among the immunoprecipitated proteins using immunodetection and α-Flag and α-GFP antibodies (Figure 3). Indeed, when pulling out Flag-EloR using the α-Flag resin we found that GFP-MltG followed in the same fraction. Strain ds515 expressing only GFP-MltG was used as a negative control for a possible GFP/α-Flag interaction. In addition, to exclude a possible GFP/Flag-EloR unspecific interaction we co-expressed Flag-tagged EloR and GFP-tagged HlpA (DNA binding protein [35]) in strain AW459. When performing anti-Flag immunoprecipitation on lysates from this strain no GFP-HlpA was pulled down together with Flag-EloR.

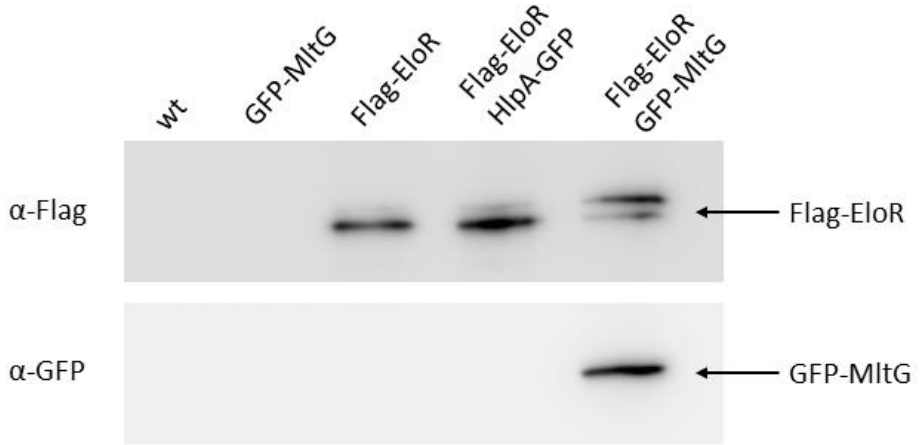

Figure 3. Immunoblot confirming the EloR – MltG interaction. Lysates from strains RH425 (wt), ds515 (*gfp-mltG*), AW98 (*flag-eloR*), AW459 (*flag-eloR, hlpA-gfp*), and AW447 (*flag-eloR, gfp-mltG*) were incubated with resin beads tethered with α-Flag antibodies to pull down Flag-EloR. As expected, immunoprecipitated Flag-EloR was found in strain AW98, AW459 and AW447, but not in strain ds515. GFP-MltG was only found in immunoprecipitated fractions when it was co-expressed with a Flag-tagged EloR.

This proves that MltG specifically follows EloR in the pull-down assay, i.e EloR is in complex with MltG *in vivo* in *S. pneumoniae*. Based on our BACTH results the EloR/MltG interaction seems to be direct. Since MltG is located at the division zone of *S. pneumoniae* it is plausible that EloR is recruited to midcell through its interaction with MltG. Nevertheless, we cannot completely exclude the possibility that MltG is pulled down with EloR because both EloR and MltG interact with a third protein. Further investigations (BACTH, co-IPs and cross-linking) are required to rule out this possibility.

We have previously found that knocking out the essential PBP2b results in suppressor mutations in *mltG, eloR* or *khpA* relieving the requirement of the elongasome in *S. pneumoniae* [1]. The same discovery regarding MltG was found in a parallel study performed by Tsui et al., 2016 [20]. The current finding that EloR and MltG interact therefore corroborate that MltG and EloR are part of the same regulatory pathway. KhpA is most probably also part of this complex since we have shown previously that it interacts directly with EloR at the division zone. In sum we can conclude that MltG, EloR and KhpA form a protein complex at the division zone which regulates the elongasome on command from StkP. In a previous study, we speculated that EloR/KhpA might regulate the expression levels of MltG. This, however, turned out to be wrong [1]. Another hypothesis is that the EloR/KhpA complex regulates the activity of MltG. MltG in *E. coli* have been shown to possess endolytic transglycosylase activity, i.e. breaking glycosidic bonds within a glycan strand [19]. Structural modelling and site directed mutagenesis of the active site of the pneumococcal MltG suggest that it has the same muralytic activity [20]. It has been hypothesized that MltG in *S. pneumoniae* releases glycan strands made by PBP1a so that they can be cross linked to new PG made by the PBP2b/RodA complex [20]. In light of the recent discoveries regarding the function of class A PBPs that suggest PBP1a to be involved in maturing the newly synthesized PG by filling in gaps, we propose a different model: MltG works together with amidases to open the PG layer so that PBP2b/RodA can add new PG to the existing layer and hence elongate the dividing cell (Figure 4). MltG must therefore be strictly regulated to avoid uncontrolled damage to the PG layer. Based on the data presented here the EloR/KhpA complex appears to play a role in regulation of MltG. Since inactivation of the RNA binding domains of EloR gives the same phenotype as inactivation of the catalytic

domain of MltG (PBP2b/RodA becomes redundant) [1, 20], one could speculate that the EloR/KhpA complex modulates the activity of MltG through RNA binding. Another possibility is that EloR regulates the MltG activity directly through protein-protein interaction. This must be confirmed or rejected by further experimental evidence.

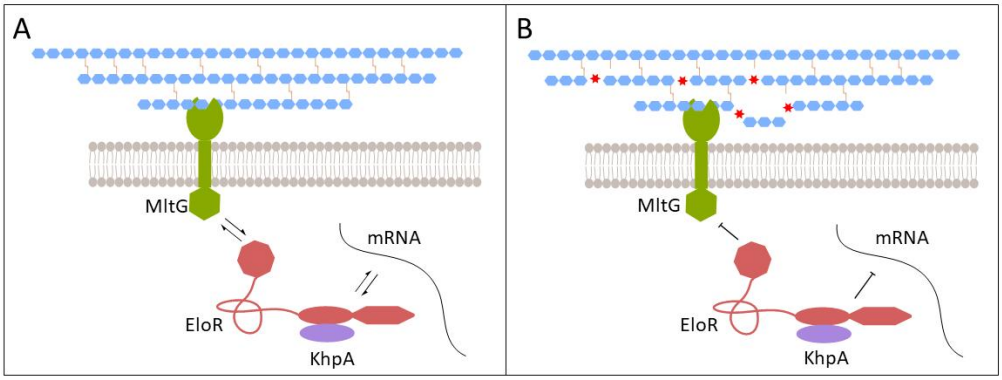

Figure 4. Modell of MltG/EloR/KhpA function. In a wild type setting as depicted in panel A, the communication between EloR/KhpA/mRNA and MltG allows for a controlled opening of the PG. These openings are utilized by PBP2b/RodA to insert new PG in the lateral direction of the cell and in this way elongate the cell. If the EloR-pathway is disturbed (panel B), MltG can cut the PG at will. This weakens the cell wall.

Methods

Bacterial strains, cultivation and transformation. All bacterial strains used in this work are listed in Table 1. All *E. coli* strains were grown in liquid Luria Bertani (LB) broth with shaking or on LB agar plates at 30°C or 37°C. When necessary, the following antibiotic concentrations were used: 100 µg/ml ampicillin and 50 µg/ml kanamycin. Transformation of *E. coli* was performed with heat shock at 42°C for 30 seconds. All *S. pneumoniae* strains were grown in C-medium [36] without shaking or on Todd-Hewitt (TH) agar plates in an oxygen-depleted chamber using AnaeroGenTM bags from Oxoid at 37°C. Concentrations of 200 µg/ml streptomycin or 400 µg/ml kanamycin was employed when necessary. When introducing genetic

changes, natural transformation was utilized. Exponentially growing cells were diluted to an OD_{550} of 0.05-0.1 and grown for two hours with 100-200 ng of the transforming DNA and 250 ng/ml CSP (final concentration) added to the growth medium. Thirty µl of the transformed cell cultures were plated on TH agar plates with the appropriate antibiotic and incubated at 37°C overnight.

DNA constructs. All primers used in this study are listed in Table 2. DNA constructs used to transform *S. pneumoniae* were made using overlap extension PCR [37]. In short, in order to create deletion mutants, the approximately 1000 bp sequence upstream and downstream of the gene in question were amplified and fused with the 5' end and 3' end of the Janus cassette [38], respectively. The same flanking regions were then used to replace the Janus cassette with an alternative DNA sequence [39]. Constructs used to produce BACTH plasmids were amplified from *S. pneumoniae*, cleaved with restriction enzymes (XbaI and EcoRI from New England BioLabs), and ligated into the preferred plasmid using Quick ligase (New England BioLabs). The plasmids used in this study are listed in Table 1. All constructs were verified with DNA sequencing.

Bacterial two hybrid assay. Bacterial two hybrid (BACTH) assays are based on the two tags T18 and T25 that make up the catalytic domain of *Bordetella pertussis* adenylate cyclase (CyaA). In order to test whether two proteins interact, their genes are cloned in frame with one tag each and co-expressed in *E. coli* BTH101 cells (*cyaA*-). If the two proteins interact, T18 and T25 are brought into close proximity to make up an active CyaA catalytic domain. This results in cAMP production which induces expression of *lacZ* (β-galactosidase). β-galactosidase cleaves X-gal, resulting in blue bacteria on X-gal containing agar plates. In instances where the two tested proteins do not interact, no β-galactosidase is expressed, and the bacteria remain white. The BACTH experiments were performed as described by the manufacturer (Euromedex). The genes encoding our proteins of interest were cloned in reading frame with either the T18 or T25 encoding gene in the plasmids pUT18, pUT18C and pKT25. The plasmids were then transformed into *E. coli* XL1-Blue cells, then isolated and sequenced. In order to test the interaction between two proteins, they were co-expressed with one tag (T18, T25) each in *E. coli* BTH101 cells. After overnight incubation, five random colonies were picked, grown to exponential phase, and

spotted (2 µl) onto LB agar plates containing ampicillin (100 µg/ml), kanamycin (50 µg/ml), IPTG (0.5 mM) and X-gal (40µg/ml). After overnight incubation at 30°C the results were documented.

Co-immunoprecipitation and western blotting. Co-IP was performed using ANTI-FLAG® M2 affinity gel (Sigma-Aldrich). In short, *S. pneumoniae* strains were grown to OD_{550} = 0.3 and lysed with 1 ml lysis buffer (50 mM Tris HCl, pH 7.4, 150 mM NaCl, 1 mM EDTA, 1% Triton X-100) by triggering LytA activity at 37°C for 5 minutes. The lysate was incubated with 40 µl ANTI-FLAG® M2 affinity gel with gentle rotation at 4°C overnight. After washing the affinity gel three times with 500 µl TBS, SDS sample buffer was added and the samples were incubated at 95°C for 10 minutes. Proteins from eight µl of each sample were separated in a 12 % SDS PAGE gel. After electrophoresis the separated proteins were blotted onto a PVDF membrane using a Trans-Blot Turbo Transfer System (Bio-Rad) with a standard protocol for seven minutes. Finally, Flag-tagged proteins were detected as previously described by Stamsås et al., 2017. GFP-tagged proteins were detected with Chromotek abbit polyclonal antibody to GFP, using the same protocol as above and dilutions as recommended by the manufacturer.

Phase contrast and fluorescent microscopy. Cells were prepared for microscopic imaging by growing them to OD_{550} = 0.4, dilution to OD_{550} = 0.1 and grown for another hour in the presence of 2 µM ComS inducer. Proteins fused with the fluorescent mKate were visualized as previously described [1] using a Zeiss AxioObserver with ZEN Blue software, an ORCA-Flash 4.0 V2 Digital CMOS camera (Hamamatsu Photonics), and a 1003 phase-contrast objective. An HXP 120 Illuminator (Zeiss) was used as a fluorescence light source. Images were prepared using the ImageJ software.

Acknowledgements

The authors would like to thank Zhian Salehian for excellent technical support and Gro Anita Stamsås for proofreading. Parts of this work were funded by The Research Council of Norway.

Table 1. Bacterial strains and plasmids.

***S. pneumoniae* strains**	**Relevant characteristics**	**Source**
R704	R6 derivative, *comA*::*ermAM*; Ery^r	J. P. Claverys
RH425	R704, but streptomycin resistant; Ery^r, Sm^r	[40]
SPH131	Δ*comA,* P1*::*P_{comR}*::comR,* P_{comX}*::Janus*; Ery^r Kan^r	[30]
AW407	Δ*comA,* P1*::*P_{comR}*::comR,* P_{comX}*::eloR-mKate*; Ery^r Sm^r	This work
AW408	Δ*comA,* P1*::*P_{comR}*::comR,* P_{comX}*::jag-mKate*; Ery^r Sm^r	This work
AW409	Δ*comA,* P1*::*P_{comR}*::comR,* P_{comX}*::jag-linker-mKate*; Ery^r Sm^r	This work
AW420	Δ*comA,* P1*::*P_{comR}*::comR,* P_{comX}*::linker-mKate*; Ery^r Sm^r	This work
AW447	Δ*comA, mltG-gfp, flag-eloR*; Ery^r Sm^r	This work
AW459	Δ*comA, flag-eloR, hlpA-gfp-chloramphenicol*; Ery^r, Sm^r, Cam^r	This work
DS515	Δ*comA, gfp-mltG*; Ery^r, Sm^r	[1]
AW98	Δ*comA, flag-eloR*; Ery^r, Sm^r	[1]
***E. coli* strains**		
XL1-Blue	Host strain	Agilent Technologies
BTH101	BACTH expression strain, *cya-*	Euromedex
Plasmids		
pKT25	Plasmid used in BACTH analysis	Euromedex
pUT18C	Plasmid used in BACTH analysis	Euromedex
pUT18	Plasmid used in BACTH analysis	Euromedex
pKT25-eloR	T25 domain fused to the N-terminus of EloR	[1]
pUT18C-eloR	T18 domain fused to the N-terminus of EloR	[1]
pKT25-jag-linker	T25 domain fused to the N-terminus of the Jag-linker domains of EloR	This work
pKT25-jag	T25 domain fused to the N-terminus of the Jag domain of EloR	This work
pUT18C-mltG	T18 domain fused to the N-terminus of MltG	[1]
pUT18C-mltG$_{cyt}$	T18 domain fused to the N-terminus of the cytoplasmic domain of MltG	This work
pUT18C-pbp2b	T18 domain fused to the N-terminus of PBP2b	[41]
pUT18C-rodA	T18 domain fused to the N-terminus of RodA	[41]
pUT18C-rodZ	T18 domain fused to the N-terminus of RodZ	[1]
pUT18C-mreC	T18 domain fused to the N-terminus of MreC	[1]
pUT18C-mreD	T18 domain fused to the N-terminus of MreD	This work
pUT18-cozE	T18 domain fused to the C-terminus of CozE	[41]
pUT18-yidC2	T18 domain fused to the C-terminus of YidC2	This work

Table 2. Primers.

Primer name	Sequence (5' → 3')	Reference
Primers used to create the *eloR-mKate* amplicon, place it behind P_{comX} and screen		
DS433	ATTTATATTTATTATTGGAGGTTCAGTGGTAGTATTTACAG GTTCAAC	This work
AW236	CTTCTCCACCAGATCCGGATTCTGTATCTACAACAACATAG CG	This work
AW234	TCCGGATCTGGTGGAGAAG	This work
AW249	ATTGGGAAGAGTTACATATTAGAAATTAACGGTGTCCCAAT TTACTAG	This work
KHB31	ATAACAAATCCAGTAGCTTTGG	[30]
KHB36	TGAACCTCCAATAATAAATATAAAT	[30]
KHB33	TTTCTAATATGTAACTCTTCCCAAT	[30]
KHB34	CATCGGAACCTATACTCTTTTAG	[30]
Primers used to create the *jag-mKate* amplicon, place it behind P_{comX} and screen		
DS433	ATTTATATTTATTATTGGAGGTTCAGTGGTAGTATTTACAG GTTCAAC	This work
AW238	CTTCTCCACCAGATCCGGATTTGACAACAGTCGTTTCACTA AT	This work
AW234	TCCGGATCTGGTGGAGAAG	This work
AW249	ATTGGGAAGAGTTACATATTAGAAATTAACGGTGTCCCAAT TTACTAG	This work
KHB31	ATAACAAATCCAGTAGCTTTGG	[30]
KHB36	TGAACCTCCAATAATAAATATAAAT	[30]
KHB33	TTTCTAATATGTAACTCTTCCCAAT	[30]
KHB34	CATCGGAACCTATACTCTTTTAG	[30]
Primers used to create the *jag-linker-mKate* amplicon, place it behind P_{comX} and screen		
DS433	ATTTATATTTATTATTGGAGGTTCAGTGGTAGTATTTACAG GTTCAAC	This work
AW240	CTTCTCCACCAGATCCGGATTGTTCAATATCAAAGTTCGTT TCAA	This work
AW234	TCCGGATCTGGTGGAGAAG	This work
AW249	ATTGGGAAGAGTTACATATTAGAAATTAACGGTGTCCCAAT TTACTAG	This work
KHB31	ATAACAAATCCAGTAGCTTTGG	[30]

KHB36	TGAACCTCCAATAATAAATATAAAT	[30]
KHB33	TTTCTAATATGTAACTCTTCCCAAT	[30]
KHB34	CATCGGAACCTATACTCTTTTAG	[30]
Primers used to create the *linker-mKate* amplicon, place it behind P_{comX} and screen		
AW239	GAAATAAATAAGGAGGAATCTGGTAGTGGCAAATCAACAG GTAGTAA	This work
AW240	CTTCTCCACCAGATCCGGATTGTTCAATATCAAAGTTCGTT TCAA	This work
AW234	TCCGGATCTGGTGGAGAAG	This work
AW249	ATTGGGAAGAGTTACATATTAGAAATTAACGGTGTCCCAAT TTACTAG	This work
KHB31	ATAACAAATCCAGTAGCTTTGG	[30]
KHB36	TGAACCTCCAATAATAAATATAAAT	[30]
KHB33	TTTCTAATATGTAACTCTTCCCAAT	[30]
KHB34	CATCGGAACCTATACTCTTTTAG	[30]
Primers used to create the *hlpA-gfp-chloramphenicol* amplicon		
MK180	AACAAGTCAGCCACCTGTAG	[35]
MK181	CGTGGCTGACGATAATGAGG	[35]
Primers used to create the *flag-eloR* amplicon		
DS374	CGAAACCTTGGGATACGCAG	[1]
DS377	CAGCACCCACGTTAAGCAAC	[1]
Primers used to introduce *jag-linker* into BACTH plasmids pKT25 and pUT18C		
AW271	GATCTCTAGAGGTAGTATTTACAGGTTCAACTGTT	This work
AW272	GTACGAATTCTTATTTGACAACAGTCGTTTCACTAAT	This work
Primers used to introduce *jag* into BACTH plasmids pKT25 and pUT18C		
AW113	GATCTCTAGAGGTAGTATTTACAGGTTCAACTGTT	This work
AW116	GATCGAATTCGATTCAATATCCACTTGGGCTGG	This work
Primers used to introduce *mltGcyt* into BACTH plasmids pKT25 and pUT18C		
AW268	GATCTCTAGAGTTGAGTGAAAAGTCAAGAGAAGAA	This work
AW269	GATCGAATTCTTAGAATGAAATCACAAAAGCTTTCAC	This work
Primers used to introduce *mreD* into BACTH plasmid pKT25 and pUT18C		
KHB455	TACGAAGCTTG ATGAGACAGTTGAAGCGAGTT	This work

GS336	TACGGAATTCGATAGATAATATTTTTCAAAAATAAATTG	This work
Primers used to introduce *yidC2* into BACTH plasmid pKT25 and pUT18C		
MK19	GAGCGGATCCCGGAGTGAAAAAGAAACTAAAGTTG	This work
MK20	GCATGAATTCGAACCAGAACCACCTTTCGTTTTCTGAGCCTTTTTCTTG	This work

References

1. Stamsås, G.A., et al., *Identification of EloR (Spr1851) as a regulator of cell elongation in* Streptococcus pneumoniae. Molecular microbiology, 2017. **105**(6): p. 954-967.
2. Sun, X., et al., *Phosphoproteomic analysis reveals the multiple roles of phosphorylation in pathogenic bacterium* Streptococcus pneumoniae. 2009. **9**(1): p. 275-282.
3. Ulrych, A., et al., *Characterization of pneumococcal Ser/Thr protein phosphatase* phpP *mutant and identification of a novel PhpP substrate, putative RNA binding protein Jag.* 2016. **16**(1): p. 247.
4. Winther, A.R., et al., *Prevention of EloR/KhpA heterodimerization by introduction of site-specific amino acid substitutions renders the essential elongasome protein PBP2b redundant in* Streptococcus pneumoniae. Scientific Reports, 2019. **9**(1): p. 3681.
5. Zheng, J.J., et al., *Absence of the KhpA and KhpB (JAG/EloR) RNA-binding proteins suppresses the requirement for PBP2b by overproduction of FtsA in* Streptococcus pneumoniae *D39.* Molecular microbiology, 2017. **106**(5): p. 793-814.
6. Vollmer, W., D. Blanot, and M.A. De Pedro, *Peptidoglycan structure and architecture.* FEMS microbiology reviews, 2008. **32**(2): p. 149-167.
7. Pinho, M.G., M. Kjos, and J.-W.J.N.r.m. Veening, *How to get (a) round: mechanisms controlling growth and division of coccoid bacteria.* 2013. **11**(9): p. 601.
8. Cho, H., et al., *Bacterial cell wall biogenesis is mediated by SEDS and PBP polymerase families functioning semi-autonomously.* Nature microbiology, 2016. **1**: p. 16172.
9. Typas, A., et al., *From the regulation of peptidoglycan synthesis to bacterial growth and morphology.* Nature Reviews Microbiology, 2012. **10**(2): p. 123.
10. Sauvage, E., et al., *The penicillin-binding proteins: structure and role in peptidoglycan biosynthesis.* FEMS microbiology reviews, 2008. **32**(2): p. 234-258.
11. Zapun, A., T. Vernet, and M.G. Pinho, *The different shapes of cocci.* FEMS microbiology reviews, 2008. **32**(2): p. 345-360.
12. Morlot, C., et al., *Crystal structure of a peptidoglycan synthesis regulatory factor (PBP3) from* Streptococcus pneumoniae. 2005. **280**(16): p. 15984-15991.
13. Berg, K.H., et al., *Effects of low PBP2b levels on cell morphology and peptidoglycan composition in* Streptococcus pneumoniae *R6.* Journal of bacteriology, 2013. **195**(19): p. 4342-4354.
14. Tsui, H.C.T., et al., *Pbp2x localizes separately from Pbp2b and other peptidoglycan synthesis proteins during later stages of cell division of* Streptococcus pneumoniae *D39.* Molecular microbiology, 2014. **94**(1): p. 21-40.
15. Perez, A.J., et al., *Movement dynamics of divisome proteins and PBP2x: FtsW in cells of* Streptococcus pneumoniae. Proceedings of the National Academy of Sciences, 2019. **116**(8): p. 3211-3220.
16. Meeske, A.J., et al., *SEDS proteins are a widespread family of bacterial cell wall polymerases.* Nature, 2016.

17. Straume, D., et al., *Class A PBPs have a distinct and unique role in the construction of the pneumococcal cell wall.* 2019: p. 665463.
18. Vigouroux, A., et al., *Cell-wall synthases contribute to bacterial cell-envelope integrity by actively repairing defects.* 2019: p. 763508.
19. Yunck, R., H. Cho, and T.G.J.M.m. Bernhardt, *Identification of MltG as a potential terminase for peptidoglycan polymerization in bacteria.* 2016. **99**(4): p. 700-718.
20. Tsui, H.C.T., et al., *Suppression of a deletion mutation in the gene encoding essential PBP2b reveals a new lytic transglycosylase involved in peripheral peptidoglycan synthesis in* Streptococcus pneumoniae *D39.* 2016. **100**(6): p. 1039-1065.
21. Wheeler, R., et al., *Super-resolution microscopy reveals cell wall dynamics and peptidoglycan architecture in ovococcal bacteria.* 2011. **82**(5): p. 1096-1109.
22. Manuse, S., et al., *Role of eukaryotic-like serine/threonine kinases in bacterial cell division and morphogenesis.* 2015. **40**(1): p. 41-56.
23. Fleurie, A., et al., *Mutational dissection of the S/T-kinase StkP reveals crucial roles in cell division of* Streptococcus pneumoniae. 2012. **83**(4): p. 746-758.
24. Fleurie, A., et al., *MapZ marks the division sites and positions FtsZ rings in* Streptococcus pneumoniae. Nature, 2014. **516**(7530): p. 259-262.
25. Holečková, N., et al., *LocZ is a new cell division protein involved in proper septum placement in* Streptococcus pneumoniae. 2015. **6**(1): p. e01700-14.
26. Falk, S.P. and B.J.F.m.l. Weisblum, *Phosphorylation of the* Streptococcus pneumoniae *cell wall biosynthesis enzyme MurC by a eukaryotic-like Ser/Thr kinase.* 2013. **340**(1): p. 19-23.
27. Fenton, A.K., et al., *Phosphorylation-dependent activation of the cell wall synthase PBP2a in* Streptococcus pneumoniae *by MacP.* 2018. **115**(11): p. 2812-2817.
28. Fleurie, A., et al., *Interplay of the serine/threonine-kinase StkP and the paralogs DivIVA and GpsB in pneumococcal cell elongation and division.* 2014. **10**(4): p. e1004275.
29. Morlot, C., et al., *Interaction of P enicillin-B inding P rotein 2x and Ser/Thr protein kinase StkP, two key players in* Streptococcus pneumoniae *R 6 morphogenesis.* 2013. **90**(1): p. 88-102.
30. Berg, K.H., et al., *Peptide-regulated gene depletion system developed for use in* Streptococcus pneumoniae. Journal of bacteriology, 2011. **193**(19): p. 5207-5215.
31. Hirschfeld, C., et al., *Proteomic Investigation Uncovers Potential Targets and Target Sites of Pneumococcal Serine-Threonine Kinase StkP and Phosphatase PhpP.* 2019. **10**.
32. Karimova, G., et al., *A bacterial two-hybrid system based on a reconstituted signal transduction pathway.* Proceedings of the National Academy of Sciences, 1998. **95**(10): p. 5752-5756.
33. Wu, Z.C., et al., *Interaction of* Streptococcus mutans *YidC1 and YidC2 with translating and nontranslating ribosomes.* 2013. **195**(19): p. 4545-4551.
34. Shiomi, D., M. Sakai, and H.J.T.E.j. Niki, *Determination of bacterial rod shape by a novel cytoskeletal membrane protein.* 2008. **27**(23): p. 3081-3091.
35. Kjos, M., et al., *Bright fluorescent* Streptococcus pneumoniae *for live-cell imaging of host-pathogen interactions.* 2015. **197**(5): p. 807-818.
36. Lacks, S. and R.D.J.B.e.b.a. Hotchkiss, *A study of the genetic material determining an enzyme activity in pneumococcus.* 1960. **39**(3): p. 508-518.
37. Higuchi, R., B. Krummel, and R.J.N.a.r. Saiki, *A general method of in vitro preparation and specific mutagenesis of DNA fragments: study of protein and DNA interactions.* 1988. **16**(15): p. 7351-7367.
38. Sung, C., et al., *An* rpsL *cassette, janus, for gene replacement through negative selection in* Streptococcus pneumoniae. Applied and environmental microbiology, 2001. **67**(11): p. 5190-5196.

39. Johnsborg, O., et al., *A predatory mechanism dramatically increases the efficiency of lateral gene transfer in* Streptococcus pneumoniae *and related commensal species.* Molecular microbiology, 2008. **69**(1): p. 245-253.
40. Johnsborg, O. and L.S.J.J.o.b. Håvarstein, *Pneumococcal LytR, a protein from the LytR-CpsA-Psr family, is essential for normal septum formation in* Streptococcus pneumoniae. 2009. **191**(18): p. 5859-5864.
41. Straume, D., et al., *Identification of pneumococcal proteins that are functionally linked to penicillin-binding protein 2b (PBP2b).* Molecular microbiology, 2017. **103**(1): p. 99-116.

Supplementary information

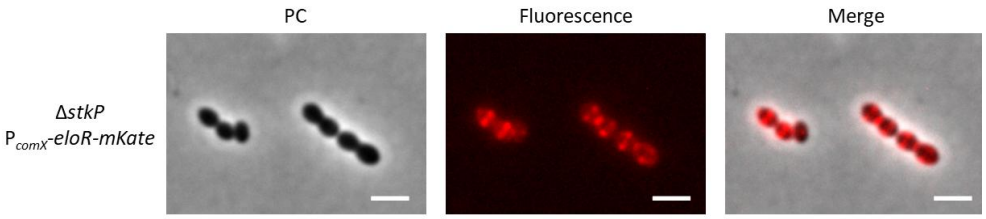

Figure S1. Localization of EloR-mKate in a Δ*stkP* mutant. EloR-mKate is concentrated at midcell. Scale bars are 2 µm.

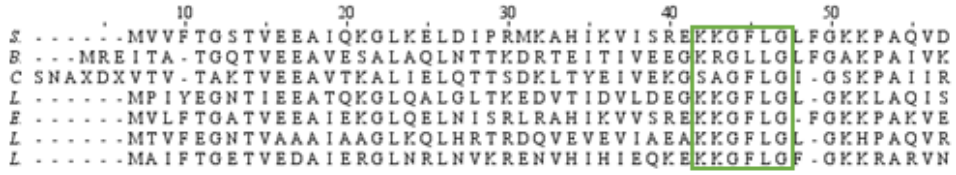

Figure S2. Alignment of the Jag domains from (listed in same order as they appear in image) *S. pneumoniae*, *B. subtilis*, *C. symbiosium*, *Listeria monocytogenes*, *Enterococcus faecalis*, *Lactobacillus plantarum*, and *Lactococcus lactis*. The conserved KKGFLG (green box) is indicated.

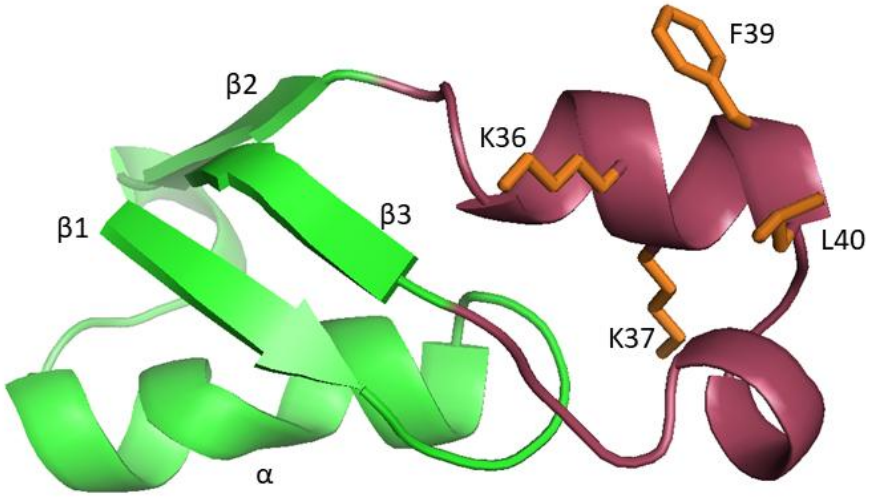

Figure S3. Predicted structure (iTasser) of the Jag domain of *S. pneumoniae* EloR. The β-α-β-β fold with the α-helix laying on top of a three-stranded β-sheet is portrayed in green. The loop connecting the second and third β-strand is portrayed in red. The KKGFLG motif is shown in orange sticks.

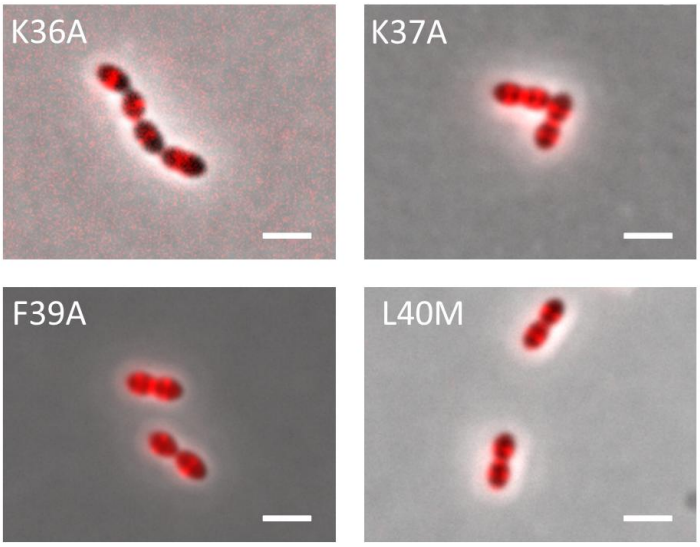

Figure S4. Localization of EloR-mKate harboring the amino acid substitutions K36A, K37A, F39A and L40M. EloR-mKate is found concentrated at midcell with all the introduced mutations. Scale bars are 2 µm.

Figure S5. Alignment of EloR from (listed in same order as they appear in image) *S. pneumoniae*, *B. subtilis*, *C. symbiosium*, *Listeria monocytogenes*, *Enterococcus faecalis*, *Lactobacillus plantarum*, and *Lactococcus lactis*. The linker domain of EloR from *S. pneumoniae* (green box) is made up of approximately 135 amino acids, while the equivalent domain from *B. subtilis* (green box) only consists of approximately 10 amino acids.

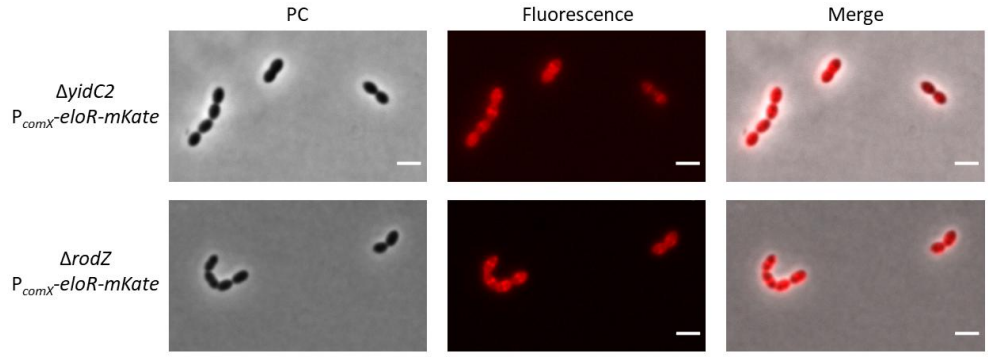

Figure S6. Localization of EloR-mKate in cells devoid of *yidC* and *rodZ*. EloR-mKate is concentrated at midcell. Scale bars are 2 µm.

ISBN: 978-82-575-1700-7
ISSN: 1894-6402

Norwegian University
of Life Sciences

Postboks 5003
NO-1432 Ås, Norway
+47 67 23 00 00
www.nmbu.no